THESIS APPROVAL

GRADUATE SCHOOL, KASETSART UNIVERSITY

Doctor of Philosophy (Chemistry)

DEGREE

Chemistry	Chemistry
FIELD	**DEPARTMENT**

TITLE: Effect of Dicarboxylic Acids on the Formation of the Metal Organic Framework Complexes Containing 1,10-Phenanthroline

NAME: Miss Panana Kitiphaisalnont

THIS THESIS HAS BEEN ACCEPTED BY

THESIS ADVISOR

(Associate Professor Sutatip Siripaisarnpipat, Ph.D.)

THESIS CO-ADVISOR

(Associate Professor Ladda Meesuk, Ph.D.)

THESIS CO-ADVISOR

(Assistant Professor Noojaree Prasitpan, Ph.D.)

DEPARTMENT HEAD

(Associate Professor Supa Hannongbua, Dr.rer.nat.)

APPROVED BY THE GRADUATE SCHOOL ON _____

DEAN

(Associate Professor Gunjana Theeragool, D.Agr.)

THESIS

EFFECT OF DICARBOXYLIC ACIDS ON THE FORMATION OF THE METAL ORGANIC FRAMEWORK COMPLEXES CONTAINING 1,10-PHENANTHROLINE

PANANA KITIPHAISALNONT

A Thesis Submitted in Partial Fulfillment of
the Requirements for the Degree of
Doctor of Philosophy (Chemistry)
Graduate School, Kasetsart University
2010

Panana Kitiphaisalnont 2010: Effect of Dicarboxylic Acids on the Formation of the Metal Organic Framework Complexes Containing 1,10-Phenanthroline. Doctor of Philosophy (Chemistry), Major Field: Chemistry, Department of Chemistry. Thesis Advisor: Associate Professor Sutatip Siripaisarnpipat, Ph.D. 169 pages.

Under solvothermal conditions at 150°C 24 hr and 72 hr, the effect of anions of copper salt on the reactions of Cu(II) ions, phenanthroline and hydroxyl dicarboxylate anions was observed. $Cu(NO_3)_2 \cdot 3H_2O$ cleavaged malate and tartrate into oxalate resulting in two different structures. The former is mononuclear complex, $[Cu(ox)(phen)(H_2O)] \cdot H_2O$ **(1)** and the latter is polymeric complex, $[Cu(\mu\text{-}ox)(phen)]_n$ **(3)**. Their structures are different from the complex **4**, which is synthesized by direct reaction of $Cu(NO_3)_2 \cdot 3H_2O$ and oxalic acid at the same condition. The non-hydroxycarboxylate succinate anions solvothermally react with $Cu(NO_3)_2 \cdot 3H_2O$ and phenanthroline yielding tetranuclear complex **2**, $[Cu_4(\mu\text{-}suc)_2(phen)_4(H_2O)_4](NO_3)_4 \cdot 4H_2O$. The solvothermal reactions of $CuSO_4 \cdot 5H_2O$ with malate and with tartrate give isostructural sulfato copper(II) complexes, $[Cu(\mu\text{-}SO_4)(phen)(H_2O)_2]_n$, **(6)**. The elemental and infrared analyses reveal that the complexes obtained from the reaction of $CuCl_2 \cdot 2H_2O$, malate (or tartrate) and phenanthroline (**7**, **8**) are isostructure with the formula $[Cu(phen)_2Cl_2]$.

The complexes obtained from the reactions of $MnCl_2 \cdot 4H_2O$ with malate, tartrate or succinate by simple wet method have same structures as that obtained by solvothermal method. Their structural formula is *cis*-$[Mn(phen)_2Cl_2]$.

The infrared, UV-Vis and thermal analyses are consistent with their crystal structures.

_____ _____ __ / __ / __

Student's signature Thesis Advisor's signature

ACKNOWLEDGEMENTS

I am gratefully thank and deeply indebted to Assoc. Prof. Dr. Sutatip Siripaisarnpipat, my advisor, for her patience, encouragement and valuable advice and suggestions during my study at Kasetsart University. I also take this opportunity to thank Assoc. Prof. Dr. Ladda Meesuk and Asst. Prof. Dr. Noojaree Prasitpan, who are my thesis committees for their valuable suggestions. I would like to thank Asst. Prof. Dr. Marisa Arunchaiya, the Graduate School representative, for her advice. I am sincerely thank Asst. Prof. Dr. Chaveng Pakawatchai from Prince of Songkla University and Assoc. Prof. Dr. Narongsak Chaichit from Thammasat University for single X-ray crystal data collections and valuable discussions. I would like to give a special thanks to Prof. Dr. Omar M. Yaghi from University of California, Los Angeles (UCLA), who is my foreign co-advisor for giving me an opportunity to work in his Recticular chemistry laboratory (2007-2008) and to Prof. Dr. Michael O'Keeffe from Arizona State University for teaching me about metal organic frameworks.

I'm especially grateful to the Royal Golden Jubilee Ph. D. Program for my RGJ scholarship (3.C.KU /48 / H.1).

Special appreciations are given to Dr. Supakit Archivavanish, Dr. Tanwawan Duangthongyou, Dr. Upsorn Boonyang, Dr. Norased Nasongkla, Mr. Anusorn Seubsai, Mr. Wachirapun Punkawee and Ms. Utaiwan Watcharosin for their good help, and to all of my friends who are not named here for their encouragements during the period of this study.

Finally, I am especially appreciated to my parents, my brother and Mr. Siri Khuharuangrong for their encouragement, support and providing me a chance to experience the world of science and learning.

Panana Kitiphaisalnont

October, 2010

TABLE OF CONTENTS

Page

LIST OF TABLES

Appendix Table

LIST OF TABLES (Continued)

LIST OF TABLES (Continued)

LIST OF FIGURES

LIST OF FIGURES (Continued)

LIST OF FIGURES (Continued)

LIST OF FIGURES (Continued)

LIST OF FIGURES (Continued)

LIST OF SYMBOLS AND ABBREVIATIONS

Å	=	angstrom
F	=	structure factor
F_c	=	calculated structure factor
F_o	=	observed structure factor
I	=	integrated intensity
h,k,l	=	miller indices
R_1	=	an index that gives a crude measurement of the correctness of a structure and the quality of the data
wR_1	=	a number assigned to express the relative precision of each measurement
S	=	goodness-of-fit
σ	=	estimated standard deviation
μ	=	absorption coefficient
θ	=	Bragg reflection angle
λ	=	wavelength
suc	=	succinate ion
ox	=	oxalate ion
phen	=	1,10-phenanthroline
UV	=	ultraviolet
Vis	=	visible
LMCT	=	ligand to metal charge transfer

EFFECT OF DICARBOXYLIC ACIDS ON THE FORMATION OF THE METAL ORGANIC FRAMEWORK COMPLEXES CONTAINING 1, 10- PHENANTHROLINE

INTRODUCTION

The bulk properties of a molecular material depend critically on its crystal structure and intermolecular interactions. In recent years, enormous interest has been aroused in using coordination polymeric networks containing transition metal centers in concert with supramolecular interactions as the basis for the attempted design of solid-state structures with pre-assigned properties. The studies on metal organic frameworks are focused on material science as well as structural chemistry for potential applications such as catalysis (Marioka *et al.*, 1993; Fujita *et al*., 1994 and Seo *et al*., 2000), gas adsorption (Yaghi *et al*, 1995; Eddaoudi *et al.*, 2000), chemical adsorption (Reineke *et al*., 1999) or magnetism (Ribas *et al*, 1994; Chaudhury *et al*, 2000 and Mukherjee *et al.*, 2001). The general strategy for designing such extended system relies on the use of multidentate ligands which have the potential capacity to bridge between metal centers to form polymeric structures.

Dicarboxylic acids have proved to be a good choice for assembling high dimensional metal organic framework owing to their interesting structures. First, they contain two bridging moieties, which lead to a variety of connection modes with transition metal centers and provides abundant structural motifs. Second, they can act not only as hydrogen bond donors but also as acceptor. On the other hand, most of high dimensional networks are not purely bridge by one ligand. They usually employ two or more ligands in the construction of polymers. In case of mix ligands complexes, usually one is ligand such as dicarboxylate ions which processes many modes to connect to metal centers and the other is rigid ligand such as pyridine, 2,2′-bipyridine and phenanthroline which can form π-π interaction and create various high dimentional structure of complexes.

The carboxylate ligands are known in various coordination modes to bond toward metal ions, such as terminal monodentate, bridging bidentate or chelate, as shown in Scheme A (Su *et al*, 2007, Wojtezak *et al*., 1998).

Scheme A

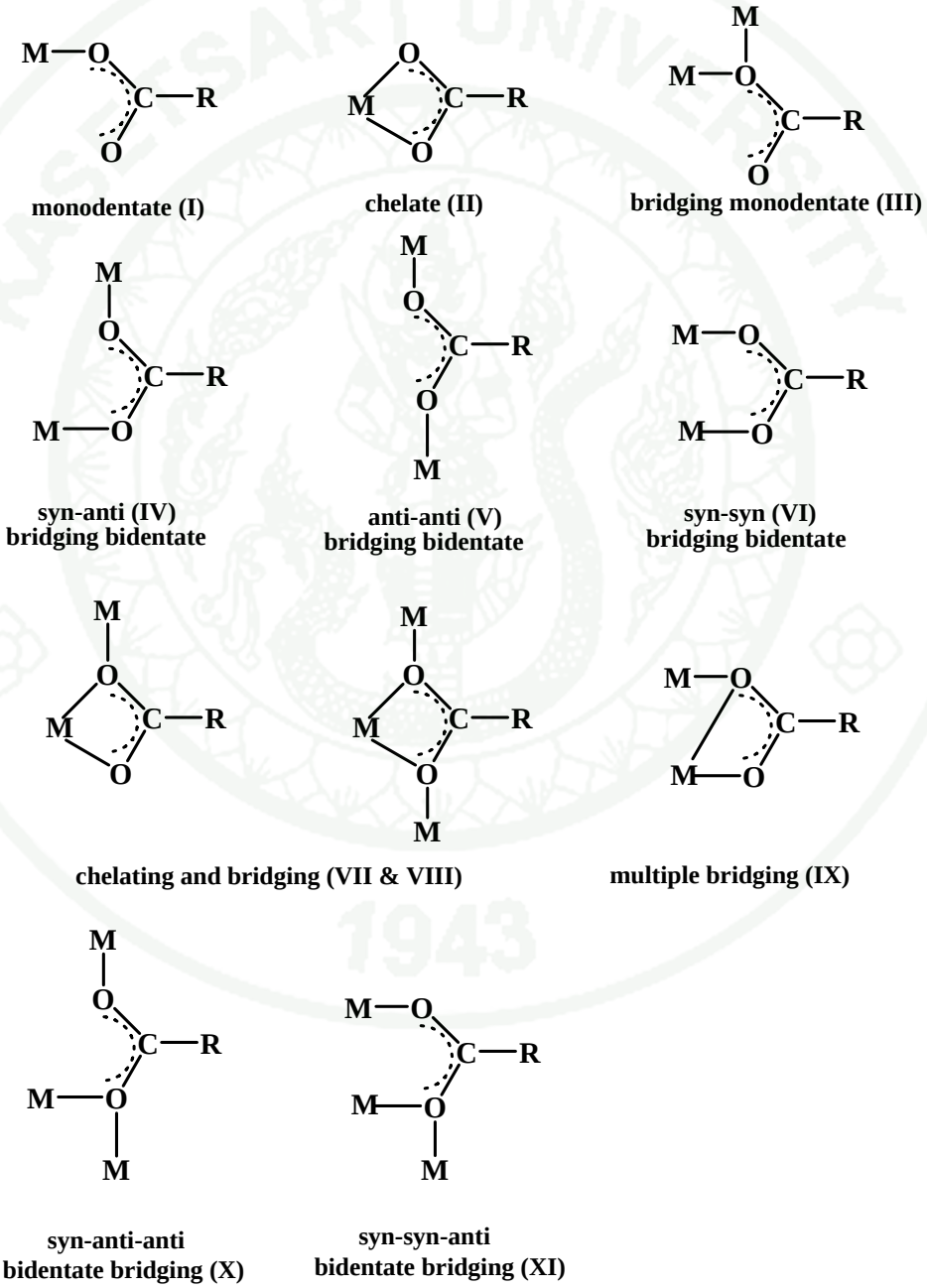

The coordination modes for each carboxylate group in dicarboxylate ligand may be similar or different as shown in scheme B.

Scheme B

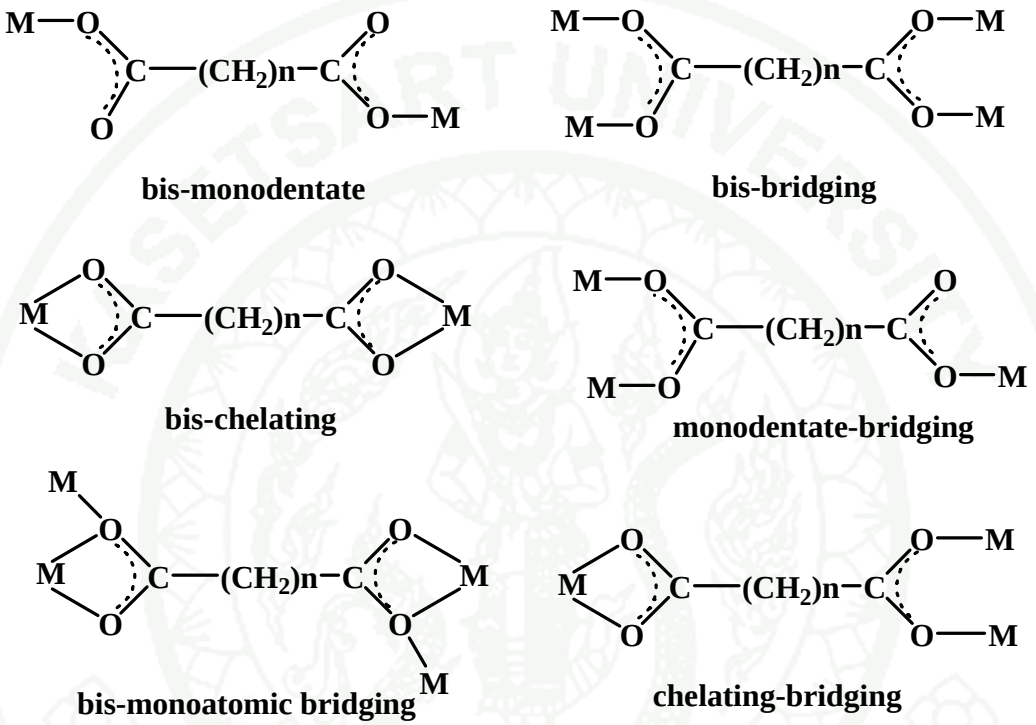

Unlike rigid spacers, the flexible dicarboxylate ligands can adopt various conformations resulting in novel topologies. The conformational isomerism of long chain dicarboxylate ligands has driven much interest in crystal engineering (Fujita *et al*,. 1994; Hennigar *et al*., 1997; Moulton *et al*., 2001). The aliphatic carbon backbone of long chain dicarboxylate ligands may be present in different conformations for example, alkyl chain of succinate ligand exists in two conformations which are *anti* and *syn* conformation (Scheme C) which are considered from the torsion angles of aliphatic carbon backbone (Mao *et al*., 2004). The torsion angles of aliphatic carbon backbone of anti form is about 160-180° while those for gauche form is less than 90°.

Scheme C

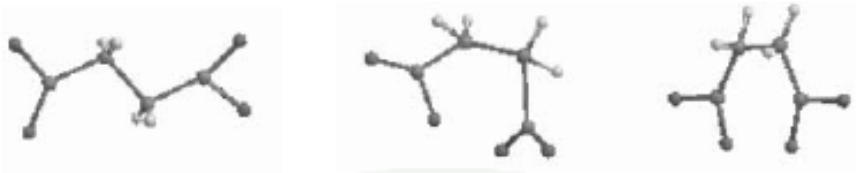

Anti **Syn**

The hydroxypolycarbonates ligands, such as malate, citrate and tartrate, have been less studied as building blocks in the construction of metal-organic frameworks. The unique features of hydroxypolycarboxylic acids have drawn our attention. First of all, these acids possess terminal carboxylic acid and hydroxyl groups that may be completely or partially deprotonated. This leads to a versatile coordination behavior, and as such, distinct bonding modes towards metal cations, such as nonchelating, chelating, and bridging modes can be realized. Secondly, hydroxypolycarboxylic acids can act not only as hydrogen-bond acceptors, but also as hydrogen bond donors to form new extended structures by means of additional hydrogen-bond interactions.

As mentioned above the dicarboxylate ligand can coordinate with transition metal centers in different fashions. Not only bridging ligands are important for the designing coordination polymer network, but also a proper choice of the planar N-donor ligands such as pyridine, imidazole, bipyridine and phenanthroline. Their rigidity and planarity can efficiently provide π-π stacking interactions among their aromatic moieties. This feature potentially contributes the stability of structures as well as creation of extended dimensionality.

Aromatic-aromatic or π-π interactions are important noncovalent inter molecular forces similar to hydrogen bonding. They can contribute to self-assembly or molecular recognition process when extended structures are formed from building blocks with aromatic moieties. In the arrangement of aromatic rings one can distinguish generally between a stacked arrangement and an edge- or point-to-face, T-shaped conformation (Scheme D). Usually the interplanar distances of about 3.3 – 3.8

Å between the parallel aromatic planes are sufficent for the π-π interaction between the stacks of aromatic groups (Janiak, 2000).

Scheme D

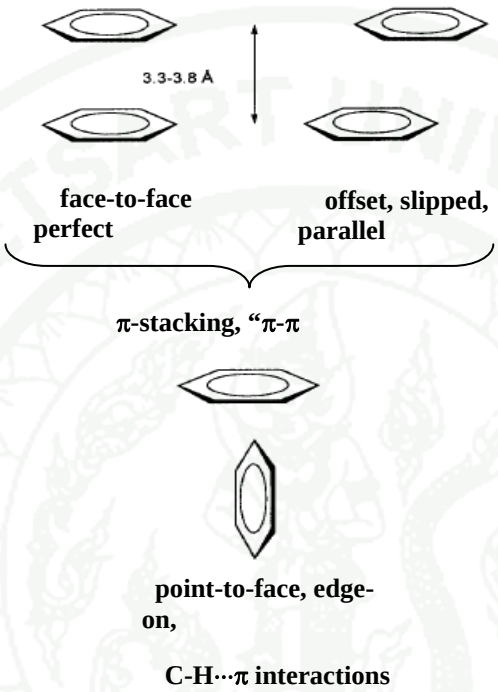

The focus of this study is to examine the influence of the hydroxyl group and the alkyl chain length of hydroxydicarboxylate on the structures and properties of Cu(II) and Mn(II) complexes. Two hydroxydicarboxylate ligands with alkyl chains of four carbon atoms (Scheme E) are used as flexible spacer ligands in this study. The coordination mode and conformational variation of the flexible ligands will be comparable with those of non- hydroxydicarboxylate acid (succinic acid).

Scheme E

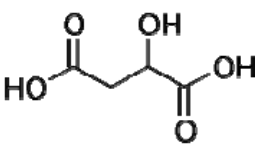

malic acid ($C_4H_6O_4$)

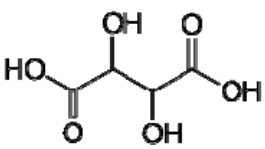

tartaric acid ($C_4H_6O_5$)

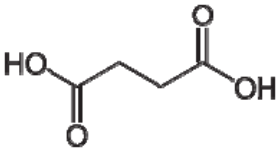

succinic acid ($C_4H_6O_6$)

OBJECTIVES

1. To synthesize Cu(II) and Mn(II) complexes containing
   (i) malic acid and 1, 10-phenanthroline
   (ii) succinic acid and 1, 10-phenanthroline
   (iii)tartaric acid and 1, 10-phenanthroline

2. To determine the crystal structures of the synthesized complexes by single crystal X-ray diffraction technique and investigate the coordination and bridging modes of oxalate and succinate as well as conformation of aliphatic backbone in the prepared complexes.

3. To study spectroscopic and thermal gravimetric properties of the prepared complexes.

LITERATURE REVIEW

Dicarboxylic acids have proved to be a good choice for assembling high dimensional metal-organic framework owing to their interesting structural features. First, they contain two bridging moieties, which lead to a variety of connection modes with transition metal centers and provide abundant structural motifs. Second, they can act not only as hydrogen bond donors but also as acceptor. On the other hand, most of high dimensional networks are not purely bridged by one ligand. They usually employ two or more ligands in the construction of polymers. In case of mixed ligand complexes, usually one is flexible ligand such as dicarboxylate ions which possesses many modes to connect to metal centers and the other is pyridyl ligand such as pyridine, 2,2′-bipyridine and phenanthroline which can form π-π interaction and create various high dimentional structure of complexes. Several coordination polymers containing C4 aliphatic carboxylate ligands are firstly planned for this study. In the course of study, it was found that the malato-copper complex and tartrato-copper complex could not be obtained. The malate and tartrate ions were converted into oxalate ion. Thus, this section will include the reviews of oxalato-copper complexes and exclude those of malato-copper complexes and tartrato-copper complexes.

The metal (II) oxalate complexes

Oxalic acid (ox, $C_2O_4^{2-}$) is a dicarboxylic acid which consists of two carboxylic group without carbon backbone. Oxalate ligands can act as either bridging or chelate which are classified as shown in Scheme A. In the pass decades there have been many studies on the synthesis and magnetic exchange interaction between metal ions through oxalate bridging group in dinuclear and polyneclear metal complexes. The literature surveys reveal that there are three types of coordination geometry around copper ion in the oxalate complexes, which are square pyramid (Julve *et al.*, 1984 ; Gleizes *et al.*, 1992; Smékal *et al.*, 1999; Castillo *et al.*, 1999; Zhang *et al.*, 2000; Du *et al.*, 2002; Sujittra *et al.*, 2006 and Boonmark *et al.*, 2008), trigonal bipyramid (Smékal *et al.*, 1999 and Wang *et al.*, 2007) and octahedron (Castillo *et al.*,

1998, 2001; Tang *et al.*, 2000; Núñes *et al.*, 2001; Sujittra *et al.*., 2003, 2006). In addition, the structural units are mostly dimeric and polymeric units. The coordination mode of oxalate in most complexes is bis-chelate bridging.

Three new complexes , $[tmen(H_2O)Cu(C_2O_4)Cu(H_2O)tmen](C1O_4)_2 \cdot 1.25H_2O$ (**I**), $[dienCu(C_2O_4)Cu(H_2O)_2tmen](C1O_4)_2$ (**2**), and $[tmen(2\text{-}MeIm)Cu(C_2O_4)Cu(2\text{-}MeIm)tmen](PF_6)_2$ (**3**), where tmen = N,N,N′,N′-tetramethylethylenediamine,die n = diethylenetri amine, and 2-MeIm = 2-methylimidazole were synthesized. Each copper atom in **I** is in a square-pyramidal environment with the two nitrogen atoms of tmen and two oxygen atoms of $C_2O_4^{2-}$ in the basal plane and a water molecule occupying the apical position (Figure 1a). The structure of **2** is made up of dissymmetrical binuclear cations and non coordinated perchlorate anions. On the dien side, the four nearest neighbors of copper are the three nitrogen atoms of dien and only one oxygen atom of $C_2O_4^{2-}$ while on the tmen side, the basal plane is again made of two oxygen atoms of tmen (Figure 1b). The environment of each copper in **3** is intermediate between the square pyramid with only one oxygen atom of $C_2O_4^{2-}$ in the basal plane and the trigonal bipyramid (Figure 1c). The magnetic properties of the three compounds were investigated in the 2-300 K temperature range. All oxalato ligands are tetradentate with the coordination mode of bis-chelate bridging. Their magnetic properties exhibit a behavior characteristic of antiferromagnetically coupleed copper (II) pairs with a rounded maximum in the susceptibility occurring at about 300 K for (1), at 62 K for (2) and 10.8 K for (3) (Julve *et al.*, 1984). The structure of $[(Cu(Medpt)_2ox](NO_3)_2 \cdot 2.2/3H_2O$ (Medpt = 3,3′-diamino-N-methyldipropylamine) is name up of dinuclear $[Cu(Medpt)_2ox]^{2+}$ cation units, uncoordinated nitrate and lattice water molecules. The environment of each copper(II) ion is distorted square pyramidal with an oxalate-oxygen atom in the apical position and the three Medpt-nitrogen and one oxalate-oxygen atoms in the equatorial plane. The $\nu_{asym}(COO^-)$ (1632-1652 cm^{-1}), $\nu_{sym}(COO^-)$ (1304-1324 cm^{-1}) and $\delta(COO^-)$ (788-794 cm^{-1}) are consistent with tetradentate oxalate. Magnetochemical measurement showed that this Cu(II) complex is antiferromagnetic and ferromagnetic in nature (Smékal *et al.*, 1999).

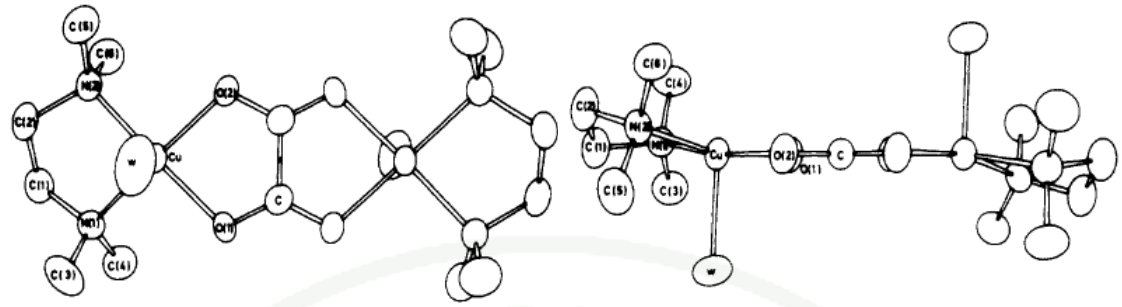

(a)

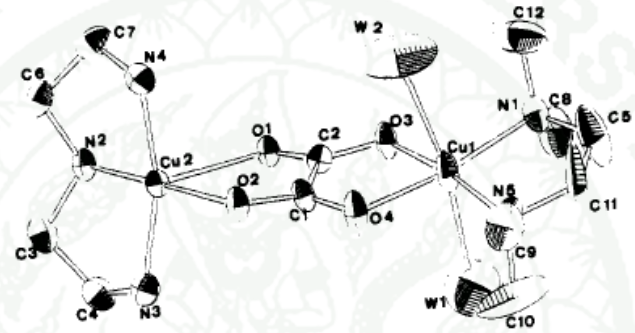

(b)

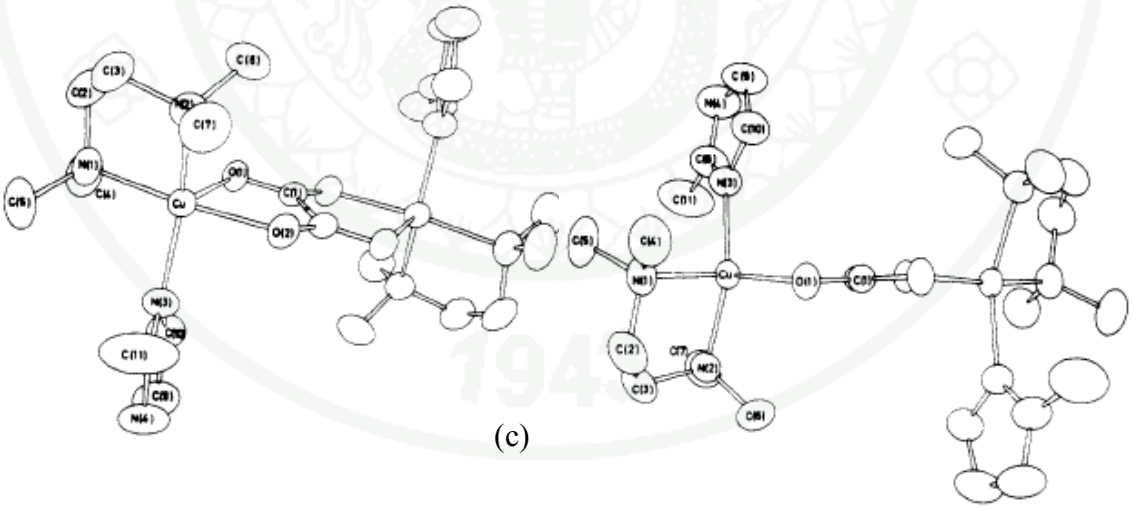

(c)

Figure 1 Perspective views of the binuclear cations (a) [tmen-(H_2O)Cu(C_2O_4)Cu (H_2O)tmen]$^{2+}$, (b) [dienCu(C_2O_4)Cu(H_2O) tmen]$^{2+}$ and (c) [tmen(2-MeIm) Cu(C_2O_4)Cu(2-MeIm)tmen]$^{2+}$.

Source: Julve *et al.* (1984)

Two compounds, $Cu_2(tacn)_2(\mu\text{-}ox)(ClO_4)_2$ and $[Cu_2(bdpm)_2(H_2O)_2(\mu\text{-}ox)](ClO_4)_2 \cdot H_2O$, where tacn = 1,4,7-triazacyclononane, ox = oxalate dianion, bdpm = bis(3,5-dimethyl-pyrazol-1-yl)methane), were prepared and characterized. The former has two copper metal centers bridged by a planar bis(didentate) oxalate ligand. The geometry around each copper(II) ion is considered as an elongated octahedral environment with two nitrogen atoms of tacn and two oxygen atoms of oxalate bridge in the equatorial plane CuN2O2, and the third nitrogen atom of tacn occupying the apical position. The Cu(1) and Cu(2) atoms lie 0.043 Å and 0.049 Å from the basal planes towards the apical nitrogen. The four equatorial atoms around Cu atoms are planar (Figure 2a). The structure of the latter is made up of water molecules of crystallization, uncoordinated perchlorate anions and binuclear $[Cu_2(bdpm)_2(H_2O)_2(\mu\text{-}ox)]^{2+}$ (Figure 2b). The copper coordination geometry is distorted square pyramidal with two nitrogen atoms from bdpm and two oxygen atoms from the oxalato bridging ligand in the basal plane and the other oxygen atom from water molecule in the axial position. The oxalate anion is almost planar and the copper (II) ions are 0.3293 Å out of the plane towards the axial position. Both compounds showed the weak magnetic coupling. These results lead to three special comments which are : (1) The bending magnitude of the basal plane of the $C_2O_4^{2-}$ bridge is sensitive to the magnetic coupling interaction. The bonding significantly reduces antiferromagnetic interaction. (2) The difference in coordination environments of copper (II) ions is able to weaken the antiferromagnetic interactions, especially in the systems in which one of the oxalate oxygen atoms is in the basal plane and the other is apical. (3) The height of metal atoms above the basal plane is significant, which permits antiferromagnetic interaction; i.e. the height reduces the overlap of both magnetic orbitals through the σ-orbital of the oxalate: the higher the distance, the weaker the interaction observed (Zhang *et al.*, 2000).

The oxalate ligands in $[Cu_2(BIBM)_2(C_2O_4)_2]$ act in a tridentate mode (Figure 3). One copper ion connects to two oxalate oxygen atoms forming a chelate ring. The other copper ion connect to one oxygen atom of the same oxalate ligand. The coordination about the copper atom is a very elongated octahedron. The equatorial plane is comprised of two oxygen atoms belonging to an oxalate group and two nitrogen

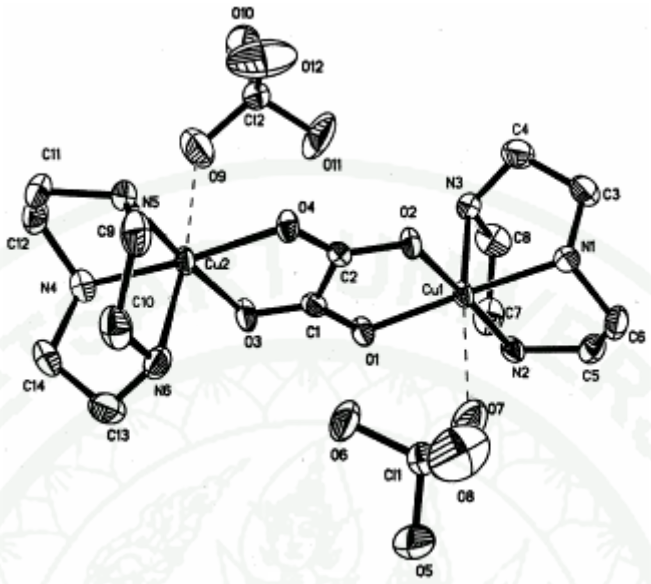

(a)

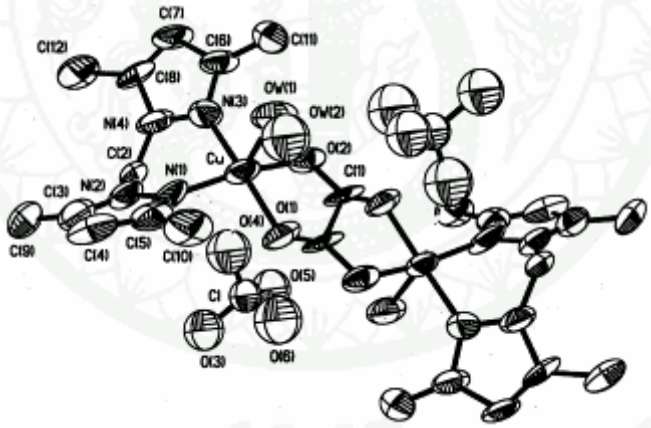

(b)

Figure 2 ORTEP drawing (30% of thermal ellipsoid probability) of (a) $Cu_2(tacn)_2(\mu\text{-}ox)(ClO_4)_2$ and (b) $[Cu_2(bdpm)_2\ (H_2O)_2(\mu\text{-}ox)](ClO_4)_2{\cdot}H_2O$ with atom-labeling scheme.

Source: Zhang *et al.* (2000)

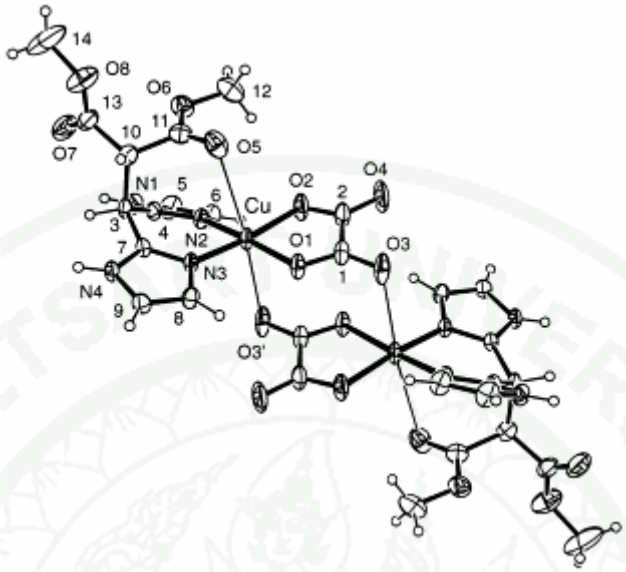

Figure 3 Perspective view and atomic numbering of the $[Cu_2(BIBM)_2(C_2O_4)_2]$ dimeric units. Carbom symbol are omitted for clarity.

Source: Núñes *et al.* (2001)

atoms from a BIBM molecule. This approximately square-planar coordination is octahedrally extended by weak apical contacts to two oxygen atoms (one from a carboxymethyl group, the other from the oxalate ion). The oxalate ligand is not planar. Magnetic susceptibility measurements in the range 1.8-200K show very weak antiferromagnetic exchange between the copper(II) ions. The diffuse reflectance spectrum of the title compound exhibits a very broad absorption in the visible region with a maximum centered at ca 16,900 cm^{-1}, which is consistent with the presence of very elongated $CuN_2O_2O_2'$ chromophores (Núñes *et al.*, 2001).

The molecular structure of $[Cu_2(DACO)_2(\mu\text{-ox})Br_2]\cdot CH_3OH$, where DACO=1,5-diazacyclooctane consists of two identical Cu(II) centers bridged by a planar bis(didentate) oxalate ligand. Each Cu(II) center is penta-coordinated to two nitrogen atoms of DACO, two oxygen atoms of the oxalate group, and one bromide

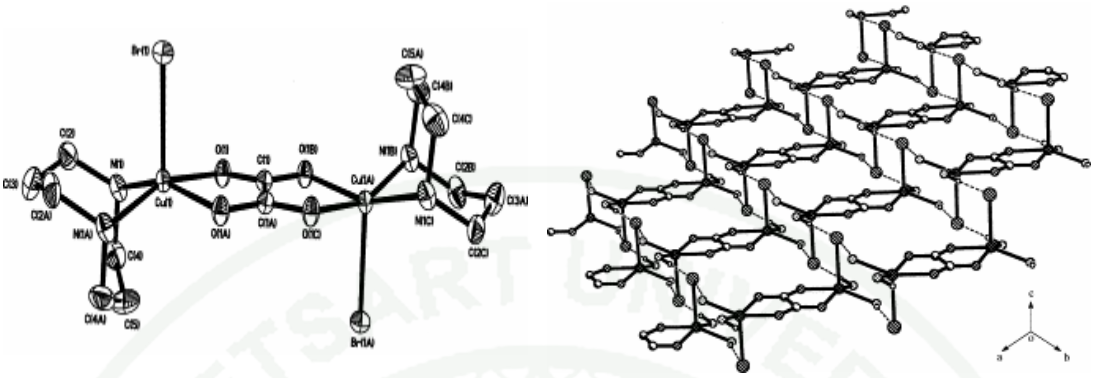

(a) (b)

Figure 4 ORTEP drawing (30% thermal ellipsoid probability) of (a) $[Cu_2(DACO)_2(\mu\text{-}ox)Br_2]$ unit and (b) packing diagram in the unit cell showing the step-like structure .

Source: Du *et al.* (2002)

ion (Figure 4a). The coordination geometry around each copper ion is square-pyramid. The molecules are assemble into a two-dimensional step-like extended network through hydrogen bond (Figure 4b). The magnetic susceptibility indicates that this compound is anti-ferromagnetic coupling (Du *et al.*, 2002).

The crystal structures, spectroscopic properties and magneto-structural correction of the complex type $[Cu_2(dpyam)_4(\mu\text{-}C_2O_4)X_2]\cdot nH_2O$ where X = ClO_4, BF_4, PF_6, $[Cu_2(dpyam)_2(\mu\text{-}C_2O_4)(NO)_3(Y)_2]$ where Y = $(CH_3)_2SO$, $(CH_3)_2NCOH$ and $[Cu_2(dpyam)_2(\mu\text{-}C_2O_4)(Z)_2]_n$ where z = Cl, n=0 and z= CF_3SO_3 n>1 were studied. Oxalate ligands in those complexes act as bis-chelate bridge. The coordination geometry of copper ion in these complexes is distorted octahedral except $[Cu_2(dpyam)_2(\mu\text{-}C_2O_4)Cl_2]$ which is square pyramidal (Figure 5a-6b). A very weak ferromagnetic interaction between the Cu (II) ions was found in $[Cu_2(dpyam)_4(C_2O_4)](ClO)_4\cdot 3H_2O$ and $[Cu_2(dpyam)_4(C_2O_4)](BF_4)_3\cdot 3H_2O$ while strong antiferromagnetic interaction was found in the rest of these complexes (Sujittra, *et al.*, 2003, 2006).

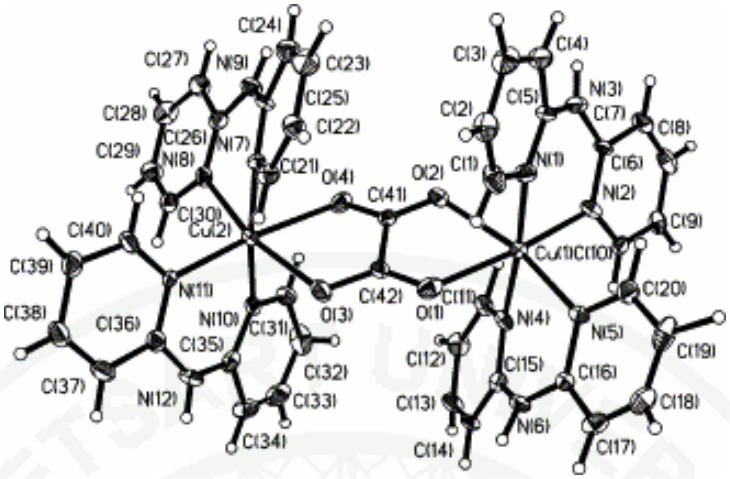

(a)

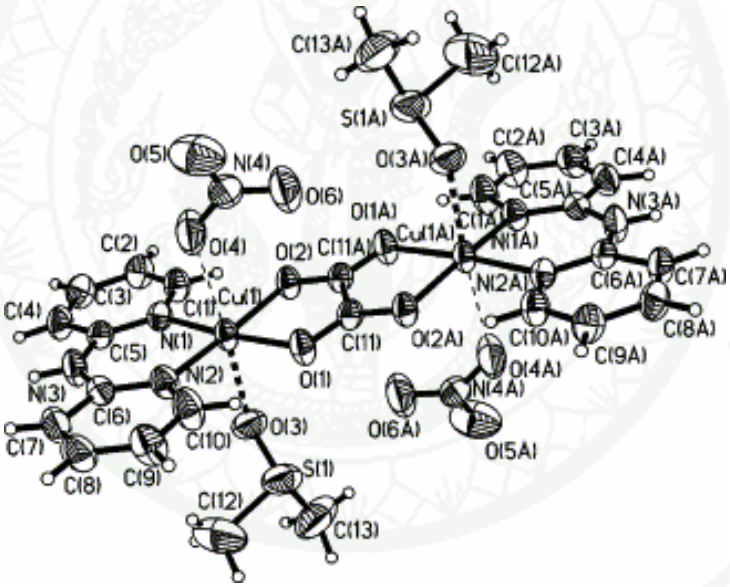

(b)

Figure 5 ORTEP 50% probability plot of the cation in (a) $[Cu_2(dpyam)_4(C_2O_4)](BF_4)_2(H_2O)_3$ and (b) $[Cu_2(dpyam)_2(C_2O_4)(NO_3)_2((CH_3)_2SO)_2]$. Atoms with an 'A' are generated by an inversion centre.

.

Source: Sujitra, *et al.*, (2003)

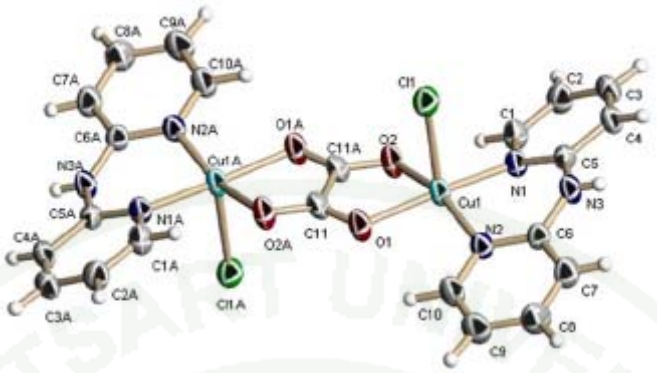

(a)

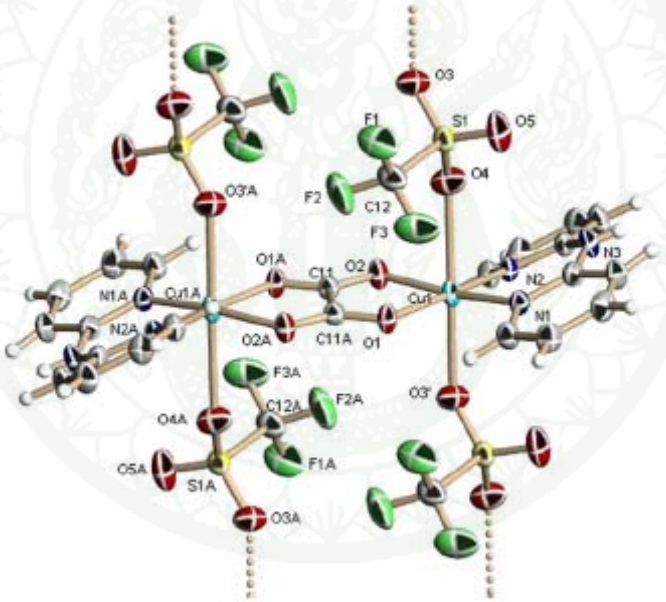

(b)

Figure 6 An ORTEP 50% probability plot of (a) $[Cu_2(dpyam)_2(\mu\text{-}C_2O_4)(CF_3SO_3)_2]_n$ and (b) $[Cu_2(dpyam)_2(\mu\text{-}C_2O_4)Cl_2]$

Source: Sujittra *et al.* (2006)

Three complexes of formula $[Cu_2(bpy)_2(H_2O)_2(C_2O_4)]X_2 \cdot [Cu(bpy)(C_2O_4)]$ (bpy = 2,2′-bipyridine; $C_2O_4^{2-}$ = oxalate, X= NO_3^-, BF_4^- or ClO_4^- were synthesized. Their structures consist of cationic centrosymmetric dinuclear $[Cu_2(bpy)_2(H_2O)_2(C_2O_4)]^{2+}$ units, neutral mononuclear $[Cu(bpy)(C_2O_4)]$ entities and either NO_3^-, BF_4^- or ClO_4^- as counter ion . Each copper atom of the dinuclear species is in a square pyramidal environment with two oxalate oxygen and two bipyridine nitrogen atoms as a base and a water molecule at the apical position. The copper atom of the mononuclear complex is in a slightly tetrahedrally distorted square comprised of two bipyridine nitrogen and two oxalate oxygen atoms (Figure 7). Variable-temperature (20-300 K) magnetic susceptibility measurements revealed a strong antiferromagnetic interaction within the dinuclear unit (Gleizes *et al.*, 1992).

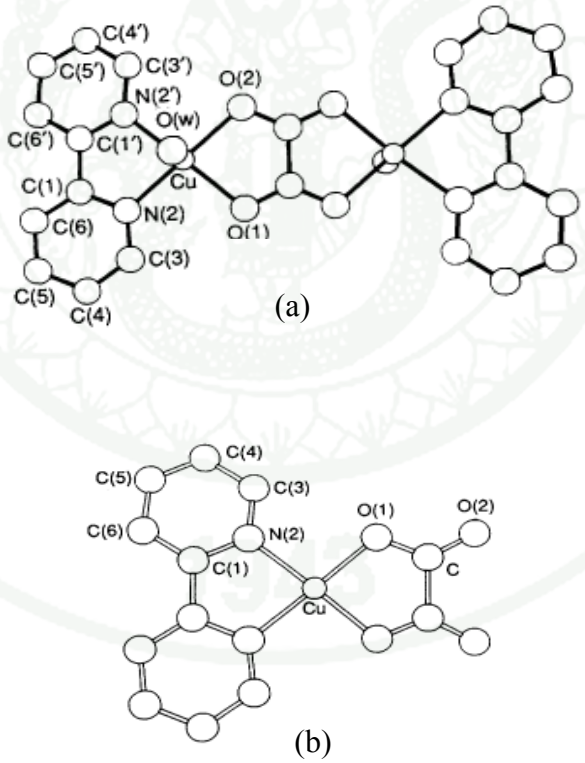

Figure 7 The structure view of (a) centrosymmetric dinuclear cationic complex $[Cu_2(bpy)_2(H_2O)_2(C_2O_4)]^{2+}$ and (b) mononuclear unit of $[Cu_2(bpy)_2(C_2O_4)]$.

Source: Gleizes *et al.* (1992)

Many research involve the studies of the role or effect of alpha-diimine chelating bidentate ligands, especially 2,2′-bipyridine (bpy) and 1,10-phenanthroline (phen), on the stability of polynuclear structures as well as coordination behavior of the copper ions. Two μ-oxalato binuclear copper(II) complexes, [{$Cu(NO_3)(H_2O)(bpy)_2$}(ox)] **(1)** and [{$Cu(dien)$}$_2$(ox)]$(NO_3)_2$ **(2)** where ox = oxalate, dien = diethylenetriamine and bpy = 2,2′-bipyridine were synthesized. The molecular structure of **1** consists of centrosymmetric binuclear neutral entities [$(bipy)(H_2O)(NO_3)Cu(C_2O_4)$ $Cu(NO_3)(H_2O)(bipy)$] held together by hydrogen-bond O_w–H···$O_{nitrate}$ and π–π interactions involving the aromatic rings of the bipy ligands (Figure 8a). The planar oxalato group, with a center of symmetry lying in the middle of the C–C bond, bridges the two copper atoms in the usual bis(bidentate) fashion: each copper atom is bound to two oxygen atoms from the two different carboxylic groups, with a Cu–Cu distance across the dimeric unit of 5.143 Å. The "bite" angles of bpy and oxalate are 82.4 and 85.0, respectively which are in good accord with the expected values. The structure of 2 is made up of non-coordinated nitrate anions and asymmetric binuclear cations in which copper atoms are in a distorted square pyramidal coordination with one oxygen atom of the oxalate ligand filling the apical position (Figure 8b). The two compounds exhibit antiferromagnetic exchange (Oscar *et al.*, 1999). The structure of $[Cu_2(\mu\text{-}C_2O_4)(bpy)_2(H_2O)_2(NO_3)_2]$ consists of The structure consists of centro symmetric $[Cu_2(\mu\text{-}C_2O_4)(bpy)_2(H_2O)_2(NO_3)_2]$ molecules with each Cu(II) ion in a distorted octahedral environment: two nitrogen atoms from bpy, two oxygen atoms from the oxalate ion in the basal plane and two oxygen atoms from H_2O and the nitrato group in the two axial positions (Figure 9) (Tang *et al.*, 2000).

Blue crystals of $\{[Cu(ox)(bpy)]\cdot 2.5H_2O\}_n$ (where ox=oxalate dianion, bpy= 2,2′-bipyridine) were obtained by slow evaporation at room temperature of an aqueous solution containing 2,2′-bipyridine, potassium oxalate monohydrate and $Cu(NO_3)_2\cdot 3H_2O$ in a molecular ratio 2:1:2. The coordination sphere of the copper atom can be described as a very elongated octahedron. The pyridine and the oxalate ligands are both bidentate in the equatorial plane of copper. The tetragonal distorted coordination around the copper is completed by weak axial contacts a coordinated oxygen-oxalato

(a)

(b)

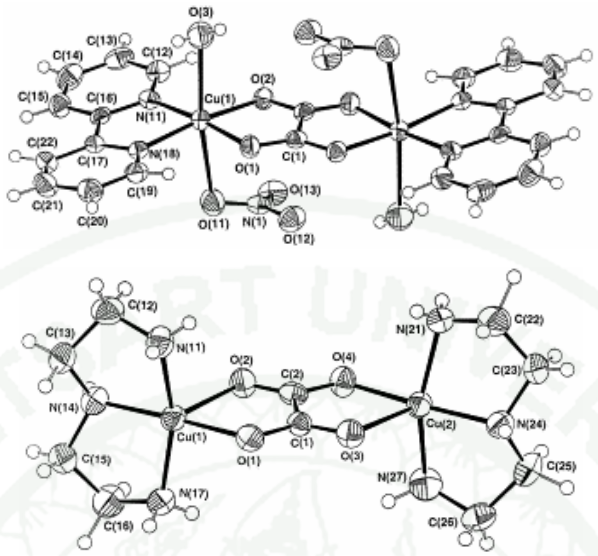

Figure 8 Thermal ellipsoid plot (50% probability level) for (a) dimeric unit [{Cu(NO_3)(H_2O)(bipy)}$_2$(ox)] and (b) [{Cu(dien)}$_2$(ox)]$^{2+}$ cation with a labeling scheme.

Source: Oscar *et al.* (1999)

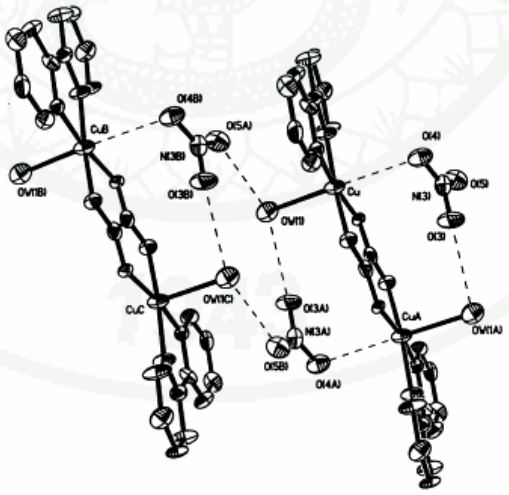

Figure 9 Hydrogen bonds plane formed by intramolecular and intermolecular hydrogen bonds in [Cu_2(μ-C_2O_4)(bpy)$_2$(H_2O)$_2$(NO_3)$_2$].

Source: Tang *et al.* (2000)

atom and to an uncoordinated one from two equivalent units (Figure 10). The magnetic properties show the occurrence of alternating-ferroantiferromagnetic interaction (Castillo *et al.*, 2001).

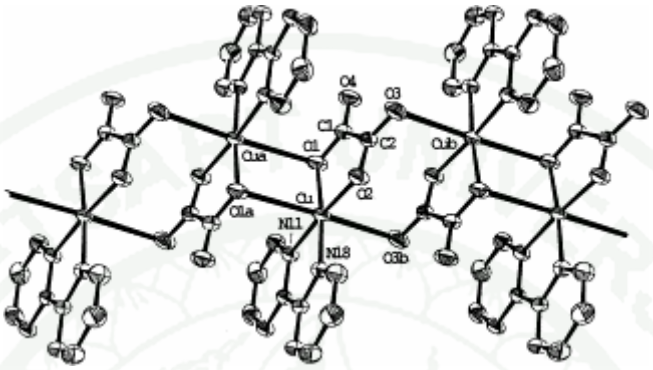

Figure 10 ORTEP diagram of the polymeric chain in $\{[Cu(ox)(bpy)]\cdot 2.5H_2O\}_n$

Source: Castillo *et al.* (2001)

Phenanthroline is an alpha-diimine ligand which is resemble to the 2,2′-bipyridine but more rigid. The plan is usually stabilized the crystal structure through the π-π stacking of aromatic rings. For the dimeric complex $[Cu_2(\mu\text{-}C_2O_4)(Cl_2)(phen)_2]$, the copper (II) ion is in distorted trigonal-bipyramidal coordination geometry (Figure 11). There is π-π stacking interaction along the *c*-axis (Wang *et al.*, 2007).

The hexanuclear Cu(II) complex, $[Cu_6(bpy)_6(\mu\text{-}O_2CC_2H_5)_7\,(H_2O)_2](PF_6)_5 \cdot 2H_2O$ is constructed from three different dinuclear units connected to each other via two *syn–anti*-μ_3-$\eta^1;\eta^2$ carboxylato bridges. All copper(II) ions are in the distorted square-pyramidal geometry. Two terminal dinuclear units are similar in structure in which both Cu(II) ions are doubly bridged by the *syn–syn* carboxylato anions, while those of the central dinuclear entity are triply bridged by two μ_3-$\eta^1;\eta^2$ carboxylato anions via monoatomic bridging fashion and one *syn–syn* carboxylato anion (Figure 12). The magnetic susceptibility of this compound was measured at 5-350K showing a weak antiferromagnetic interaction between the Cu(II) centers (Boonmark *et al.*, 2008).

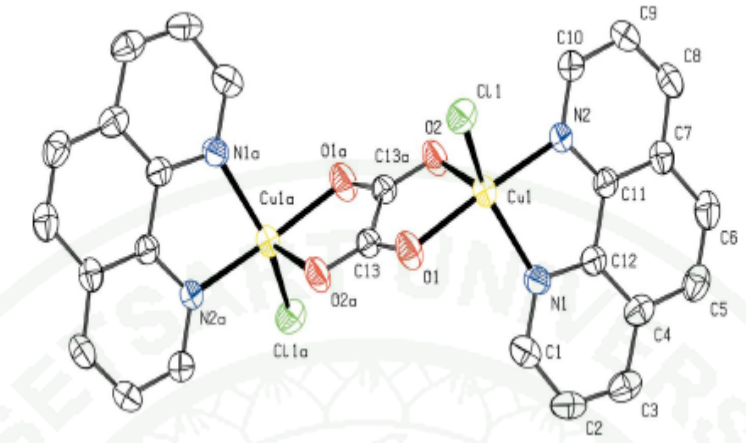

(a)

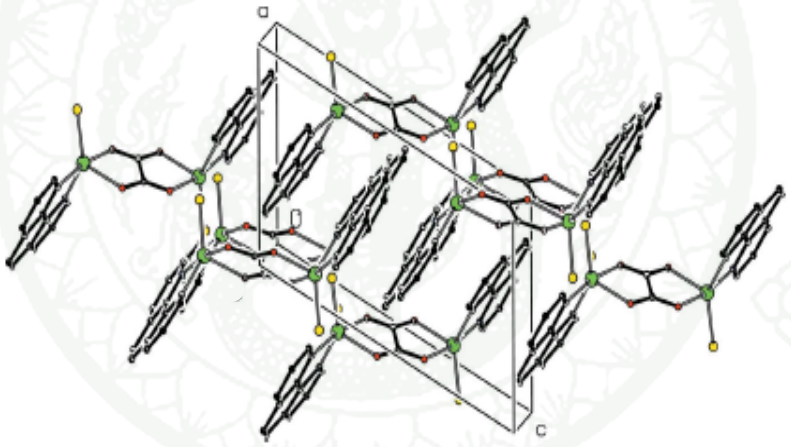

(b)

Figure 11 (a) The molecular structure of $[Cu_2(\mu\text{-}C_2O_4)(Cl_2)(phen)_2]$, with displacement ellipsoids drawn at the 50% probalility level. (b) Part of the crystal structure of $[Cu_2(\mu\text{-}C_2O_4)(Cl_2)(phen)_2]$. Hydrogen atoms are omitted for clarity.

Source: Wang *et al.* (2007)

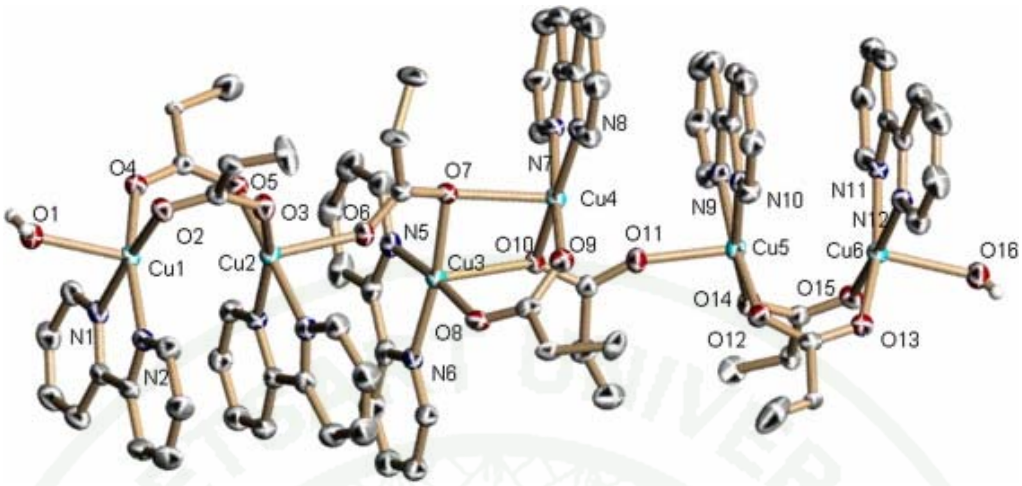

Figure 12 Plot of $[Cu_6(bpy)_6(\mu\text{-}O_2CC_2H_5)_7(H_2O)_2](PF_6)_5 \cdot 2H_2O$. Hydrogen atoms in bpy and the non coordinating anions and water molecules are omitted for clarity.

Source: Boonmark *et al.* (2008)

The metal (II) succinate complexes

Succinate dianions (suc, $C_4H_4O_4^{2-}$), which is a α,ω-alkanedicarboxylates, have good conformational freedom and prossess some desirable features such as being a versatile ligand because of the four-electron donor oxygen atoms. They carry, their linking ability between inorganic moiety and the generation of secondary building units through their carboxylate group. Among the coordination modes of succinate ligand, the bidentate chelating and bridging modes (Pajunen *et al.*, 1996; Xiang *et al.*, 1998; Subramanian *et al.*, 1998; Ang *et al.*, 2004; Kumar *et al.*, 2006; Vuckovic *et al.*, 2008; Zheng *et al.*, 2004; Padmanabha *et al.*, 2005; Ang and Sun, 2005; Vaidhyanathan *et al.*, 2002) are more common compared to the monodentate coordination. Recently; some complexes containing the succinate counter ions have been reported (Ying *et al.*, 2004; Mao *et al.*, 2004; Xu *et al.*, 2007; Jin and Chen, 2007; Ghosh *et al.*, 2006). Some of these complexes have shown the simultaneous presence of succinate as a ligand and a counter ion (Zheng *et al.*, 2002; Padmanabha *et al.*, 2005) or as a ligand and a H_2suc molecule (Zheng *et al.*, 2002). Several divalent

metal ions can coordinate to succinate ligands such as Co^{2+}, Ni^{2+}, Zn^{2+}, Cd^{2+}, Cu^{2+},Mn^{2+} (Zheng *et al.*, 2002, Vuckovic *et al.*, 2008; Zhou *et al.*, 2005; Demir *et al.*, 2010; Zhou *et al.*, 2005; Shyu and LaDuca, 2009; Mao *et al.*, 2004). In this review, several reports involve the function of succinate ligand as bidentate chelate and bidentate bridging are presented here.

$[Cu(C_4H_4O_4)(C_4H_{13}N_3)]_n$ has a polymeric structure in which the Cu atom is coordinated by three N atoms from the diethylenetriamine molecule ($C_4H_{13}N_2$), two oxygen atoms from the succinate ion and one oxygen atom from the succinate ion of the adjacent complex unit. The coordination polyhedron around the Cu atom can be regarded as a severely distorted octahedron (Figure 13a). The chains are joined together by hydrogen bonds between the amine H atoms and the O1 and O4 atoms of the succinate ion (Figure 13b)(Pajunen *et al.*, 1996).

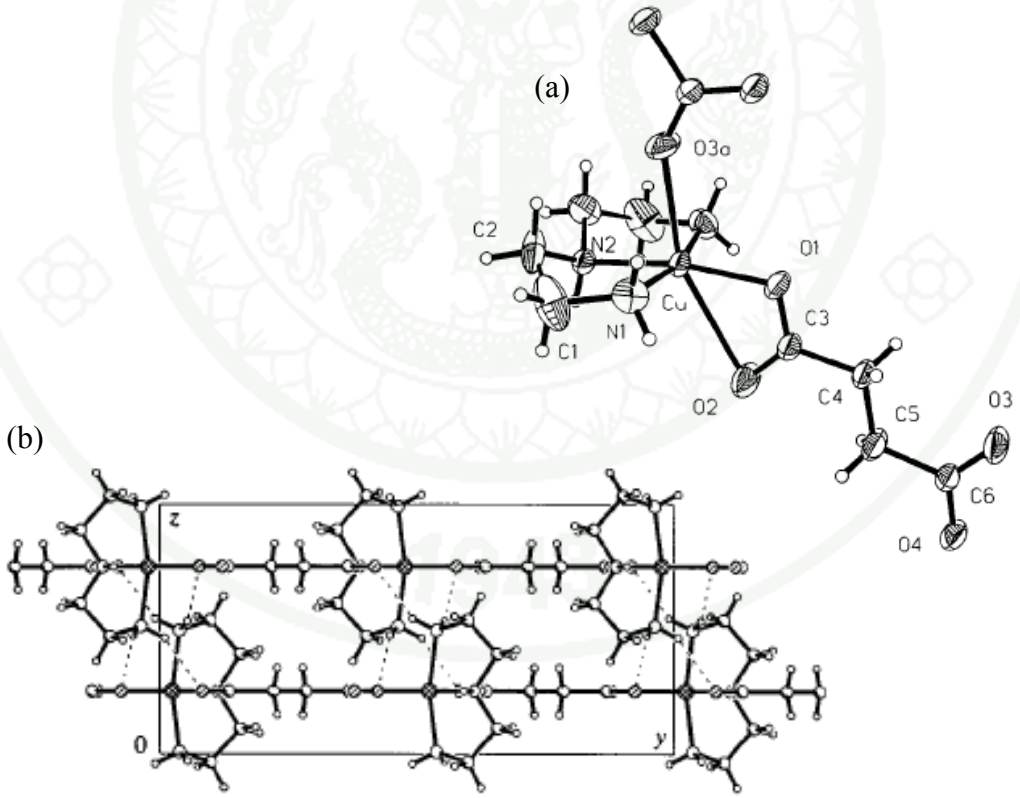

Figure 13 (a) The structure of $[Cu(C_4H_4O_4)(C_4H_{13}N_3)]_n$ showing 50% probability displacement ellipsoids and (b) packing diagram viewed along the a axis.

Source: Pajunen *et al.* (1996)

The Cu ions in $[Cu_2(C_4H_4O_4)_2(C_7H_6N_2S)_4]$, where $C_7H_6N_S$ = 2-amino-1,3-benzothiazole, are enclosed in a 14-membered ring. They adopt a distorted square-pyramidal coordination. Two nitrogen atoms of 2-amino-benzothiazole ligands ($C_7N_6N_2S$) and two oxygen atoms of succinate ligands form a square planar cis arrangement. The remaining oxygen atoms of the carboxylate groups complete the sixfold coordination of the Cu atoms (Figure 14). The conformations on the two terminal C-C bonds of the succinate ion are different. On the C18-C19 bond, the conformations are synperiplanar and antiperiplanar [torsion angles O11-C18-C19-C9i = 5.0 (6)° and O12-C18-C19-C9i = -175.2 (4)°], and on the C8-C9 bond, the conformations are antiperiplanar and synclinal [torsion angles O1-C8-C9-C19 = 151.4 (4)°and O2-C8-C9-C19 = 32.0 (6)°]. The structure illustrates the influence of weak hydrogen bonds on the conformation of the aliphatic chain and the differentiation of Cu-O bond lengths (Sieroń *et al.*, 1999).

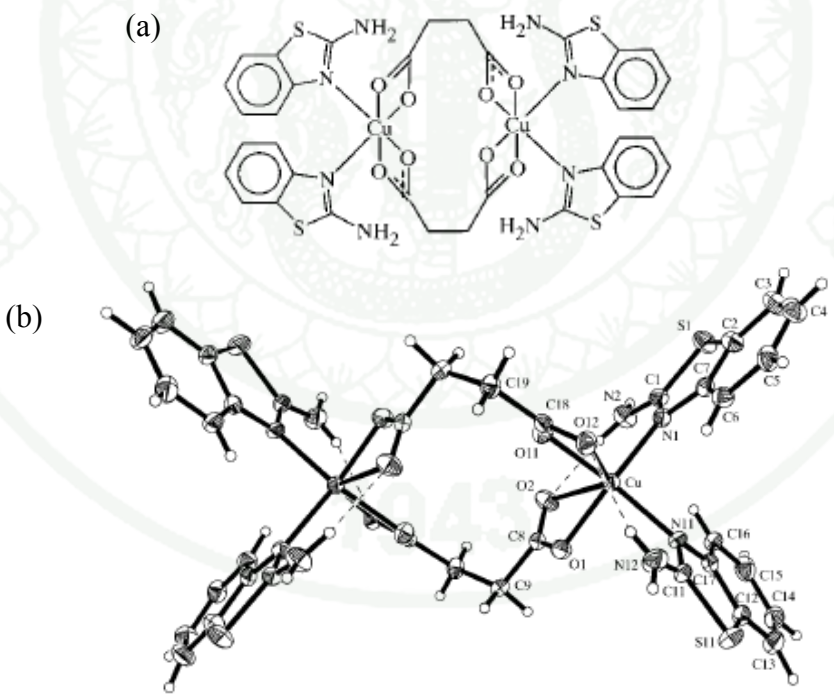

Figure 14 (a) scheme of $[Cu_2(C_4H_4O_4)_2(C_7H_6N_2S)_4]$ and (b) view of the molecule of $[Cu_2(C_4H_4O_4)_2(C_7H_6N_2S)_4]$.

Source: Sieroń *et al.* (1999)

The copper ion is chelated by a 2,2′- bipyrimidine (bpm) ligand and a succinate anion in the basal plane. Water molecule in the apical position completes the slightly distorted square-pyramidal coordination geometry. Extensive O—H···O and O—H···N hydrogen bonding is present in the crystal structure (Figure 15). The coordination mode of the succinate ligands is bidentate chelate forming a seven-membered ring (Ke *et al.*, 2009)**.**

The succinate ligands in the complexes mentioned above behave as chelate forming four-or seven-memberwd ring. This ligand not only can chelate metal ions but also can bridge metal ions. In $[Cu(C_4H_4O_4)(C_3H_4N_2)_2]_n$, the Cu^{II} ion assumes a distorted CuO_2N_2 square-planar coordination geometry formed by two succinate dianions and two imidazole molecules. The Cu^{II} complex units are bridged by the succinate dianions, forming polymeric chains (Figure 16) (Wang *et al.*, 2006).

Each Cu atom in $\{[Cu(C_4H_4O_4)(H_2O)(NH_3)]\cdot 2H_2O\}_n$ us coordinated by two oxygen atoms of two different succinato ligands, one water oxygen atom and one ammonia nitrogen atoms to complete CuO3N square plane. The succinate dianions are maximally extended (C-C-C-C torsion angle is 177.44°) and link Cu atoms in bismonodentate fashion to generate infinite chains along [101] (Figure 17)(Jin *et al.*, 2006). The complex $\{Cu(C_4H_4O_4)(H_2O)_2]\cdot 2H_2O\}_n$ is a one-dimensional coordination chain of copper(II) bridged through the succinate ligand aligned approximately along the crystallographic *ac* diagonal. In the chain, each Cu(II) is ligated with two bridging succinate ligands and two water molecules in square planar environment with CuO4 chromophore (Figure 18). Hydrogen bonding between coordinated water (O1w) and succinate oxygen (O1) of adjacent chains connect copper atoms resulting a layer in ab plane. The layers are held together through bridging succinate ligands leading to an overall 3D solid state structure with small channels. The low temperature magnetic study reveals significant antiferro-magnetic interactions between the copper centers (Ghoshal *et al.*, 2007).

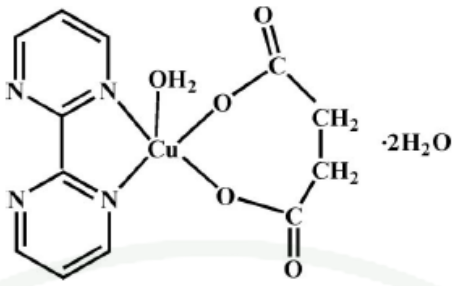

Figure 15 Molecular view of $[Cu(C_4H_4O_4)(C_8H_6N_4)(H_2O)]\cdot 2H_2O$ showing the atom-labeling scheme.

Source: Ke *et al.* (2009)

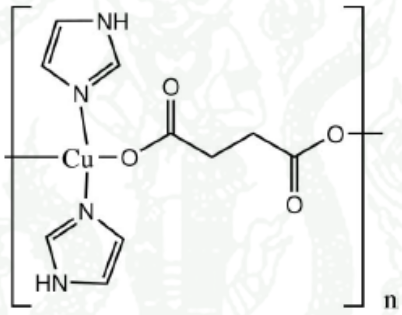

Figure 16 Molecular view of $[Cu(C_4H_4O_4)(C_3H_4N_2)_2]_n$ showing the atom-labelling scheme.

Source: Wang *et al.* (2006)

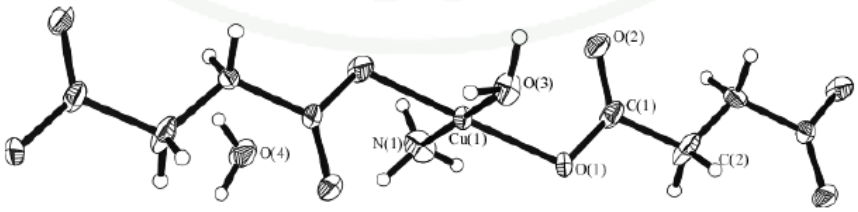

Figure 17 ORTEP view of $\{[Cu(C_4H_4O_4)(H_2O)(NH_3)]\cdot 2H_2O\}_n$

Source: Jin *et al.* (2006)

Figure 18 ORTEP diagram of the 1D coordination chain of $[Cu_4(succinato)(tpmc)_2](ClO_4)_6 \cdot 2C_2H_5OH \cdot 4H_2O$ with atom labeling scheme.

Source: Ghoshal *et al.* (2007)

The molecular structure of the tetranuclear complex unit $[Cu_4(succinato)(tpmc)_2]^{6+}$ in $[Cu_4(succinato)(tpmc)_2](ClO_4)_6 \cdot 2C_2H_5OH \cdot 4H_2O$ is presented in Figure 19. In the unit cell, the tetranuclear $[Cu_4(succinato)(tpmc)_2]^{6+}$ cation is positioned on the inversion centre at 1/2 1/2 1/2. Consequently, the two binuclear complex units are equivalent. Each copper(II) ion is pentacoordinated with four nitrogen atoms (two from adjacent pyridyl groups and two from the cyclam moiety) and oxygen atom from the succinate anion. The two metal centres in the complex are bridged with bidentate carboxylate group of the succinate anion. The other bidentate carboxylate group of same succinate ligand also bridge other two copper ions. Therefore each succinate ligand bridges four copper atoms (Vučković *et al.*, 2008).

Two neutral polymeric chains with the formula $[Cu_2(\textit{trans}\text{-L})(suc)(H_2O)_2]_n \cdot 2nH_2O$ (L=oxap, N,N′-bis(2-aminopropyl)oxamide and L= oxen, N,N′-bis(2-amino ethyl) oxamide) were synthesized from the mononuclear precursors $Cu(oxen) \cdot 2H_2O$ and Cu(oxap). The succinate ligands act as spacer ligand connecting two building blocks $[Cu_2(trans\text{-L})]^{2+}$ to form the infinite zigzag chains. The copper(II) atom is located in a square pyramidal environment of N_2O_3. The basal plane consists of N_2O from L and one oxygen from succinate while the axial position is occupied by a water molecule. The spacer succinate ligand adopts the trans-configuration bound to the copper atom in the end-to-end bis-monodentate bridging mode through two oxygen atoms, each from a carboxyl group (Figure 20).

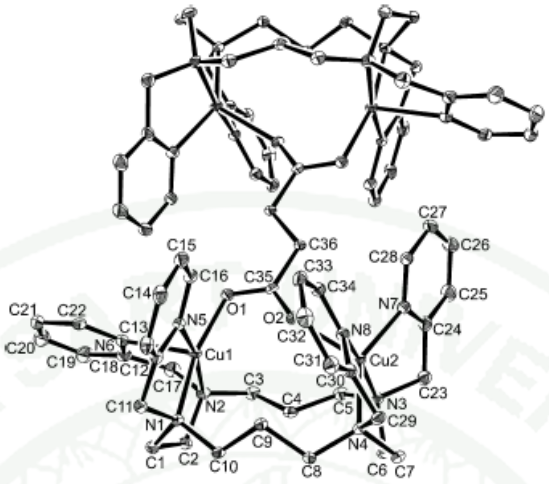

Figure 19 Molecular structure of the $[Cu_4(succinato)(tpmc)_2]^{6+}$ complex cation in $[Cu_4(succinato)(tpmc)_2](ClO_4)_6 \cdot 2C_2H_5OH \cdot 4H_2O$.

Source: Vučvić *et al.* (2008)

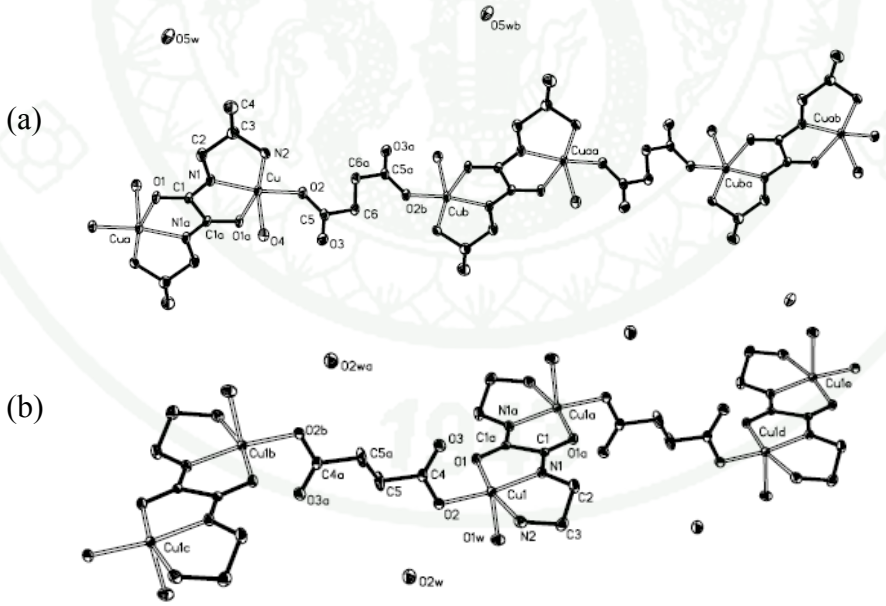

Figure 20 Crystal structure of (a) $[Cu_2(trans\text{-}oxap)(suc)(H_2O)_2]n \cdot 2nH_2O$ and (b) $[Cu_2(trans\text{-}oxen)(suc)(H_2O)_2]n \cdot 2nH_2O$. Hydrogen atoms are omitted.

Source: Zhang *et al.* (2001)

The absorption bands of succinate fall in the 1550–1580 and 1350–1340 cm^{-1} regions, corresponding to the asymmetric and symmetric vibrations of the carboxylate moiety, respectively. TGA results showed that both compounds lost the water molecules from 100 to 140 °C. When the temperature comes up to about 247 °C, the weight lost sharply in a very narrow temperature range, which meant the breakdown and decomposition of the polymeric chains. The final residue was black and amorphous (Zhang *et al.*, 2001).

Two coordination polymers, $[Cu_2(H_2O)_2(suc)_2]\cdot 2H_2O$ **(1)** and $[Cu_4(pmo)_4(suc)_2]\cdot H_2O$ **(2)** (suc = succinate, Hpmo = 2-pyridine-methanol), were obtained by changing the amounts of Hpmo used in the reactions. Hpmo not only behaves as a versatile ligand in compound **2**, but also acts as an important buffer in the formation of compound **1**. Structure of **1** consists of a H-bonded 2D open framework assembled from a 1D coordination polymer that is constructed from a succinate-bridged dinuclear framework with a Cu…Cu distance of 2.60 (1) Å. Four *syn, syn* $\eta^1:\eta^1:\mu_2$ carboxylate groups bridge the two Cu(II) atoms to form a paddle-wheel structure. Each Cu is also coordinated to a terminal water molecule to result in a slightly distorted square pyramidal geometry. Adjacent binuclear units were connected by a succinate ligand to give a one-dimensional chain running along the *a*-axis. The adjacent chains are shifted by 1/2a along the *a* axis. In addition, the adjacent chains are connected to produce a 2D sheet in the *ab* plane via four kinds of hydrogen bonds among guest and coordinated H_2O molecules at Cu(II) atoms and oxygen atoms of carboxylates (Figure 21a). Although one of the starting materials, Hpmo, is not contained in the product, it plays a very important buffer role in the process of crystal growing. In compound **2**, all Cu(II) ions are found in the same slightly distorted square-planar NO_3 coordination environment, involving one nitrogen atom, one oxygen atom from one pmo, and another oxygen atom from a different pmo ligand, while the fourth coordinate position is occupied by an oxygen atom from the carboxylate group of the succinate ligand. Each oxygen atom of pmo bridges two neighboring Cu(II) atoms. As a result, an open cubane-like Cu_4O_4 core is generated (Figure 21b). The bridged Cu…Cu separation is 3.07 (1), while the unbridged Cu…Cu separation is 3.62(1) Å. The open cubane is linked to four neighboring tetrameric units by succinate ligands to form a 2D $4,8^2$ sheet with two different large

metallacycles. A careful examination shows that all three starting materials have undergone different transformations in the two resulting structures of **1** and **2**: (1) in the dimer **1**, Cu atoms are separated by a short copper–copper distance 2.60 (1) Å, while in **2**, we observe an open cubane-like Cu_4O_4 core; (2) the succinate group bridged two dimers in a *syn, syn* η^1:η^1:μ_2 manner and bridged adjacent cubanes with $\mu_{1,6}$ model in **1** and **2**, respectively; (3) Hpmo functions as a buffer in the formation of **1** and as a deprotonated ligand in **2**. A variable temperature magnetic susceptibility investigation shows that the dimeric copper (II) in the complex **1** are strong antiferromagnetically exchanges and there are ferromagnetic couple among adjacent copper (II) ions in the tetramer of complex **2** (Ang, *et al.*, 2004).

A mixed ligand and dimeric Cu^{II} complex $[(phen)_2Cu(\mu\text{-}L)Cu(phen)_2]$ $L \cdot 12.5H_2O$ (H_2L = succinic acid) containing bridging succinate moiety and also non-coordinated succinate dianion was prepared from polymeric Cu(II) succinate by nucleophilic reaction with *o*-phenanthroline (*phen*) followed by depolymerization. The complex crystallizes in triclinic crystal system and is composed of succinate bridged $[(phen)_2Cu(\mu\text{-}L)Cu(phen)_2]^{2+}$ complex cations, noncoordinated succinate anions and hydrogen bonded water molecules. Within the dimeric cationic unit, each of the Cu atoms is octahedrally coordinated by four nitrogen atoms of both *phen* ligands and both oxygen atoms of a carboxylate moiety of the bridging succinate group in chelating form (Figure 22). The intermolecular π-π stacking interactions are observed. In solid state a broad band at 710 nm was obtained, which is indicative of a tetragonal configuration around the copper (II) ion with CuN_4O_2 chromophoric group. This band is essentially due to $^2B_{1g} \rightarrow {}^2A_{1g}$ transition which, in comparison with the square planar complexes, occurs at lower energy region due to the energetically lifted d_z^2 orbital (Padmanabhan *et al.*, 2005).

Three isostructural polymers with formula $[M(suc)(bpmp)(H_2O)_2]_n$ (M=Co, **1** ; M=Ni, **2**; M=Cu, **3** and bpmp= bis(4-pyridylmethyl) piperazine) were prepared cleanly either by hydrothermal technique or via slow diffusion of aqueous solutions of

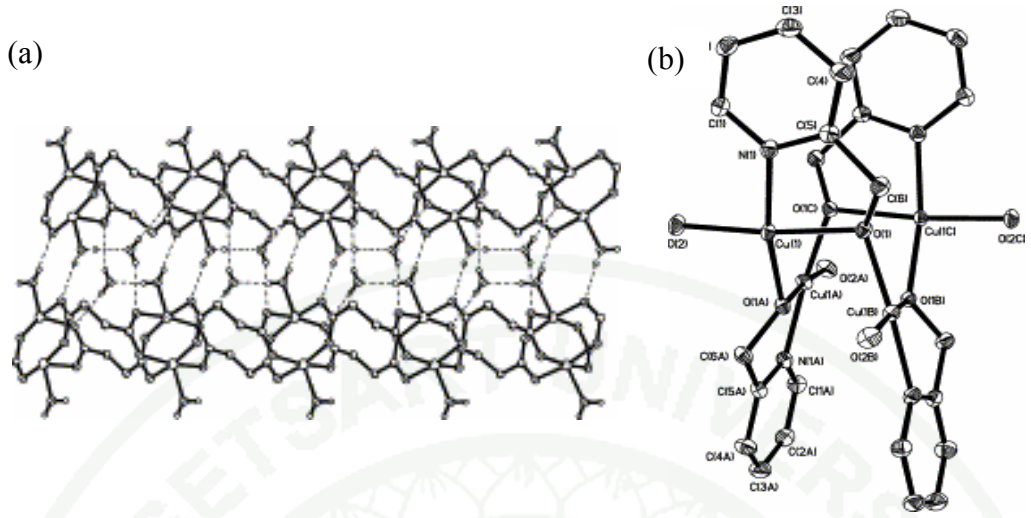

Figure 21 (a) View of the 1D dimer chain of $\{[Cu_2(H_2O)_2(suc)_2]\cdot 2H_2O\}$ down the *c* axis and (b) ORTEP drawing 30% of thermal ellipsoid probability of $[Cu_4(pmo)_4(suc)_2]\cdot H_2O$ with atom labeling scheme.

Source: Ang, *et al.* (2004)

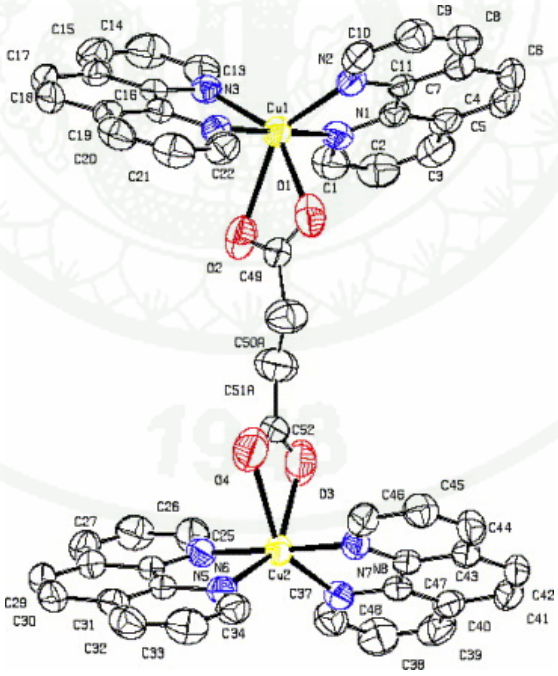

Figure 22 ORTEP view of the dinuclear $[(phen)_2Cu(\mu\text{-}L)Cu(phen)_2]^{2+}$ complex cation with displacement ellipsoids (45% probability).

Source: Padmanabhan *et al.* (2005)

the appropriate metal chloride and succinic acid with ethanolic solution of bpmp. The asymmetric unit of compound **1-3** are very similar and consist of a divalent metal ion whose coordination geometry is distorted octahedral. The equatorial plane are occupied by two trans aqua ligands and two oxygen atoms from two different succinate ligands. Pyridyl nitrogen atoms from two different bpmp ligands are situated in axial positions (Figure 23). The bis-bridging bismonodentate succinate anions forms one-dimensional $[M(suc)(H_2O)_2]_n$ chain motifs parallel to the *c* crystal direction. These chains are then connected into a two-dimension (4,4) rhomboid grid $[M(suc)(bpmp)(H_2O)_2]_n$ coordination polymer layer motif (Figure 24). While there is no direct covalent interaction between interpenetrated layers, structural stability is provided by hydrogen bonding between the aqua ligands in one layer and unligated carboxylate oxygen atoms belonging to suc ligands in another layer. These hydrogen bonding patterns construct supramolecular $[M(suc)(H_2O)_2]_n$ 1D chain patterns that course along the *b* crystal direction (Martin, *et al.*, 2008).

A red coordination polymers assembled by bridging succinate ligand, [Mn(dpdo) $(H_2O)_2$(suc)] was synthesized by the reaction of $MnCl_2 \cdot 6H_2O$, succinic acid and dpdo (4,4′-dipyridyl N,N′-dioxide). Its structure is isomorphous with the zinc derivative. The coordination sphere of the manganese (II) ions is definded by two atoms of coordinate aqua molecules and two carboxylate oxygen atoms of two succinate ligands in the equatorial plane and two oxygen donors of dpdo ligands in the apical position leading to a slightly distorted MnO_6 octahedron. The Mn ions are bridged by succinate ligand along the [001] direction,yielding a linear chain. These adjacent chains are further linked through dpdo, leading to a 2-D grid sheet, in which the dpdo adopts a trans connection fashion (Figure 25a). The two pyridyl groups of the dpdo ligand are completely coplanar, and it is nearly perpendicular to the 2-D sheet. No significant π-π stacking interactions are found between these dpdo molecules. These adjacent 2-D sheets are further connected through hydrogen bonds between the coordinated water molecules and bridging dpdo ligand or uncoorginated carboxylate oxygen, leading to a 3-D structure motif (Figure 25b) (Ang, *et al.*, 2004).

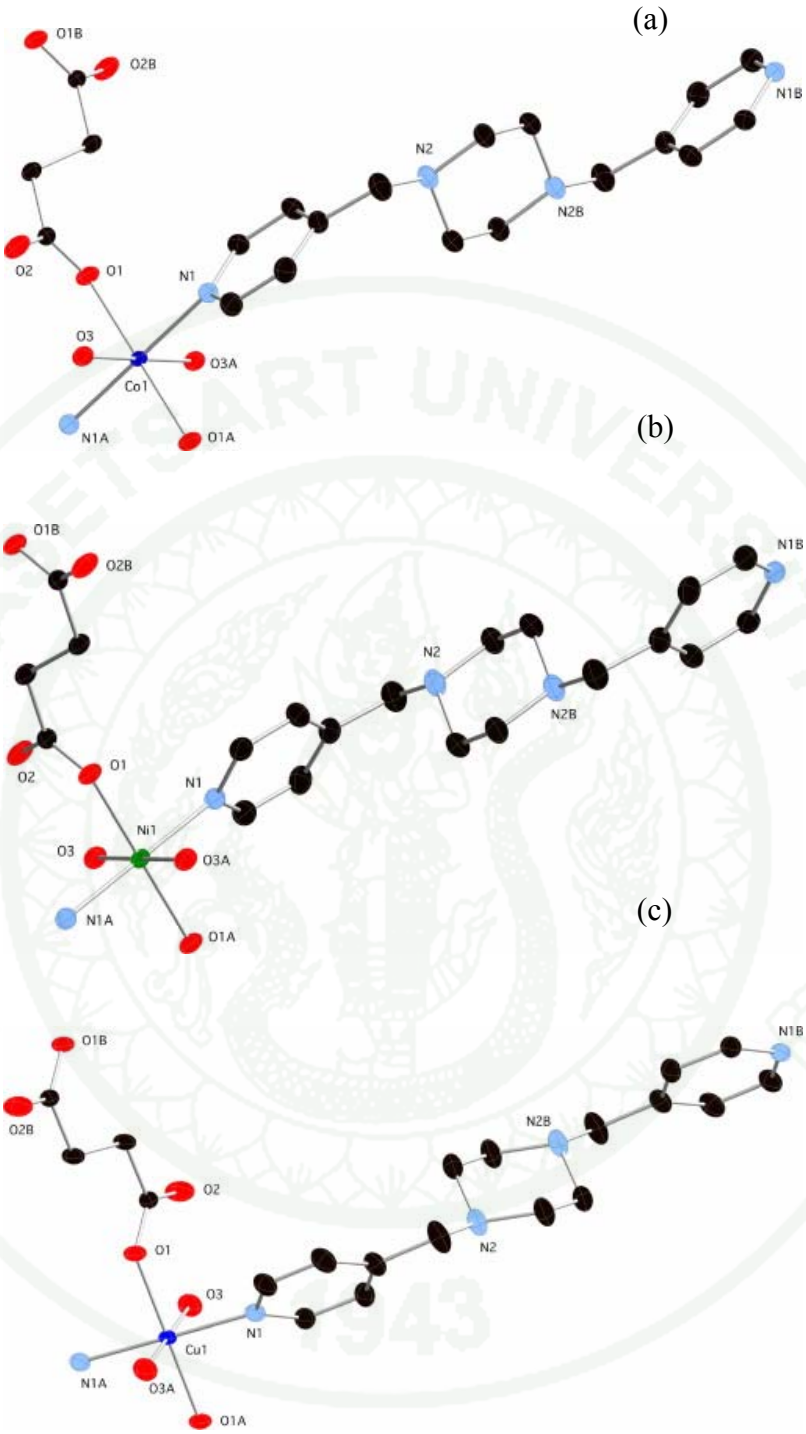

Figure 23 Coordination environment of (a) Co (b) Ni and (c) Cu with thermal ellipsoids drawn at 50% probability and partial atom numbering scheme.

Source: Martin, *et al.* (2008)

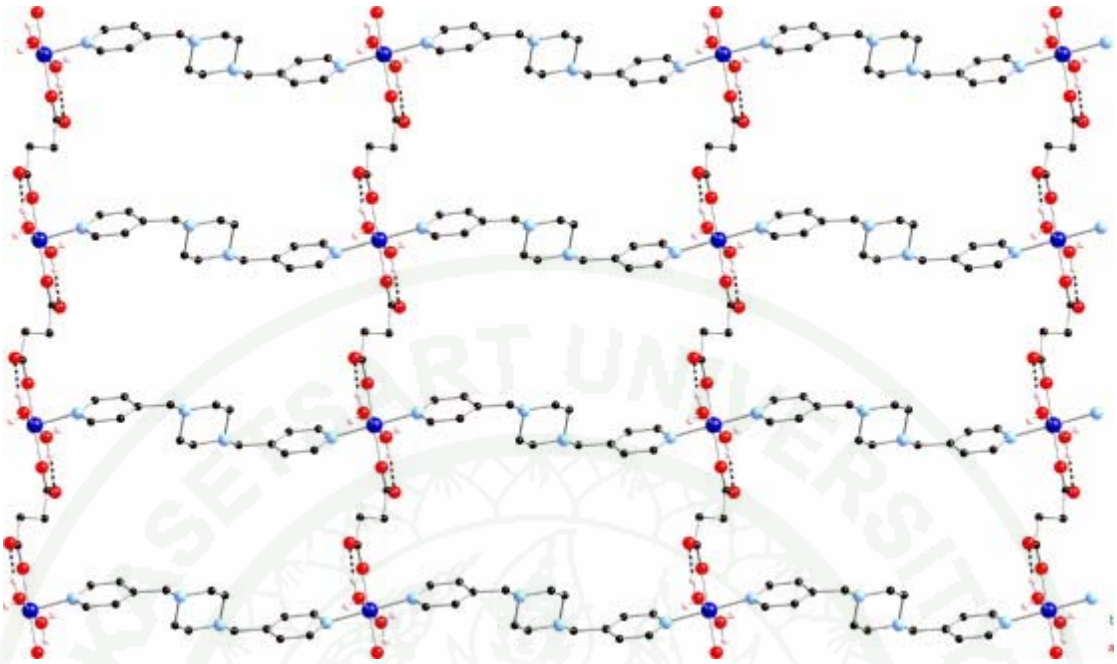

Figure 24 A single $[Co(suc)(bpmp)(H_2O)_2]_n$ layer. Hydrogen bonding is indicated as dashed lines.

Source: Martin, *et al.* (2008)

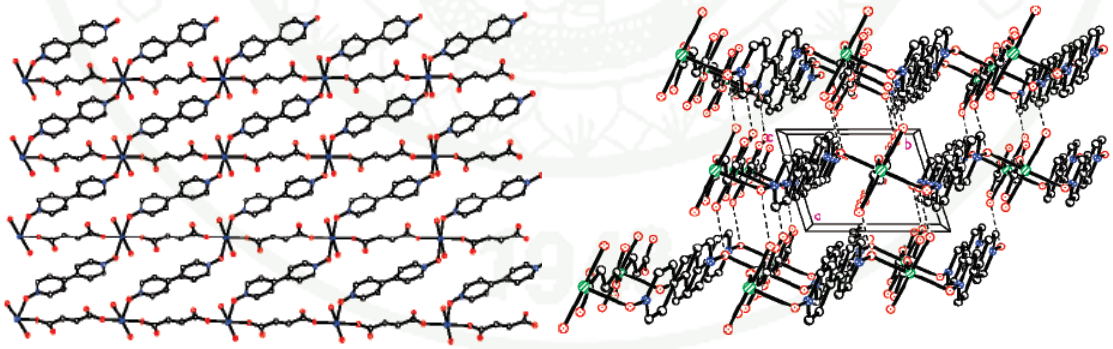

(a) (b)

Figure 25 (a) Packing view of the 2-D sheet in $M(dpdo)(H_2O)_2(C_4H_4O_4)$ and (b) down the a axis.

Source: Ang, *et al.* (2004)

Two coordination polymers $\{[Mn(C_{10}H_8N_2)(H_2O)_4](C_4H_4O_4)\cdot 4H_2O\}_n$ **(1)** and $[Mn_5(C_4H_4O_4)_4(O)]_n$ **(2)** were obtained from the hydrothermal reaction shown in Scheme F.

Scheme F

$$Mn(CH_3COO)_2\cdot 4H_2O + \underset{\text{Suc}}{C_4H_6O_4} + \underset{\text{4,4′-bpy}}{C_{10}H_8N_2} \xrightarrow[170°,\ 5\ \text{days}]{H_2O} \underline{\mathbf{1}}\ \text{yellow block crystal} + \underline{\mathbf{2}}\ \text{colorless crystals}$$

Compound **1** is a one-dimensional chain structure, which is further extended to two-dimensional supramolecular layer structure with hydrogen bond. The 4,4′-bipyridine bridges between manganese ions forming a 1D linear chain. Each manganese center displays distorted octahedral coordination geometry with four oxygen atoms of four aqua ligands in the square plane. The succinate counter ions are situated between the linear chains and formed hydrogen bond with the coordinatied aqua ligands (Figure 26a). During the synthesis of **1**, compound **2** which is a three-dimensional network composed of pentanuclear Mn(II) building units and succinate ligands. Mn(II) adopts distorted octahedral coordination mode and connects with six oxygen atoms. One Mn (2) ion connects with two Mn (2) ions and two Mn (3) ions with μ_3-oxygen atoms to form an interesting pentanuclear Mn(II) cluster. Bridging succinate anion and oxygen atoms connect such pentanuclear Mn (II) clusters to form a two-dimensional layer structure (Figure 26b). Such two-dimensional layers are connected by succinate ligands to form three-dimensional network (Xu *et al.*, 2007).

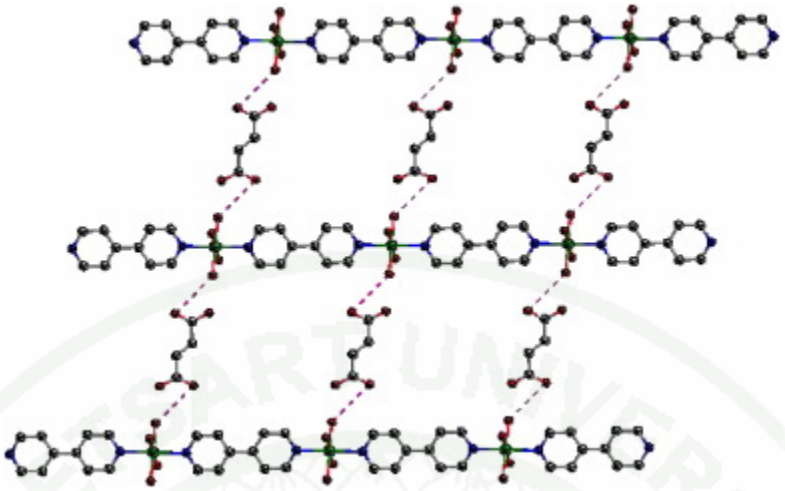

(a)

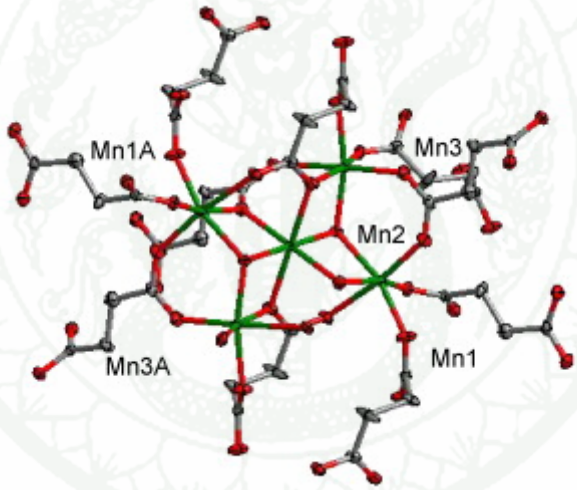

(b)

Figure 26 (a) The two-dimensional layer constructed by hydrogen bond of $\{[Mn(C_{10}H_8N_2)(H_2O)_4](C_4H_4O_4)\cdot 4H_2O\}_n$ and (b) The coordination environment of Mn(II) in compound $[Mn_5(C_4H_4O_4)_4(O)]_n$

Source: Xu *et al.* (2007)

MATERIALS AND METHODS

This part describes syntheses, characterization, spectral and thermal studies of the studied compounds. Material section consists of chemical, apparatus and instruments. Method section consists of 5 sections: (1) syntheses and characterization of the copper(II) complexes; (2) syntheses and characterization of the manganese(II) complexes (3) single crystal structure determination (4) HPLC study and (5) spectral and thermal property measurements.

Materials

1. Chemicals, apparatus and instruments

1.1 Chemicals

1.1.1 Copper(II) nitrate trihydrate (analytical grade; Merck) : $CuNO_3 \cdot 3H_2O$

1.1.2 Copper(II) chloride (analytical grade; Merck) : $CuCl_2 \cdot 2H_2O$

1.1.3 Copper(II) sulfate (analytical grade; Merck) : $CuSO_4 \cdot 5H_2O$

1.1.4 Manganese (II) chloride (analytical reagent grade; Ajex Finechem) : $MnCl_2 \cdot 4H_2O$

1.1.5 1-10-phenanthroline hydrate (analytical reagent grade; Ajex Finechem): $C_{12}H_8N_2 \cdot H_2O$

1.1.6 DL-Malic acid (reagent grade; Fluka): $C_4H_5O_5$

1.1.7 Tartaric acid (laboratory reagent grade; Fluka): $C_4H_4O_6$

1.1.8 Succinic acid (analytical reagent grade; Mag&Baker LTD): $C_4H_6O_4$

1.1.9 Oxalic acid (analytical reagent grade; Ajex Finechem) : $C_2H_2O_4$

1.1.10 Methanol (analytical reagent grade; Mallinkvodt company)

1.1.11 Sodium hydroxide (reagent grade; Fluka)

All compounds and solvent were used without further purification

1.2 Apparatus and Instruments

1.2.1 Hydrothermal apparatus

The hydrothermal apparatus consists of Teflon-lined stainless steel autoclave equipped with thermal couple, and high temperature oven (Figure 27).

(a) (b)

Figure 27 (a) The Teflon-lined stainless steel autoclave and (b) high temperature oven

1.2.2 Fourier Transform Infrared Spectrophotometer (FTIR)

Solid state infrared spectra of compounds were measured on a Bruker Model Equinox 55 Spectrophotometer in the region 4000-400 cm^{-1} with a horizontal attenuated total reflectance accessory.

1.2.3 Elemental Analyzer

All complexes were analysed by CHNS/O Analyzer Perkin Elmer Model PE2400 Series II**.**

1.2.4 X–ray Single Crystal Diffractometer (XRD)

All X–ray data for single crystals were collected on a Siemens-Smart CCD Diffractometer controlled by a digital computer.

1.2.5 X–ray Powder Diffractometer (XRD)

Powder patterns were collected on a PHILIPS X' Pert Spectrometer 2θ range 5-40° with heating rate 2°C/min.

1.2.6 SHELXTL 97 Program

All crystal structures were solved by using the SHELXTL 97 program version 5.1.

1.2.7 HPLC apparatus

The instrumental setup consisted of an HPLC Beckman Coulter (Fullerton, CA, USA) instrument, composed of a prostar photodiode array detector. The mixing took place into the flow cell by prostar 210/215 solent derivery module pump. The Star Chromatography Workstation version 5 program was used for data acquisition and treatment. Chromatography was performed using a vatian chromsep persuit 5-C18 column.

1.2.8 UV/VIS/NIR Spectrophotometer

The absorption spectra of all complexes were obtained by Jasco V-530 UV/VIS/NIR spectrophotometer. The spectra were measured from 200-1100 nm.

1.2.9 Thermogravimetric Analyzer

Thermogravimetric analyses were performed using a Perkin Elmer TGA 7.

Methods

1. Synthesis and characterization of the copper (II) complexes

This section reports the synthesis of eight copper(II) complexes using two types of ligands which are (1) oxalic acid and dicarboxylic acids with alkyl chains of four carbon atoms (malic tartaric and succinic acid) and (2) rigid N,N′-donor ligands (phenanthroline). Complex **1**-**4** and **6** give blue to green crystals. Hence their crystal structures are determined. Table 1 summarizes the solvothermal conditions for all synthesis.

1.1 $[Cu(ox)(phen)(H_2O)]\cdot H_2O$ (**1**) CuPMa

Copper(II) nitrate trihydrate (0.2416 g, 1 mmol), phenanthroline (0.1982 g, 1 mmol) and malic acid (0.1374 g, 1 mmol) were mixed in 10 cm^3 of H_2O and 5 cm^3 of methanol. This mixture was placed in a 300 teflon-lined autoclave which was heated at 150°C for 72 hr. After cooling to room temperature, black powder in green solution was obtained and was collected by filtration, washed with water and dried at room temperature. After green solution was stand at room temperature for 2 days, the green gel was obtained. The bluish green rod crystals began to form at the bottom of green gel within 2 days and was collected by filtration. The black powder was characterized as CuO by the powder X-ray diffraction technique. *Anal*. Cal.(%) for $[Cu(C_2O_4)(C_{12}H_8N_2)(H_2O)]\cdot H_2O$: C, 45.72; H, 3.29; N, 7.61. Found: C, 45.94; H, 3.37; N, 7.52. Detailed infrared and electronic spectra are given in the result section.

1.2 $[Cu_4(\mu\text{-suc})_2(phen)_4(H_2O)_4](NO_3)_4\cdot 4H_2O$ (**2**) CuPSb

Copper(II) nitrate trihydrate (0.2416 g ,1 mmol), phenanthroline (0.1982 g, 1 mmol), and succinic acid (0.1198 g, 1 mmol) were mixed in 10 cm^3 of H_2O and 5 cm^3 of methanol. This mixture was placed in a 300 teflon-lined autoclave which was heated at 150°C for 24 hr. Slow cooling to room temperature yielded green plate

Table 1 Preparative conditions for all syntheses

Metal ion	Reactant	Dicarboxylic acid	Solvent	Temperature (°C)	Time (hr)	Result
Solvothermal						
Copper						
CuPMa **(1)**	$Cu(NO_3)_2 \cdot 3H_2O$	malic acid	H_2O : MeOH 2 : 1	150	72	black powder + green crystal
CuPSu **(2)**		succinic acid				green crystal
CuPTa **(3)**	$Cu(NO_3)_2 \cdot 3H_2O$	tartaric acid	H_2O : MeOH	150	24	blue crystal
CuPOx **(4)**		oxalic acid	2 : 1			green + blue crystal
CuSMa **(5)**	$CuSO_4 \cdot 5H_2O$	malic acid	H_2O : MeOH	150	24	blue powder + blue crystal
CuSTa **(6)**		tartaric acid	2 : 1			green crystal
CuCMa **(7)**	$CuCl_2 \cdot 2H_2O$	malic acid	H_2O : MeOH	150	24	green crystal
CuCTa **(8)**		tartaric acid	2 : 1			green crystal
Manganese						
MnPMa **(9)**		malic acid				yellow solution
MnPTa **(10)**	$MnCl_2 \cdot 4H_2O$	tartaric acid	H_2O 15 ml	130	72	yellow solution
MnPSu **(11)**		succinic acid				yellow crystal

Table 1 (Continued)

Metal ion	Reactant	Dicarboxylic acid	Solvent	Temperature (°C)	Time (hr)	Result
MnPMaB **(12)**	$MnCl_2 \cdot 4H_2O$+	malic acid				yellow precipitate
MnPTaB **(13)**	NaOH	tartaric acid	H_2O 15 ml	150	72	yellow precipitate
MnPSuB **(14)**		succinic acid				yellow solution
Wet method						
Manganese						
MnPMaW **(15)**		malic acid	H_2O : MeOH	room	0.5	yellow precipitate
MnPTaW **(16)**	$MnCl_2 \cdot 4H_2O$	tartaric acid	2 : 1	temperature		yellow precipitate
MnPSuW **(17)**		succinic acid				yellow crystal
MnPOxBW**(18)**		oxalic acid				
MnPMaBW**(19)**	$MnCl_2 \cdot 4H_2O$+	malic acid	H_2O : MeOH	room	0.5	yellow precipitate
MnPTaBW **(20)**	NaOH	tartaric acid	2 : 1	temperature		yellow precipitate
MnPSuBW **(21)**		succinic acid				yellow solution

crystals. The crystals were collected by filtration, washed with water and dried at room temperature. *Anal*. Cal.(%) for $[Cu_4(\mu\text{-suc})_2(phen)_4(H_2O)_4](NO_3)_4 \cdot 4H_2O$: C, 44.16; H, 2.91; N, 11.03 Found: C, 44.17; H, 3.24; N, 10.64%. Detailed infrared and electronic spectra are given in the result section.

1.3 $[Cu(\mu\text{-ox})(phen)]_n$ **(3)** CuPTa

Copper(II) nitrate trihydrate (0.2416 g, 1 mmol), phenanthroline (0.1982 g, 1 mmol) and tartaric acid (0.1501 g, 1 mmol) were mixed in 10 cm^3 of H_2O and 5 cm^3 of methanol. This mixture was placed in a 300 teflon-lined autoclave which was heated at 150°C for 24 hr. Slow cooling to room temperature yielded blue parallelepiped crystals. The crystals were collected by filtration, washed with water and dried at room temperature. *Anal*. Cal.(%) for $[Cu(\mu\text{-ox})(phen)]_n$: C, 50.68; H, 2.43; N, 8.44. Found: C, 50.32; H, 1.99; N, 8.17%. Detailed infrared and electronic spectra are given in the result section.

1.4 $[Cu_2(\mu\text{-ox})_2(phen)_2]_n$ **(4)** CuPOx

Copper(II) nitrate trihydrate (0.2416 g, 1 mmol), phenanthroline (0.1982 g, 1 mmol) and oxalic acid (0.12607 g, 1 mmol) were mixed in 10 cm^3 of H_2O and 5 cm^3 of methanol. This mixture was placed in a 300 cm^3 teflon–lined autoclave which was heated at 150°C for 24 hr. Slow cooling to room temperature yielded mixture of green plate and blue rod crystals. The crystals are collected by filtration, washed with water and dried at room temperature. The green plate crystals were selected by hand.. *Anal*. Cal.(%) for $[Cu_2(\mu\text{-}C_2O_4)_2(C_{12}H_8N_2)_2]_n$ (green plate): C, 50.68; H, 2.43; N, 8.44. Found: C, 45.41; H, 2.44; N, 10.47%. Note: different elemental percentage between observed and calculated value may be due to contamination of small blue rod crystals.

1.5 Copper(II) sulfate + phenanthroline + malic acid **(5)** CuSMa

Copper(II) sulfate pentahydrate (0.2497g, 1 mmol), phenanthroline (0.1982

g, 1 mmol) and malic acid (0.1362 g,1 mmol) were mixed in 10 cm^3 of H_2O and 5 cm^3 of methanol. This mixture was placed in a 300 teflon-lined autoclave which was heated at 150°C for 24 hr. Slow cooling to room temperature yielded mixture of blue powder and blue crystals. The blue crystals were picked out by hand and collected by filtration, washed with water and dried at room temperature. *Anal*. Cal.(%) for [Cu(μ-SO_4)(phen)$(H_2O)_2$]: C, 32.99; H, 2.31; N, 6.41. Found: C, 33.65; H, 2.93; N, 7.54%.

1.6 $[Cu\ (\mu\text{-}SO_4)(phen)(H_2O)_2]_n$ **(6)** CuSTa

Copper(II) sulphate pentahydrate (0.2497 g, 1 mmol), phenanthroline (0.1982 g ,1 mmol) and tartaric acid (0.1501 g, 1 mmol) were mixed in 10 cm^3 of H_2O and 5 cm^3 of methanol. This mixture was placed in a 300 teflon-lined autoclave which was heated at 150°C for 24 hr. Slow cooling to room temperature yielded blue parallelepiped crystals. The crystals were collected by filtration, washed with water and dried at room temperature. *Anal*. Cal.(%) for $[Cu(\mu\text{-}SO_4)(phen)(H_2O)_2]_n$: C, 32.99; H, 2.31; N, 6.41. Found: C, 33.47; H, 2.84; N, 7.37%. Detailed infrared and electronic spectra are given in the result section.

1.7 Copper(II) chloride + phenanthroline + malic acid **(7)** CuCMa

Copper(II) chloride dihydrate (0.1705 g, 1 mmol), phenanthroline (0.1982 g, 1 mmol) and malic acid (0.1362 g, 1 mmol) were mixed in 10 cm^3 of H_2O and 5 cm^3 of methanol. This mixture was placed in a 300 teflon-lined autoclave which was heated at 150°C for 24 hr. Slow cooling to room temperature yielded green crystals. The crystals were collected by filtration, washed with water and dried at room temperature. *Anal*. Found: C, 46.02; H, 2.60; N, 8.46%. Detailed infrared spectrum is given in the result section.

1.8 Copper(II) chloride + phenanthroline + tartaric acid **(8)** CuCTa

Copper(II) chloride dihydrate (0.2497 g, 1 mmol), phenanthroline (0.1982 g, 1 mmol), and tartaric acid, 0.1501 g (1 mmol) were mixed in 10 cm^3 of H_2O and 5

cm^3 of methanol. This mixture was placed in a 300 teflon-lined autoclave which was heated at 150°C for 24 hr. Slow cooling to room temperature yielded green crystals. The crystals were collected by filtration, washed with water and dried at room temperature. *Anal*. Found: C, 45.73; H, 2.44; N, 8.44%. Detailed infrared spectrum is given in the result section.

2. Synthesis and characterization of the manganese(II) complexes

This section reports the synthesis of five manganese(II) complexes using two types of ligands which are (1) oxalic acid and dicarboxylic acids with alkyl chains of four carbon atoms (malic tartaric and succinic acid) and (2) rigid N,N′-donor ligands (phenanthroline). All reactions give yellow solution. Hence the crystal structures of them are determined. Two preparation methods used in this study are hydrothermal and simple wet methods (Table 1).

Hydrothermal Method

2.1 Manganese(II) chloride + phenanthroline + malic acid **(9)** MnPMa

Manganese(II) chloride tetrahydrate (0.2008 g, 1 mmol), phenanthroline (0.2004 g, 1 mmol) and malic acid (0.1383 g, 1 mmol) were mixed in 15 cm^3 of H_2O This mixture was placed in a 300 teflon-lined autoclave which was heated at 130°C for 24 hr. Slow cooling to room temperature. Yellow precipitates were obtained in yellow solution. This powder was collected by filtration, washed with water and dried at room temperature. Detailed electronic spectrum is given in the result section.

2.2 Manganese(II) chloride + phenanthroline + tartaric acid **(10)** MnPTa

Manganese(II) chloride tetrahydrate (0.2026 g, 1 mmol) phenanthroline (0.1991 g, 1 mmol) and tartaric cid (0.1524 g, 1 mmol) were mixed in 15 cm^3 of H_2O This mixture was placed in a 300 teflon-lined autoclave which was heated at 130°C for 24 hr. Slow cooling to room temperature. Yellow precipitates were obtained in

yellow solution. This powder was collected by filtration, washed with water and dried at room temperature. Detailed electronic spectrum is given in the result section.

2.3 *cis*-[$Mn(phen)_2Cl_2$] **(11)** MnPSu

Manganese(II) chloride tetrahydrate (0.1979 g, 1 mmol), phenanthroline (0.1982 g, 1 mmol) and succinic acid (0.111 g, 1 mmol) were mixed in 15 cm^3 of H_2O This mixture was placed in a 300 teflon-lined autoclave which was heated at 130°C for 24 hr. Slow cooling to room temperature. Yellow rod crystals began to form in 4 weeks at the bottom. The crystals were collected by filtration, washed with water and dried at room temperature. *Anal*. Cal.(%) for *cis*-[$Mn(phen)_2Cl_2$] : C, 59.28; H, 3.32; N, 11.52. Found: C, 59.51; H, 3.03; N, 11.07%. Detailed infrared and electronic spectra are given in the result section.

2.4 Manganese(II) chloride + phenanthroline + malic acid + NaOH **(12)** MnPMaB

Manganese(II) chloride tetrahydrate (0.2033 g, 1 mmol), phenanthroline (0.1995 g, 1 mmol) and malic acid (0.1368 g, 1 mmol) were dissolved in 5 cm^3 of H_2O . NaOH was added to adjust pH of mixture. After added 10 cm^3 of 0.1M NaOH into a mixture, it turned to semi-transparent yellow solution. pH of solution increased from 3 to 4. This mixture was sealed in a 300 cm^3 teflon–lined autoclave and heated at 130°C for 72 hr. Slow cooling to room temperature. Yellow precipitates were obtained in yellow solution. This powder was collected by filtration, washed with water and dried at room temperature.

2.5 Manganese(II) chloride + phenanthroline + tartaric acid + NaOH **(13)** MnPTaB

Manganese(II) chloride tetrahydrate (0.2149 g, 1 mmol), phenanthroline (0.1984 g, 1 mmol) and tartaric acid (0.1512 g, 1 mmol), were dissolved in 5 cm^3

of H_2O 10 cm^3 . Then 10 cm^3 of 0.1M NaOH was added into a mixture. The transparent yellow solution was turned to semi-transparent solution. pH of solution increase from 3 to 4. This mixture was sealed in a 300 cm^3 teflon–lined autoclave and heated at 130°C for 72 hr. Slow cooling to room temperature. Yellow precipitate were obtained in yellow solution (deeper yellow than **12**). This powder was collected by filtration, washed with water and dried at room temperature.

2.6 Manganese(II) chloride + phenanthroline + succinic acid + NaOH **(14)** MnPSuB

A mixture of manganese(II) chloride tetrahydrate, 0.2149 g (1 mmol), phen, 0.1984 g (1 mmol), and tartaric acid, 0.1512 g (1 mmol), was dissolved in 5 cm^3 of H_2O 10 cm^3 . Then 10 cm^3 of 0.1M NaOH was added into a mixture. The transparent yellow solution was turned to semi-transparent solution. pH of solution increase from 5 to 6. This mixture was sealed in a 300 cm^3 teflon–lined autoclave and heated at 130°C for 72 hr. Slow cooling to room temperature. No crystals or precipitate were obtained in deep yellow solution.

Wet Method

2.7 Manganese(II) chloride + phenanthroline + malic acid **(15)** MnPMaW

To an aqueous solution of manganese(II) chloride tetrahydrate (0.1980 g, 1 mmole in 10 cm^3 water) was added a phenanthroline solution (0.1989 g, 1mmole in 5 cm^3 methanol). Malic acid 0.1356 g (1mmole) was added to mixture. Then 0.1057 M NaOH was added to the reaction mixture. The mixture was stirred yielded yellow powder in yellow solution. This powder was collected by filtration, washed with water and dried at room temperature. For several days, the rod yellow crystals were obtained. *Anal*. Cal.(%) for $[Mn(phen)_2Cl_2]$: C, 59.28; H, 3.32; N, 11.52. Found: C, 59.60; H, 2.45; N, 11.54%. Detailed infrared spectrum is given in the result section.

2.8 Manganese(II) chloride + phenanthroline + tartaric acid **(16)** MnPTaW

To an aqueous solution of manganese(II) chloride tetrahydrate (0.1983 g, 1 mmole in 10 cm^3 water) was added a phenanthroline solution (0.1990 g, 1mmole in 5 cm^3 methanol). Tartaric acid 0.1515 g (1mmole) was added to mixture. Then 0.1057 M NaOH was added to the reaction mixture. The mixture was stirred yielded yellow powder in yellow solution. This powder was collected by filtration, washed with water and dried at room temperature. For several days, the rod yellow crystals were obtained. *Anal*. Cal.(%) for $[Mn(phen)_2Cl_2]$: C, 59.28; H, 3.32; N, 11.52. Found: C, 59.50; H, 2.65; N, 11.60%. Detailed infrared spectrum is given in the result section.

2.9 Manganese(II) chloride + phenanthroline + succinic acid **(17)** MnPSuW

To an aqueous solution of manganese(II) chloride tetrahydrate (0.2018 g, 1 mmole in 10 cm^3 water) was added a phenanthroline solution (0.1985 g, 1mmole in 5 cm^3 methanol). Succinic acid 0.1194g (1mmole) was added to mixture. Then 0.1057 M NaOH was added to the reaction mixture. The mixture was stirred and allowed to stand at room temperature for several days. The rod yellow crystals were obtained. *Anal*. Cal.(%) for $[Mn(phen)_2Cl_2]$: C, 59.28; H, 3.32; N, 11.52. Found: C, 59.61; H, 2.84; N, 11.67%. Detailed infrared spectrum is given in the result section.

2.10 Manganese(II) chloride + phenanthroline + oxaic acid **(18)** MnPOxW

To an aqueous solution of manganese(II) chloride tetrahydrate (0.2008 g, 1 mmole in 10 cm^3 water) was added a phenanthroline solution (0.1993 g, 1mmole in 5 cm^3 methanol). Oxalic acid 0.1275g (1mmole) was added to mixture. Then 0.1057 M NaOH was added to the reaction mixture. The mixture was stirred, yielded yellow powder. This powder was collected by filtration, washed with water and dried at room temperature. *Anal*. Cal.(%) for [Mn(ox)(phen)] : C, 52.03; H,2.49; N, 18.66. Found: C, 51.51; H, 2.38; N, 8.35%. Detailed infrared spectrum is given in the result section.

2.11 Manganese(II) chloride + phenanthroline + malic acid +NaOH **(19)** MnPMaBW

To a methanolic solution of manganese(II) chloride tetrahydrate (0.1979 g, 1 mmole in 10 cm^3 MeOH) was added malate solution (malic acid 1 mmole in 0.2 M NaOH 4ml). The solution mixture was stirred 20 min. A phenanthroline solution (0.1999 g, 1mmole in 5 cm^3 methanol) was added to mixture. The mixture was stirred 2 hours yielded yellow powder in yellow solution. This powder was collected by filtration, washed with water and dried at room temperature. For several days, the yellow crystals were obtained.

2.12 Manganese(II) chloride + phenanthroline + succinic acid +NaOH **(20)** MnPSuBW

To an aqueous solution of manganese(II) chloride tetrahydrate 0.2014 g (1 mmole) , phenanthroline 0.1993 g (1mmole) in 10 cm^3 MeOH was added succinate solution (succinic acid 1 mmole in 0.2 M NaOH 4ml). The solution mixture was stirred 15 min yielded yellow powder in pale yellow solution. This powder was collected by filtration, washed with water and dried at room temperature.

2.13 Manganese(II) chloride + phenanthroline + malic acid +NaOH **(21)** MnPSuRW

To a methanolic solution of manganese(II) chloride tetrahydrate (0.2012 g, 1 mmole in 10 cm^3 MeOH) was added malate solution (malic acid 1 mmole in 0.2 M NaOH 4ml). The solution mixture was refluxed 4 hr 30 min. A phenanthroline solution (0.1999 g, 1mmole in 5 cm^3 methanol) was added to mixture. The mixture was refluxed 30 min yielded yellow powder in yellow solution. This powder was collected by filtration, washed with water and dried at room temperature. For several days, the yellow crystals were obtained.

3. Single Crystal Structure Determination

In this study, the crystal structures of six complexes **1**-**4**, **6** and **11** were determined.

3.1 Data Collection

The chosen crystal must meet two main requirements: (1) it must be pure single crystal processing uniform internal structure. (2) it must be of proper size and shape. The color and shape of the selected crystals in this work are listed in Table 2.

The chosen crystal was attached to a glass fiber which was fastened to a 1/8 inch diameter brass pin. This metal pin was inserted into the goniometer head. The crystal was adjusted and shifted until the crystal was on the central axis of the head. The crystal was normally aligned so that a direct crystal axis was parallel to the axis of rotation. The goniometer head was placed on the diffractometer. The crystal was optically centered.

Table 2 Appearance of the selected crystals

complex	color	shape
$[Cu(ox)(Phen)(H_2O)]\cdot H_2O$ **(1)**	green	parallelepiped
$[Cu_4(\mu\text{-}suc)_2(phen)_4(H_2O)_4](NO_3)_4\cdot 4H_2O$ **(2)**	green	parallelepiped
$[Cu(\mu\text{-}ox)(phen)]_n$ **(3)**	blue	parallelepiped
$[Cu_2(\mu\text{-}ox)_2(phen)_2]_n$ **(4)**	green	plate
$[Cu(phen)_2(\mu\text{-}SO_4)(H_2O)_2]_n$ **(6)**	blue	parallelepiped
cis-$[Mn(phen)_2Cl_2]$ **(11)**	yellow	rod

The reflections were integrated using SAINT program. Intensity data were corrected for Lorentz and polarization effects for all the complexes. Decay correlations were also made. The structures were solved by direct methods and followed by successive Fourier and difference Fourier syntheses. Full matrix least

square refinements on F^2 were carried out using SHELXL-97 (Shedrick, 1997). Refinement of positional and anisotropic thermal parameters for non-hydrogen atoms by full-matrix least-square methods minimize the function $\Sigma w(|F_0| - |F_c|)^2$ giving lowest R1 and wR2 (where $R1 = \Sigma||F_0| - |F_c|| / \Sigma|F_0|$) and $wR_2 = \Sigma w(F_0^2 - F_c^2)^2 / \Sigma w(F_0^2)^2]^{½}$ and $w = 1/\sigma(Fo)$). Covalent radii of atoms are listed in Appendix A. All calculations were carried out using SHELXL-97 (Shedrick, 1997) and Mercury (Macrae *et al.*, 2006).

4. HPLC study to support the cleavage of malate into oxalate ion

An HPLC system equipped with an C-18 column was used to separate the organic acid. Good separation was achieved using an isocratic mobile phase composed of 0.005 M sulfuric acid. The flow rate of mobile phase (0.005M H_2SO_4) was set at 0.3 ml/min in order to obtain a reasonable analysis time (<30 min) with the window between 8 and 35 min (Ruiz *et al*, 2004). The eight fractions of cooking complex **1** were collected every 3 hour (0, 3, 6, 9, 12, 18, 21, 24 hr) and injected in HPLC system.

5. Spectral and thermal properties measurement

5.1 Infrared Spectroscopy

Infrared (IR) spectra were recorded on a Bruker Model Equinox 55 spectrophotometer in the region 4000-400 cm^{-1} equipped with a horizontal attenuated total reflectance accessory (ATR technique).

5.2 Electronic Spectroscopy

The absorption spectra at room temperature were measured in water using a Jasco V-530 UV/VIS/NIR spectrophotometer in the 200-1100 nm spectral range.

5.3 Thermal Gravimetric Analysis

Thermo gravimetric analyses were performed using a Perkin Elmer TGA 7. The complexes were placed in platinum pan and the data were recorded under a nitrogen atmosphere from room temperature to 800°C with a heating rate of 10°C/min.

RESULTS AND DISCUSSION

Total eight copper complexes and sixteen manganese complexes were synthesized either by solvothermal or wet method (Table 3). Only six complexes give single crystals which are suitable for X-ray diffraction experiments. The rest of them are characterized by elemental analysis and infrared technique. Some syntheses give neither crystal nor precipitate, thus no further experiments were done.

1. Crystal Structure Determination

1.1 The crystal structure of the copper(II) complexes

1.1.1 $[Cu(ox)(phen)(H_2O)]\cdot H_2O$ **(1)**

Complex **(1)** crystallizes in monoclinic system with cell dimensions: a = 8.482 Å, b = 9.6812(1) Å, c = 17.4677(2) Å, $\alpha = \gamma$ 90°, β = 103.75with the $P2_1/n$ space group. From 9966 reflections collected, which included all duplicate and equivalent reflections, 3970 independent reflections were obtained by averaging. Of those, 3390 reflections whose intensity were greater than $2\sigma(I)$ were used in the structure solution and least-square refinements. The program SHELXTL 97 (sheldrick, G.M. 1997) was used for data reduction, structure solution and structure refinement. Some hydrogen atoms were located in a diffraction Fourier map and refined isotropically. All hydrogen atoms are included in the final refinement. The Goodness-of-fit on F^2 (S) was 1.044 and final R valua was 0.0294. Crystal data and structure refinement are shown in Table 4. The atomic position (x, y, z) with equivalent isotropic thermal (Ueq) parameters and the anisotropic thermal (Uij) parameter expressions are shown in Appendix B and C. Bond lengths and bond angles are summarized in Appendix D and E, respectively.

The crystal structure of **1** consists of mononuclear Cu(II) complex molecules. A perspective view of the metal coordination environment of the neutral complex of

Table 3 Colours, and elemental analysis data of the prepared complexes

Complex	Synthetic Result	Elemental Analysis (%)		
		C	H	N
[Cu (ox)(phen)(H_2O)]·H_2O **(1)**	Green rod	45.94	3.37	7.52
		(45.72)	(3.29)	(7.61)
[Cu_4(μ-suc)$_2$(phen)$_4$(H_2O)$_4$](NO_3)$_4$·4H_2O **(2)**	Green plate	44.17	3.24	10.64
		(44.16)	(2.91)	(11.03)
[Cu(μ-ox)(phen)]$_n$ **(3)**	Blue precipitate	50.32	1.99	8.17
		(50.68)	(2.43)	(8.44)
[Cu_2(μ-ox)$_2$(phen)$_2$]$_n$ **(4)**	Green plate+ Blue rod	45.41	2.44	10.47
		(50.68)	(2.43)	(8.44)
CuSMa **(5)**	Blue powder + Green crystal	33.65	2.93	7.54
		(32.99)	(2.31)	(6.41)
[Cu(μ-SO_4)(phen)(H_2O)$_2$]$_n$ **(6)**	Blue parallelepiped	33.47	2.84	7.37
		(32.99)	(2.31)	(6.41)
CuCMa **(7)**	Green crystal	46.02	2.60	8.46
CuCTa **(8)**	Green crystal	45.73	2.44	8.44
MnPMa **(9)**	Deep yellow solution	-	-	-
MnPTa **(10)**	Deep yellow solution	-	-	-
cis-[Mn(phen)$_2$$Cl_2$] **(11)**	Yellow rod	59.51	3.03	11.07
		(59.28)	(3.32)	(11.52)

Table 3 (Continued)

Complex	Synthetic Result	Elemental Analysis (%)		
		C	H	N
MnPMaB **(12)**	Yellow precipitate	-	-	-
MnPTaB **(13)**	Yellow precipitate	-	-	-
MnPSuB **(14)**	Deep yellow solution	-	-	-
MnPMaW **(15)**	Yellow precipitate	59.60	2.45	11.54
		(59.28)	(3.32)	(11.52)
MnPTaW **(16)**	Yellow precipitate	59.50	2.65	11.60
		(59.28)	(3.32)	(11.52)
MnPSuW **(17)**	Yellow crystal	59.61	2.84	11.67
		(59.28)	(3.32)	(11.52)
MnPOxW **(18)**	Yellow precipitate	51.51	2.38	8.35
		(52.03)	(2.49)	(8.66)
MnPMaBW **(19)**	Yellow precipitate	-	-	-
MnPSuBW **(20)**	Yellow precipitate	-	-	-
MnPSuRW **(21)**	Yellow precipitate	-	-	-

*(…….) calculated value

Table 4 Crystal data and structure refinement for $[Cu(ox)(phen)(H_2O)]\cdot H_2O$ **(1)**

Formula	$[Cu\ (C_2H_2O_4)(C_{12}H_8N_2)(H_2O)]\cdot H_2O$	
Empirical formula	C14 H12 Cu N2 O6	
Formula weight	367.80	
Temperature	293(2) K	
Wavelength	0.71073 Å	
Radiation type	Fine-focus sealed tube	
Radiation source	K-alpha molybdenum	
Crystal system	Monoclinic	
Space group	$P2_1/n$	
Unit cell dimensions	a = 8.482 Å	α = 90°
	b = 9.6812(1) Å	β = 103.75°
	c = 17.4677(2) Å	γ = 90°
Volume	1393.34(2) $Å^3$	
Z	4	
Density (calculated)	1.753 g/cm^3	
Absorption coefficient	1.603 mm^{-1}	
F(000)	748	
θ range for data collection	2.40 to 30.58°	
No. of reflections collected	9966	
No. of independent reflections	3970 [R_{int} = 0.0181]	
No. of reflection > 2σ(I), n	3390	
No. of parameter, p	228	
Absorption correction	Semi-empirical from equivalents	
Refinement method	Full-matrix least-squares on F^2	
Goodness-of-fit on F^2	S = 1.044	
Final $R_1 = \Sigma\|\|F_0\| - \|F_c\|\| / \Sigma\|F_0\|$	0.0294	
Final $wR_2 = \Sigma w(F_0^2 - F_c^2)^2 / \Sigma w(F_0^2)^2]^{½}$	0.0783	

1, with the atomic numbering scheme is shown in Figure 28. The coordination geometry around copper ion is approximately square pyramid. The equatorial plane consists of two nitrogen atoms of a phenanthroline and two oxygen atoms of a bidentate oxalate ligand. An aqua ligand is at the apical position and forms intermolecular hydrogen bonds with the uncoordinated oxalate oxygen (O5-O6 distance = 2.754 Å). This coordinated water also forms hydrogen bonds with the free water in the crystal as shown in Figure 29 and Table 5 (O5-O2 distance=2.945 Å). The free water forms another hydrogen bond with the coordinated oxygen of oxalate ligand (O6-O1 distance = 2.878 Å). The in-plane Cu-O bond distance average 1.939(1) Å and Cu-N bond distance 2.010 Å. The former are shorter than those observed in square pyramidal oxalato copper(II) complexes (Smékal *et al.*,1999) while the latter are longer. The axial Cu-O bond distance is 2.223(2) Å. The four donor atoms on the equatorial plane are not perfectly planar showing a tetrahedral distortion, with a dihedral angle of 166.77º formed between the O-Cu-O and N-Cu-N planes. In this complex, the coordination mode of oxalate ligand is bidentate mode. The oxalato complexes of Cu(II) in the literature are mostly dimeric complex in which the oxalate ligand acts as bis-chelate bridging ligand. The crystal structure is stabilized by partial face to face π-π stacking of phenanthroline ligands with approximate interplane distances between phenanthroline molecule of 3.513-3.555 Å as shown in Figure 30. The packings of complex **1** along *a*-, *b*- and *c*-axes are shown in Figure 31.

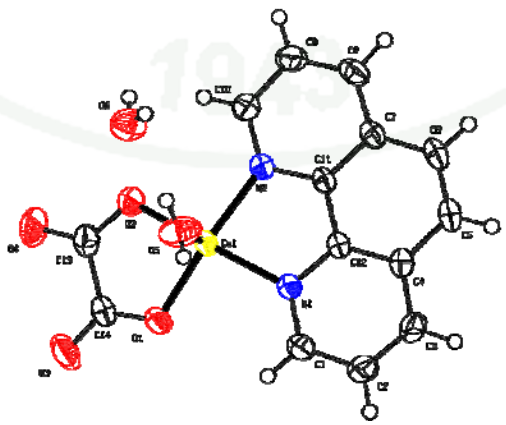

Figure 28 An ORTEP view of $[Cu(ox)(phen)(H_2O)]\cdot H_2O$ (**1**) showing the numbering scheme.

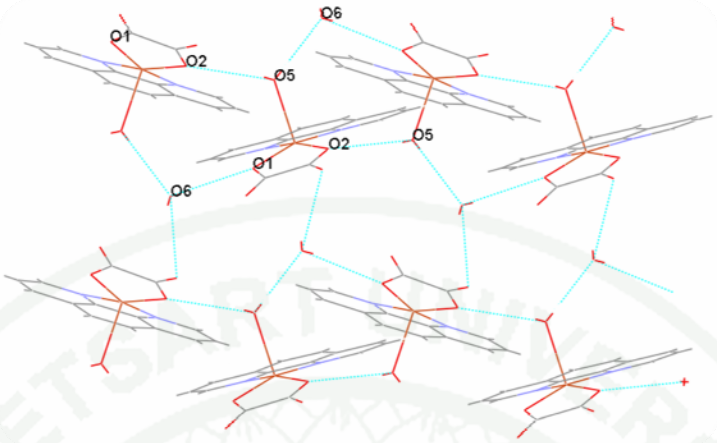

Figure 29 Packing structure view of [Cu(ox)(phen)(H_2O)]·H_2O (**1**) showing hydrogen-bonding between adjacent molecules.

Table 5 Hydrogen bonding geometry (Å, °) of **(1)**

D-H···A	D-H	H···A	D···A	D-H···A	Symmetry codes
O5-H5B···O2	0.703	2.265	2.945	163.34	-x+3/2, y-1/2, -z+1/2
O5-H5A···O6	0.791	1.964	2.754	177.41	
O6-H6B···O1	0.761	2.134	2.878	165.85	-x+3/2, y+1/2, -z+1/2

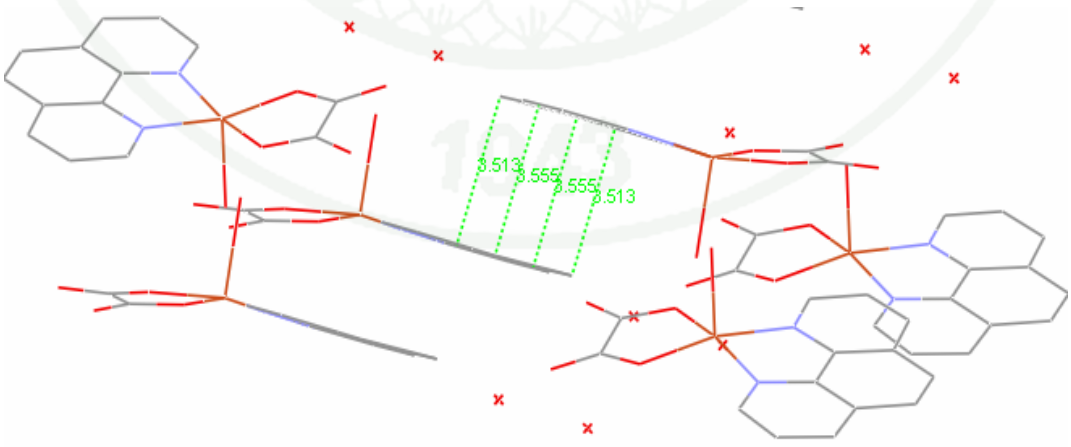

Figure 30 π-π interaction of phenanthroline ring of [Cu(ox)(phen)(H_2O)]·H_2O (**1**)

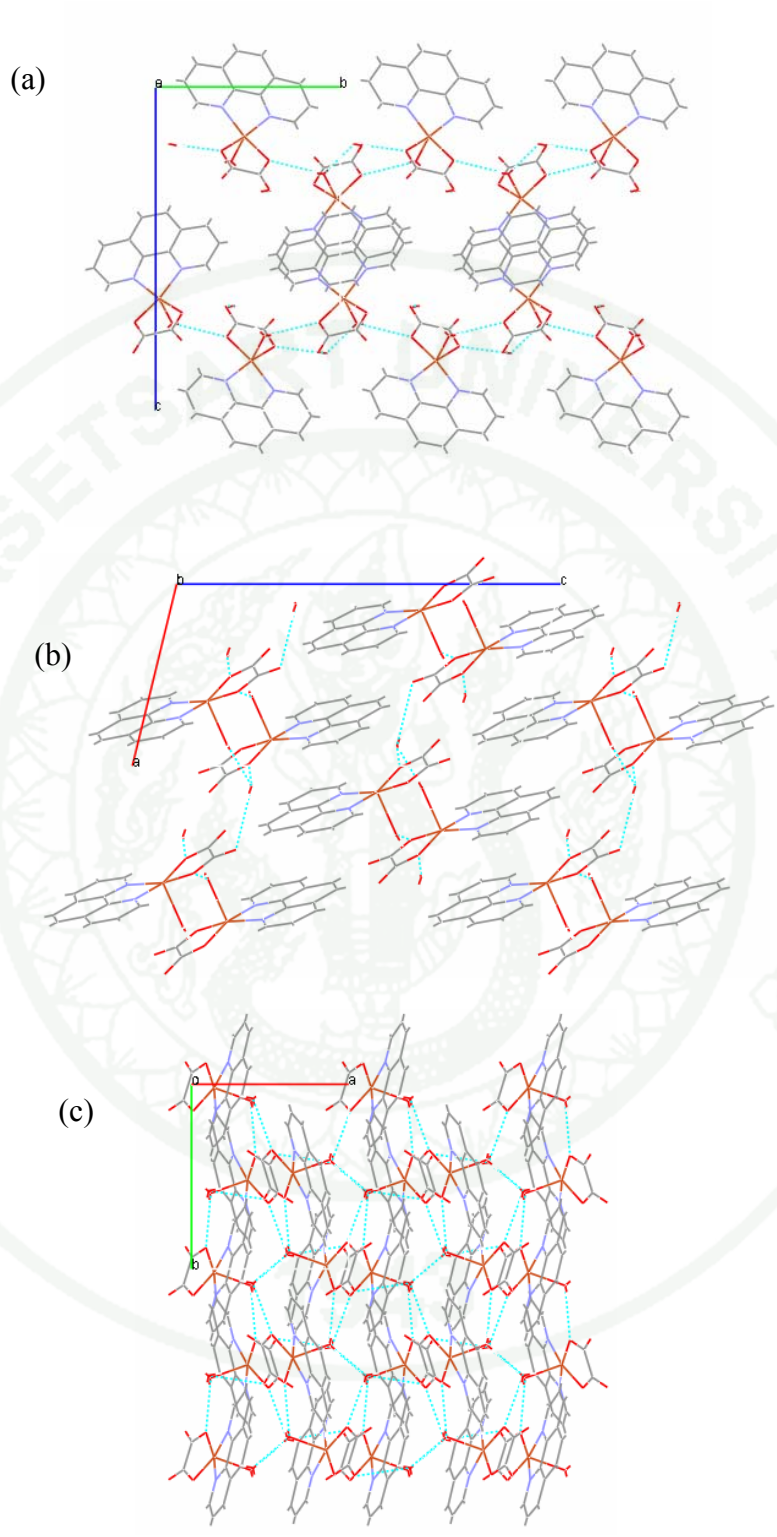

Figure 31 Packing structure of [Cu(ox)(phen)(H_2O)]·H_2O (**1**) view along (a) *a*-axis, (b) *b*-axis and (c) *c*-axis.

1.1.1 $[Cu_4(\mu\text{-suc})_2(phen)_4\ (H_2O)_4](NO_3)_4{\cdot}4H_2O$ **(2)**

Complex **2** crystallizes in monoclinic system with cell dimensions: a = 8.9180(1) Å, b = 34.1090(2) Å, c = 10.3620(2) Å, $\alpha = 90°$, $\beta = 96.031(1)°$, $\gamma = 90°$ with the $P2_1/c$ space group. From 23089 reflections collected, which included all duplicate and equivalent reflections, 8980 independent reflections were obtained by averaging. Of those, 7772 reflections whose intensity were greater than $2\sigma(I)$ were used in the structure solution and least-square refinements. The program SHELXTL 97 (sheldrick, G.M. 1997) was used for structure solution and structure refinement. Some hydrogen atoms were located in a difference Fourier map and refined isotropically. All hydrogen atoms are included in the final refinement. The Goodness-of-fit on F^2 (S) was 1.049 and final R value was 0.0644. Crystal data and structure refinement are shown in Table 6. The atomic position (x, y, z) with equivalent isotropic thermal (Ueq) parameters and the anisotropic thermal (Uij) parameter expressions are shown in Appendix B and C. Bond lengths and bond angles are summarized in Appendix D and E, respectively.

This complex consists of tetranuclear $[Cu_4(phen)_4(suc)_2(H_2O)_4]^{4+}$ species and uncoordinated water molecules and nitrate anion. The complete tetracation is generated by crystallographic inversion symmetry. Both unique Cu^{2+} ions are coordinated by an a bidentate phenanthroline molecule, two bis-bridging succinate dianions and a water molecule, resulting in distorted CuN_2O_3 square-based pyramidal geometries for the metal ions, with the water molecule occupying the apical site. The distance between two unique Cu^{2+} ions is 3.032 Å (Figure 33). The coordination mode for carboxylate groups in succinate ligand are bis-bridging mode (scheme B). As a result, a fourteen membered ring is formed between copper ions in tetranuclear cation. The distance between Cu ion in this fourteen membered ring is 6.396 Å. The average dihedral angles of alkyl chains of succinate ligands in this complex are observed to be 72.43 indicating the *syn, anti*-conformation. The Cu-O (aqua) bonds are longer than the Cu-O (succinate) bonds (Appendix D). All bond lengths and bond angles are in the usual ranges (Appendix D and E). Two unique aqua ligands in the

tetranuclear species form hydrogem bonding differently. One forms two hydrogen bonds with two nitrate ions (O4-O10 = 2.816 and O4-O12 = 3.016 Å). While the other with two free water molecules (O3-O13 = 2.773 and O3-O14 = 2.707 Å) (Appendix D). One water (O13) also forms two bonds with a nitrate ion and a coordinated carboxylate ligand. The other free water (O14) forms two hydrogen bonds with two nitrate ions (Table 7 and Figure 34). The packings of this complex along a-, b- and c- axes are shown in Figure 35.

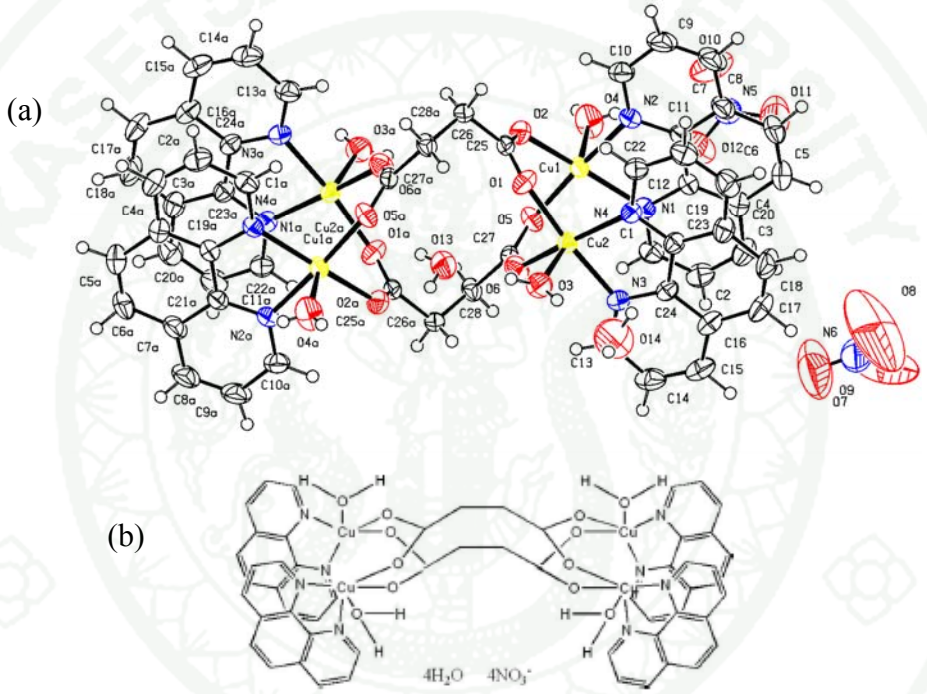

Figure 32 (a) An ORTEP view with the numbering schemeand and (b) schematic view of $[Cu_4(\mu\text{-suc})_2(phen)_4(H_2O)_4](NO_3)_4 \cdot 4H_2O$ **(2)**.

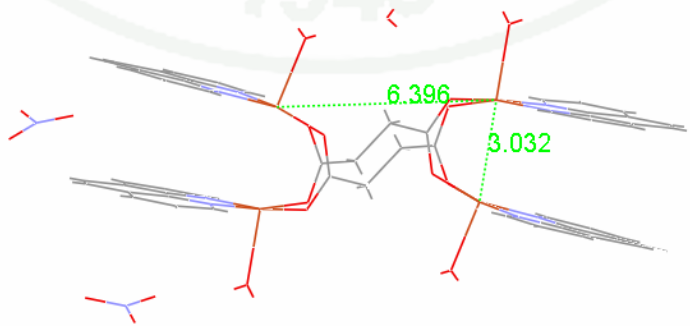

Figure 33 Cu-Cu distance (Å) in $[Cu_4(\mu\text{-suc})_2(phen)_4(H_2O)_4](NO_3)_4 \cdot 4H_2O$ **(2)**

Table 6 Crystal data and structure refinement for $[Cu_4(\mu\text{-suc})_2(phen)_4(H_2O)_4](NO_3)_4 \cdot 4H_2O$ **(2)**.

Formula	$[Cu_4(C_2H_2O_4)_2(C_{12}H_8N_2)_4(H_2O)_4](NO_3)_4 \cdot 4H_2O$	
Empirical formula	C56 H56 Cu4 N12 O28	
Formula weight	1599.29	
Temperature	293(2) K	
Wavelength	0.71073 Å	
Radiation type	Fine-focus sealed tube	
Radiation source	K-alpha molybdenum	
Crystal system	Monoclinic	
Space group	$P2_1/c$	
Unit cell dimensions	a = 8.9180(1) Å	α = 90°
	b = 34.1090(2) Å	β = 96.031(1) °
	c = 10.3620(2) Å	γ = 90°
Volume	3134.51(7) $Å^3$	
Z	2	
Density (calculated)	1.694 Mg/m^3	
Absorption coefficient	1.438 mm^{-1}	
F(000)	1632	
θ range for data collection	1.19 to 30.49°	
No. of reflections collected	23089	
No. of independent reflections	8980 [R_{int} = 0.0179]	
No. of reflection > 2σ(I), n	7772	
No. of parameter, p	463	
Refinement method	Full-matrix least-squares on F^2	
Goodness-of-fit on F^2	S = 1.049	
Final $R_1 = \Sigma\|\|F_0\| - \|F_c\|\| / \Sigma\|F_0\|$	0.0644	
Final $wR_2 = \Sigma w(F_0^2 - F_c^2)^2 / \Sigma w(F_0^2)^2]^{½}$	0.1828	

Table 7 Hydrogen bonding geometry (Å, °) of $[Cu_4(\mu\text{-suc})_2(phen)_4(H_2O)_4](NO_3)_4 \cdot 4H_2O$ **(2)**

D-H···A	D-H	H···A	D···A	D-H···A	Symmetry codes
O13-H13D···O10	0.701	2.234	2.899	158.74	x+1, y, z-1
O13-H13C···O5	0.753	2.260	3.000	167.37	-x+1, -y, -z
O3-H4···O14	0.732	1.985	2.707	168.87	
O3-H16···O13	0.701	2.073	2.773	176.31	
O4-H24···O10	0.818	2.031	2.816	160.68	-x, -y, -z+1
O4-H23···O12	0.818	2.264	3.016	153.03	
O14-H14B···O9	0.819	2.156	2.845	141.72	x+1, -y+1/2, z-1/2
O14-H14C···O7	0.822	2.093	2.874	158.49	x+1, y, z

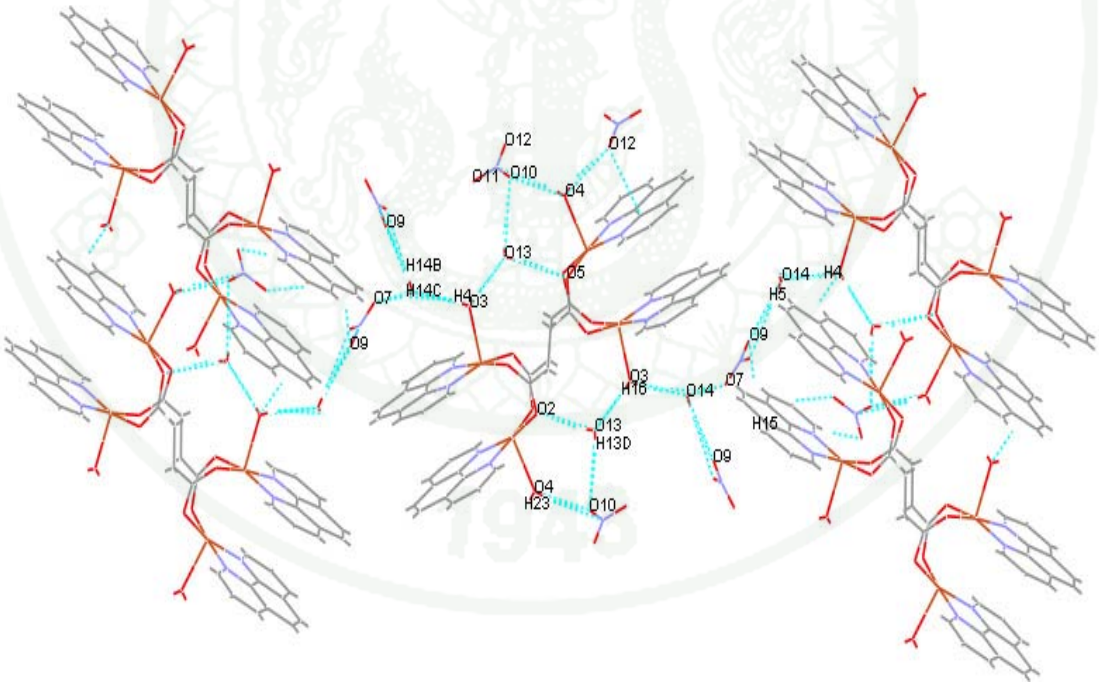

Figure 34 Packing structure view of $[Cu_4(\mu\text{-suc})_2(phen)_4(H_2O)_4](NO_3)_4 \cdot 4H_2O$ **(2)** showing hydrogen-bonding adjacent molecule.

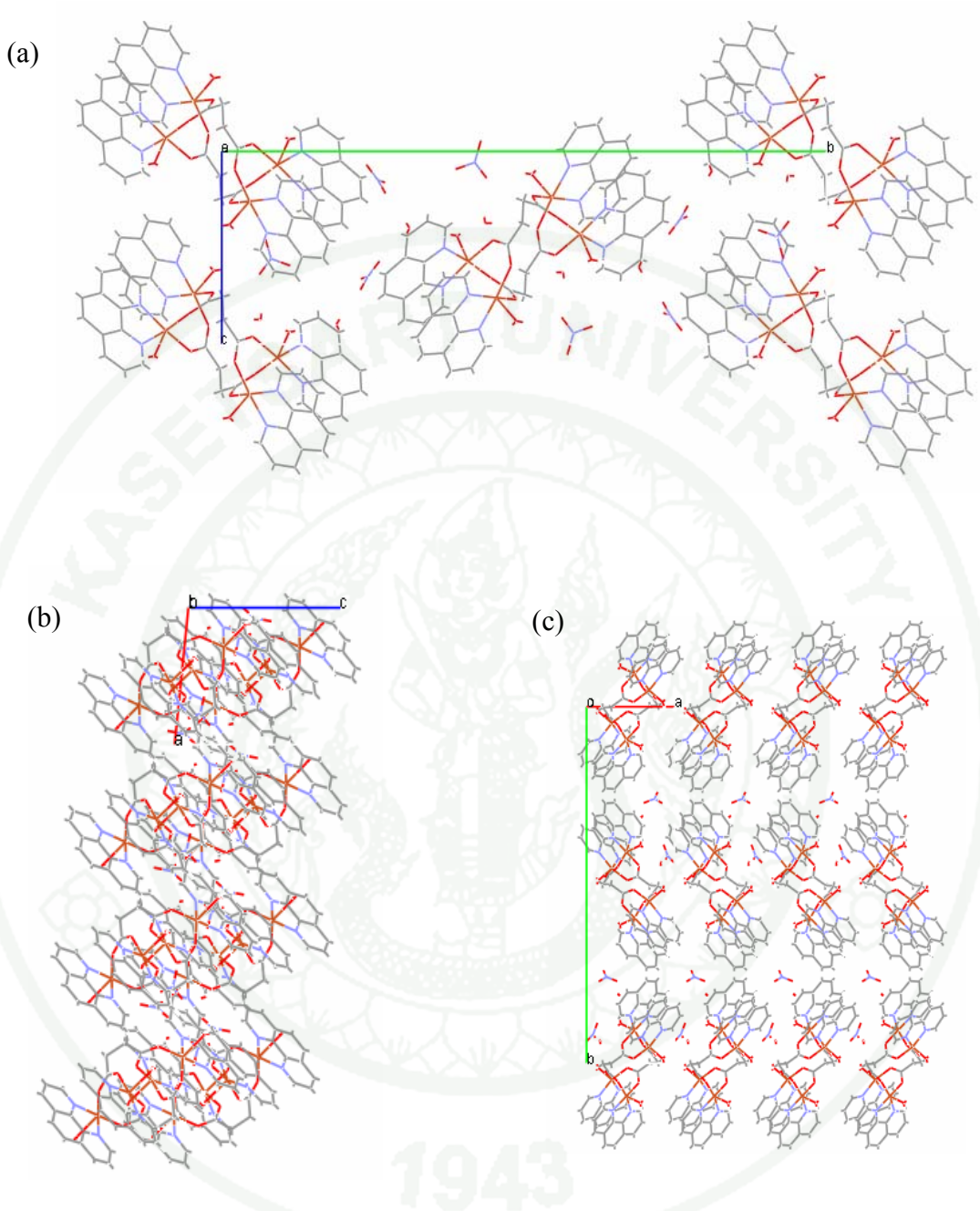

Figure 35 Packing structure of $[Cu_4(\mu\text{-suc})_2(phen)_4(H_2O)_4](NO_3)_4{\cdot}4H_2O$ **(2)** view along (a) *a*-axis, (b) *b*-axis and (c) *c*-axis.

1.1.2 $[Cu(\mu\text{-ox})(phen)]_n$ **(3)**

Complex **3** crystallizes in orthorhombic system with cell dimensions: a = 9.1483(3) Å, b = 10.1441(3) Å, c = 13.3359(3) Å, $\alpha = \beta = \gamma = 90°$ with the $Pna2_1$

space group. From 8648 reflections collected, which included all duplicate and equivalent reflections, 3101 independent reflections were obtained by averaging. Of those, 2722 reflections whose intensity were greater than 2σ(I) were used in the structure solution and least-squares refinements. The program SHELXTL 97 (sheldrick, G.M. 1997) was used for structure solution and structure refinement. All hydrogen atoms are located in a diffraction Fourier map and refined isotropically. The Goodness-of-fit on F^2 (S) was S = 1.050 and final R value was 0.0257. Crystal data and structure refinement are shown in Table 8. The atomic position (x, y, z) with equivalent isotropic thermal (Ueq) parameters and the anisotropic thermal (Uij) parameter expressions are shown in Appendix B and C. Bond lengths and bond angles are summarized in Appendix D and E., respectively.

The crystal structure of complex **3** consists of polymeric chain of [Cu(μ-ox)(phen)] moieties (Figure 36). Each moiety is composed of two copper ions linking through one bridging oxalate ligand. The coordination geometry around copper ion is distorted octahedron in which each copper ion is coordinate to two nitrogen atoms of one phenanthroline molecule and four oxygen atoms of two bridging oxalate ligands. Cu(II) ions are linked through oxalate ligands to create one-dimentional polymeric zigzag chain along the a-axis. The distance between each pair of Cu(II) ions within the polymeric chains is 5.531 Å (Figure37). Two bridging oxalate ligands are in *cis*-position. The coordination mode for each oxalate ligands is bis-chelate bridging. The planes of phenanthroline molecules within the chains are in the alternative left or right positions (Figure 38). The Cu-O and Cu-N bond distance are longer than those observed in dimeric oxalato copper(II) complex (Tang *et al.*, 2000, Castillo *et al.*, 1999, Youngme *et al.*, 2006 and Castillo *et al.*, 2001). The average bite angle of phenanthroline and oxalate are 81.5° and 78.10°, respectively. The planes of phenanthroline in adjacent chain are nearly perpendicular to each other (Figure 39b).The packing of **3** along *a*-, *b*- and *c*-axes are shown in Figure 39. The interplanar distance between parallel phenanthroline plane is 9.148 Å which is too far to form π-π interaction (Figure 36). No hydrogen bondings are observed in **(3)**.

Table 8 Crystal data and structure refinement for $[Cu(\mu\text{-}ox)(phen)]_n$ **(3)**.

Formula	$[Cu(\mu\text{-}C_2O_4)(C_{12}H_8N_2)]$	
Empirical formula	C14 H8 Cu N2 O4	
Formula weight	331.76	
Temperature	293(2) K	
Wavelength	0.71073 Å	
Radiation type	Fine-focus sealed tube	
Radiation source	K-alpha molybdenum	
Crystal system	Orthorhombic	
Space group	*Pna2₁*	
Unit cell dimensions	a = 9.1483(3) Å	a = 90°
	b = 10.1441(3) Å	b = 90°
	c = 13.3359(3) Å	γ = 90°
Volume	1237.59(6) $Å^3$	
Z	4	
Density (calculated)	1.472 Mg/m^3	
Absorption coefficient	1.353 mm^{-1}	
F(000)	555	
θ range for data collection	2.52 to 30.53°	
No. of reflections collected	8648	
No. of independent reflections	3101 [R_{int} = 0.0229]	
No. of reflection > 2σ(I), n	2722	
No. of parameter, p	222	
Absorption correction	No	
Refinement method	Full-matrix least-squares on F^2	
Goodness-of-fit on F^2	S = 1.050	
Final $R_1 = \Sigma\|\|F_0\| - \|F_c\|\| / \Sigma\|F_0\|$	0.0257	
Final $wR_2 = \Sigma w(F_0^2 - F_c^2)^2 / \Sigma w(F_0^2)^2]^{½}$	0.0580	

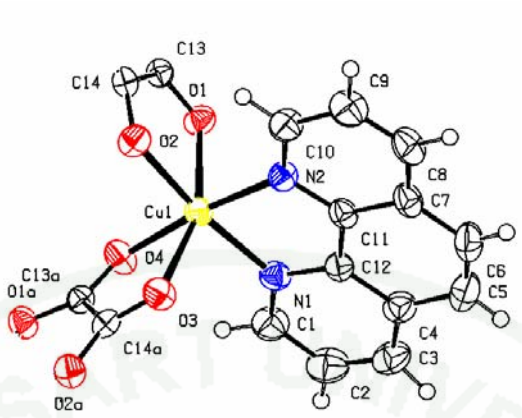

Figure 36 An ORTEP view of [Cu(μ-ox)(phen)]$_n$ **(3)** showing the numbering scheme.

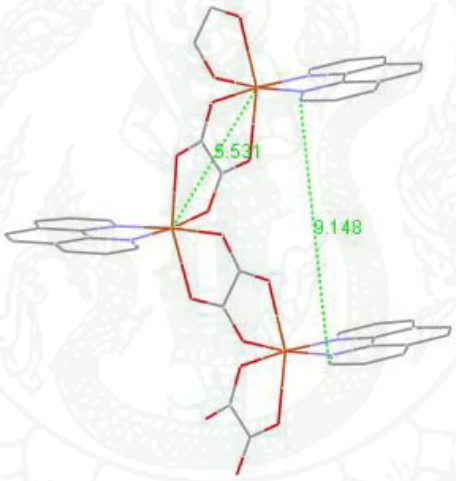

Figure 37 Cu-Cu distance (Å) in [Cu(μ-ox)(phen)]$_n$ **(3)**.

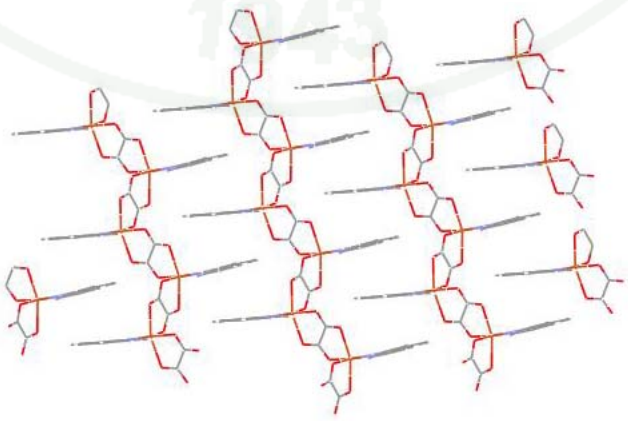

Figure 38 Alternative phenanthroline ring position in [Cu(μ-ox)(phen)]$_n$ **(3)**.

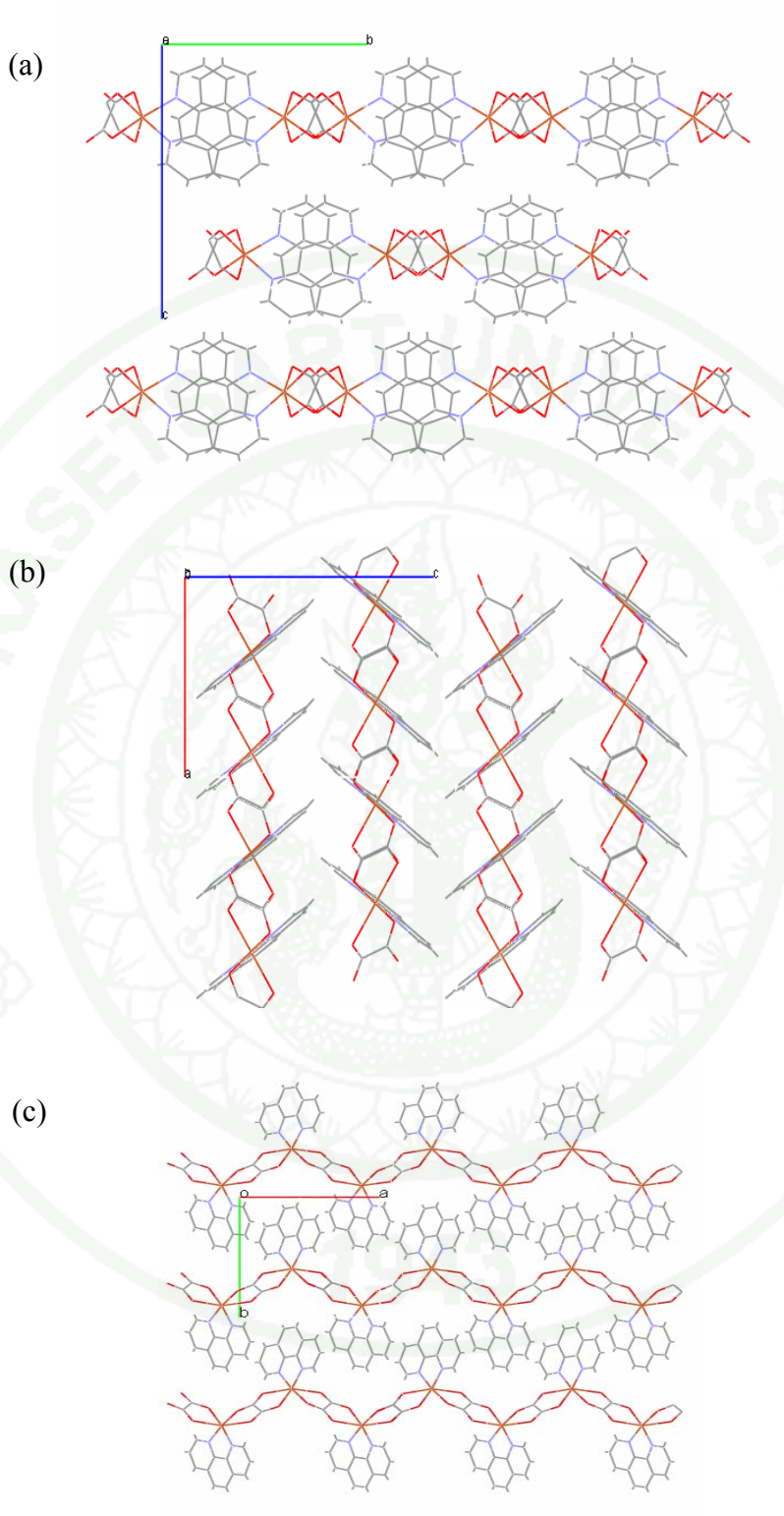

Figure 39 Packing structure of $[Cu(\mu\text{-ox})(phen)]_n$ **(3)** view along (a) *a*-axis, (b) *b*-axis and (c) *c*-axis.

1.1.3 $[Cu_2(\mu\text{-}ox)_2(phen)_2]_n$ **(4)**

Complex **4** crystallizes in triclinic system with cell dimensions: a = 9.1594(2)Å, b = 10.1686(2)Å, c = 13.3489(1) Å, α = 90.155(1) °, β= 90.042(1)°, γ= 89.983(1)° with the *P1* space group. From 9217 reflections collected, which included all duplicate and equivalent reflections, 7822 independent reflections were obtained by averaging. Of those, 5732 reflections whose intensity were greater than $2\sigma(I)$ were used in the structure solution and least-square refinements. The program, SHELXTL 97 (sheldrick, G.M. 1997) was used for structure solution and structure refinement. Some hydrogen atoms were located in a difference Fourier map and refined isotropically. All hydrogen atoms are included in the final refinement. The Goodness-of-fit on F^2 (S) was S = 0.945 and final R value was 0.361. Crystal data and structure refinement are shown in Table 9. The atomic position (x, y, z) with equivalent isotropic thermal (Ueq) parameters and the anisotropic thermal (Uij) parameter expressions are shown in Appendix B and C. Bond lengths and bond angles are summarized in Appendix D and E, respectively.

The crystal structure of complex **4** is similar to **3.** It consists of a polymeric chain of $[Cu_2(\mu\text{-}ox)_2(phen)_2]$ moieties. The asymmetric unit contains two crystallographic independent $[Cu_2(\mu\text{-}ox)_2(phen)_2]$ moieties (Figure 40). Each independent moiety consists of two copper ions linking through one bridging oxalate ligand. The coordination geometry around copper ion is distorted octahedron in which each copper ion is coordinate to two nitrogen atoms of one phenanthroline molecule and four oxygen atoms of two bridging oxalate ligands. The Cu(II) ions are linked through oxalate ligands to create one-dimentional polymeric zigzag chain along the a-axis (Figure 42). The distance between each pair of Cu(II) ions within the polymeric chains is 5.540 Å. Two bridging oxalate ligands are in *cis*-position. The coordination mode for each oxalate ligands is bis-chelate bridging. The planes of phenanthroline molecules within the chains are in the alternative left or right positions (Figure 41). The Cu-O and Cu-N bond distance are longer than those observed in dimeric oxalato copper(II) complex (Castillo *et al.*, 1999, Tang et al., 2000 and Youngmee *et al.*, 2006) . The average bite

angle of phenanthroline and oxalate are 81.4° and 78.0°, respectively. The planes of phenanthroline in adjacent chain are nearly perpendicular to each other (Figure 42b). The packing of **4** along *a*-, *b*- and *c*-axes are shown in Figure 42. The interplanar distance between parallel phenanthroline plane is 9.159 Å which is too far to form π-π interaction. No hydrogen bondings are observed in **4**.

Table 9 Crystal data and structure refinement for $[Cu_2(\mu\text{-}ox)_2(phen)_2]_n$ **(4)**

Formula	$[Cu_2(\mu\text{-}C_2O_4)_2(C_{12}H_8N_2)_2]_n$	
Empirical formula	C28 H16 Cu2 N4 O8	
Formula weight	663.53	
Temperature	293(2) K	
Wavelength	0.71073 Å	
Radiation type	Fine-focus sealed tube	
Radiation source	K-alpha molybdenum	
Crystal system	Triclinic	
Space group	*P1*	
Unit cell dimensions	a = 9.1594(2) Å	α = 90.155(1) °
	b = 10.1686(2) Å	β = 90.042(1) °
	c = 13.3489(1) Å	γ = 89.983(1) °
Volume	1243.29(4) Å ^{3}	
Z	2	
Density (calculated)	1.329 Mg/m^3	
Absorption coefficient	1.331 mm^{-1}	
F(000)	501	
θ range for data collection	1.53 to 30.44°	
No. of reflections collected	9217	
No. of independent reflections	7822 [R_{int} = 0.0186]	
No. of reflection > 2σ(I), n	5732	
No. of parameter, p	840	
Refinement method	Full-matrix least-squares on F^2	
Goodness-of-fit on F^2	S = 0.945	
Final $R_1 = \Sigma\|\|F_0\| - \|F_c\|\| / \Sigma\|F_0\|$	0.0361	
Final $wR_2 = \Sigma w(F_0^2 - F_c^2)^2 / \Sigma w(F_0^2)^2]^{½}$	0.0864	

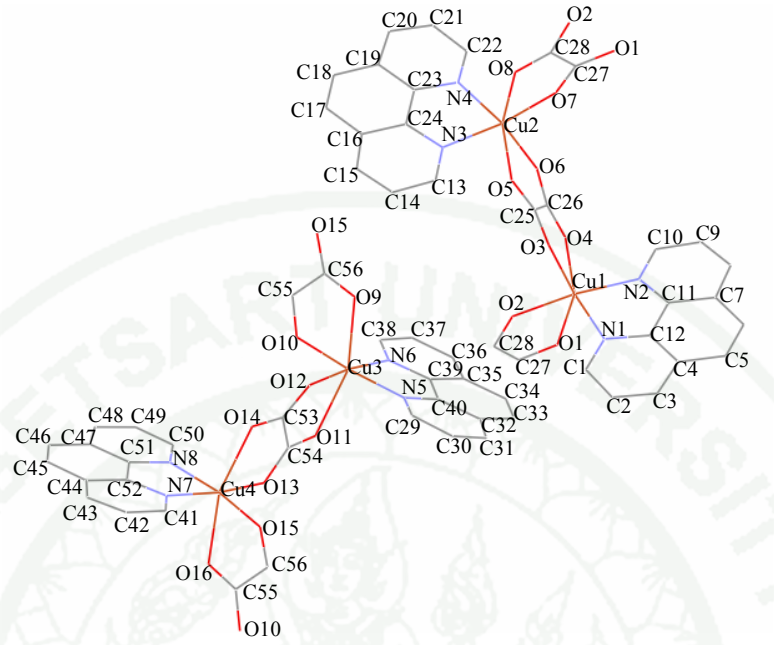

Figure 40 Schematic view of $[Cu_2(\mu\text{-ox})_2(phen)_2]_n$ **(4)** showing the numbering scheme

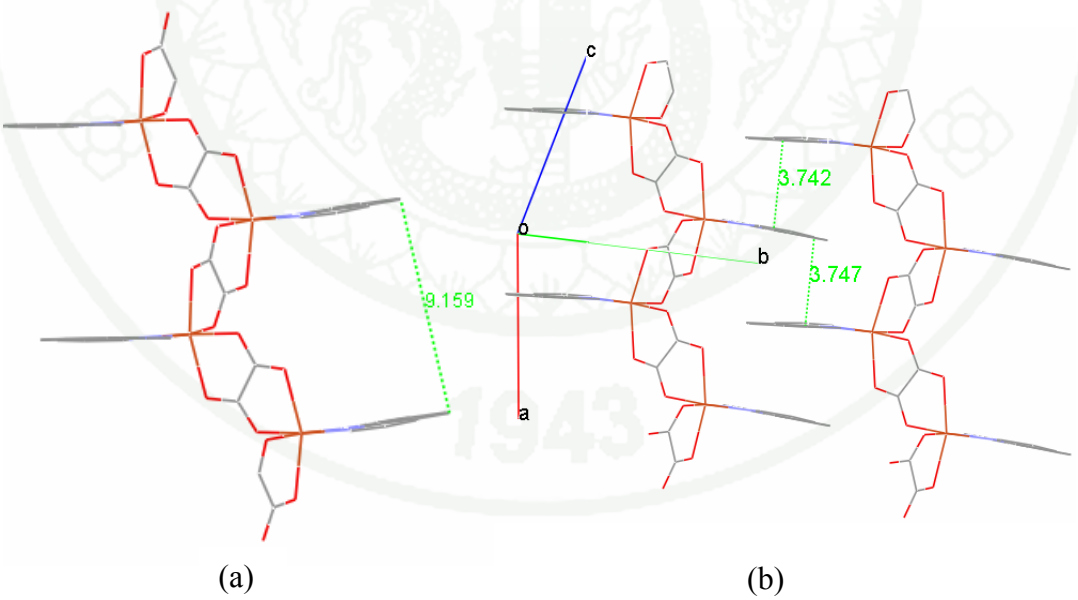

(a) (b)

Figure 41 (a) Interplanar distance of phenanthroline ring and (b) π-π interchain interaction in $[Cu_2(\mu\text{-ox})_2(phen)_2]_n$ **(4)**

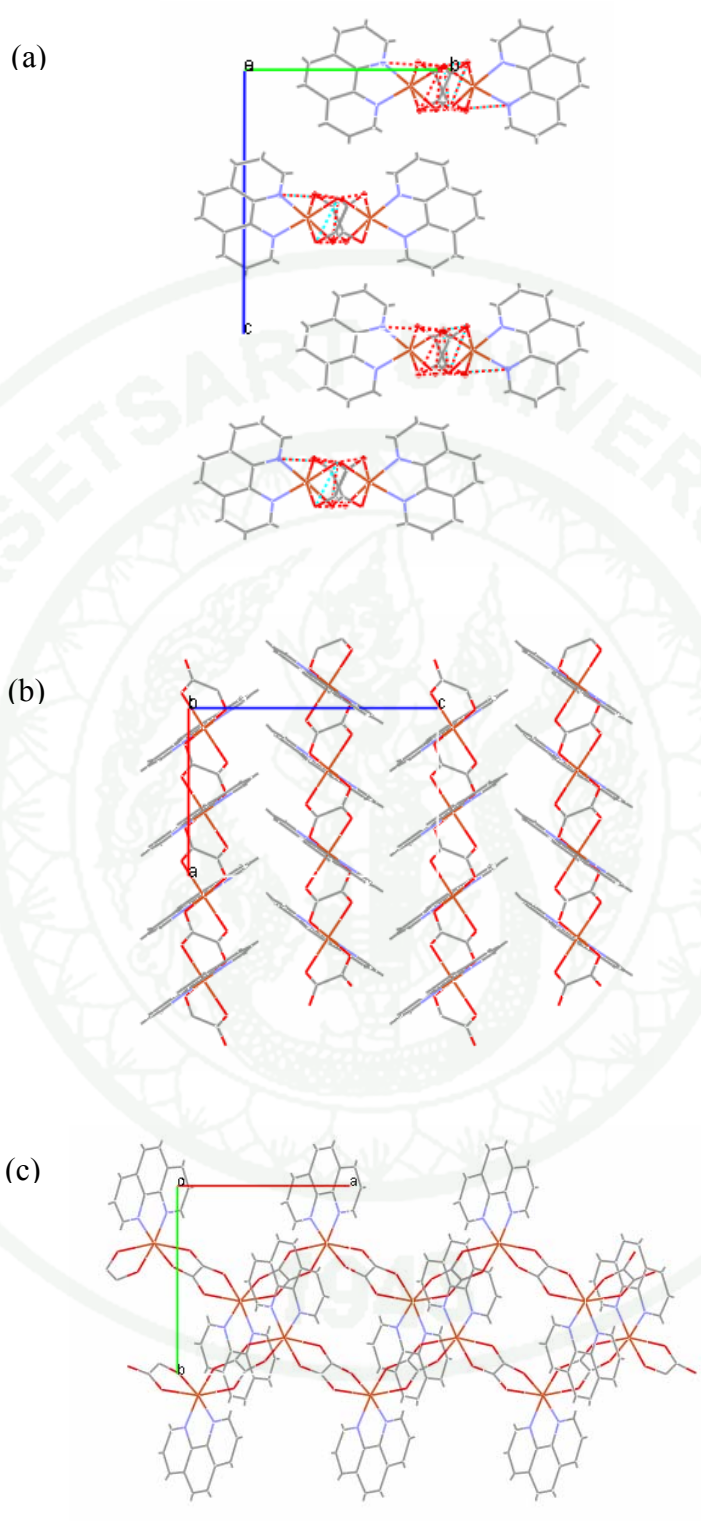

Figure 42 Packing structure of $[Cu_2(\mu\text{-ox})_2(phen)_2]_n$ **(4)** view along (a) *a*-axis, (b) *b*-axis and (c) *c*-axis.

1.1.4 $[Cu(\mu\text{-}SO_4)(phen)(H_2O)_2]_n$ **(6)**

Complex **6** crystallizes in monoclinic system with cell dimensions: a = 14.9017(8) Å, b = 13.8668(8) Å, c = 7.0277(4) Å, $\alpha = \gamma = 90°$, β= 108.506(2)° with the *Cc* space group. From 4694 reflections collected, which included all duplicate and equivalent reflections, 3035 independent reflections were obtained by averaging. Of those, 2931 reflections whose intensity were greater than $2\sigma(I)$ were used in the structure solution and least-square refinements. The program SHELXTL 97 (sheldrick, G.M. 1997) was used for structure solution and structure refinement. Some hydrogen atoms were located in a diffraction Fourier map and refined isotropically. All hydrogen atoms are included in the final refinement. The Goodness-of-fit on F^2 (S) was S = 0.945 and final R value was 0.0272. Crystal data and structure refinement are shown in Table 10. The atomic position (x, y, z) with equivalent isotropic thermal (Ueq) parameters and the anisotropic thermal (Uij) parameter expressions are shown in Appendix B and C. Bond lengths and bond angles are summarized in Appendix D and E, respectively.

The crystal structure of **6** contains neither tartrate nor oxalate ligands. Its structure is totally different from that of complex **3**. The crystal structure of complex **6** consists of 1D coordination polymers formed by square-planar $[Cu(phen)(H_2O)_2]^{2+}$ units linked by bridging SO_4^{2-} ions via the axial coordination sites (Figure 43). In each octahedral copper(II) unit, the equatorial plane is defined by two *cis*-nitrogen doners from, one phenanthroline molecule and two oxygen donors from two aqua ligands and the axial positions are occupied by two bidentate sulfate ligands. Those planar phenanthroline molecules lie parallel along the chain and nearly perpendicular to the chain extension direction. The interesting feature of this structure is the parallel double chain structure. In the double chains structure, each phenanthroline ligand on one single chain is inserted into the interspaces of the closet two phenanthroline ligands of the other single chain. Consequently, all phenanthroline planes in double chain are parallel to each other. The distance between the closest two phenanthroline planes on single chain is 8.097 Å and on double chain is 3.445 Å. The structure is thus stabilized by interchain

Table 10 Crystal data and structure refinement for $[Cu(\mu\text{-}SO_4)(phen)(H_2O)_2]_n$ **(6)**

Formula	$[Cu(\mu\text{-}SO_4)(C_{12}H_8N_2)(H_2O)_2]_n$
Empirical formula	C12 H8 Cu N2 O6 S
Formula weight	371.82
Temperature	293(2) K
Wavelength	0.71073 Å
Radiation type	Fine-focus sealed tube
Radiation source	K-alpha molybdenum
Crystal system	Monoclinic
Space group	*Cc*
Unit cell dimensions	a = 14.9017(8) Å
	b = 13.8668(8)Å β = 108.506(2) °
	c = 7.0277(4) Å γ = 90°
Volume	1377.10(13) $Å^3$
Z	2
Density (calculated)	1.534 Mg/m^3
Absorption coefficient	0.946 mm^{-1}
F(000)	646
θ range for data collection	2.06 to 30.19°
No. of reflections collected	4694
No. of independent reflections	3035 [R_{int} = 0.0154]
No. of reflection > 2σ(I), n	2931
No. of parameter, p	211
Refinement method	Full-matrix least-squares on F^2
Goodness-of-fit on F^2	S = 1.110
Final $R_1 = \Sigma\|\|F_0\| - \|F_c\|\| / \Sigma\|F_0\|$	0.0272
Final $wR_2 = \Sigma w(F_0^2 - F_c^2)^2 / \Sigma w(F_0^2)^2]^{½}$	0.0848

π-π interaction. In addition, the double chain structure is also stabilized by hydrogen bonding between sulfate ion and aqua ligand. Two types of hydrogen bond are observed. One is the intrachain hydrogen bonds (O-O = 2.608 Å), the other is interchain hydrogen bonds (O-O =2.660 Å). The interesting feature of **6** is its double one-dimensional chains structures. These two one-dimensional chains lie parallel to each other along *c*-axis (Figure 44). The packing of **6** along *a*- *b*- and *c*- axes are shown in Figure 45.

The equatorial Cu-O band distances are 1.955(4) Å and 2.002 Å, while those axial Cu-O bond distances are 2.483 and 2.476 Å. Such long bond distances indicate the existence of Jahn-Teller distortion on copper ions along axial position. A copper (II) ion has nine *d* electrons, Jahn-Teller distortion causes a splitting of e_g and t_{2g} orbital. In this case, the severe elongation in z direction is observed, therefore the axial Cu-O bonds must be very week. Similar observation was found in $[Cu(phen)(\mu\text{-}SO_4)(C_2H_8N)_2]_n$. The Cu-O (sulfate) bond lengths are 2.3575(9) and 2.4673(9) Å (Lutz *et al.*, 2010).

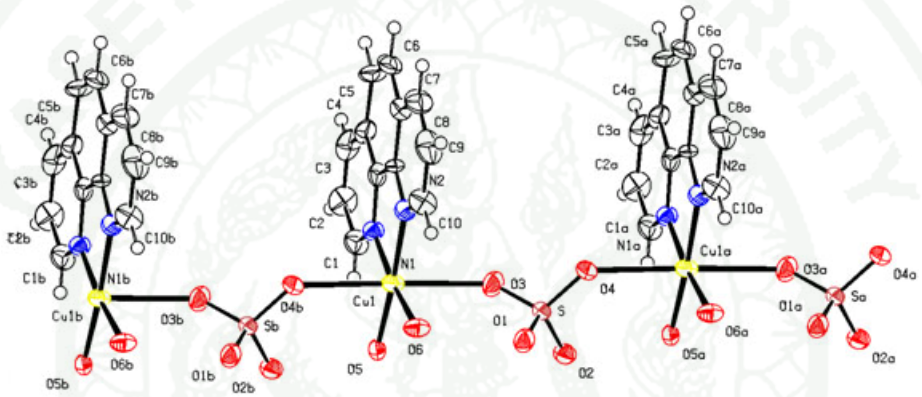

Figure 43 An ORTEP view of $[Cu(\mu\text{-}SO_4)(phen)(H_2O)_2]_n$ **(6)** showing the numbering scheme.

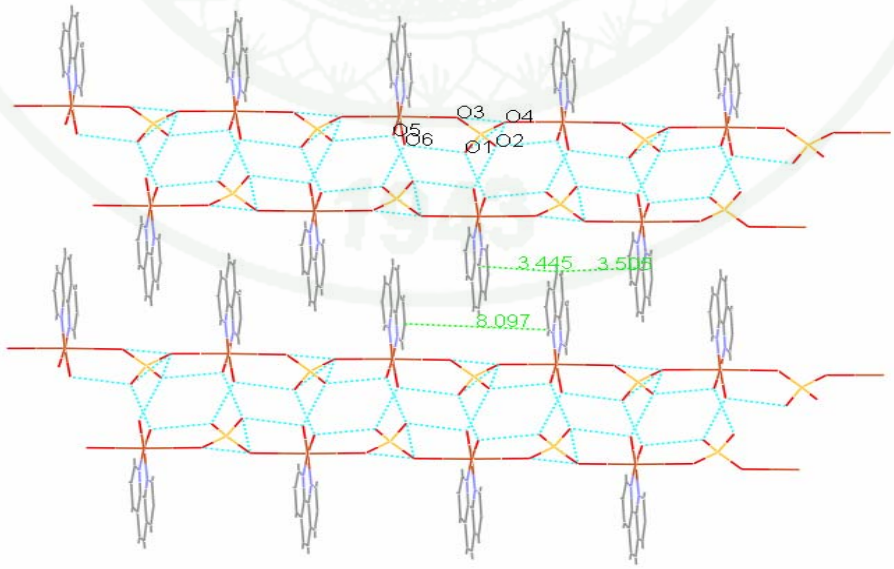

Figure 44 H-bonding and π-π distance (Å) of $[Cu(\mu\text{-}SO_4)(phen)(H_2O)_2]_n$ **(6).**

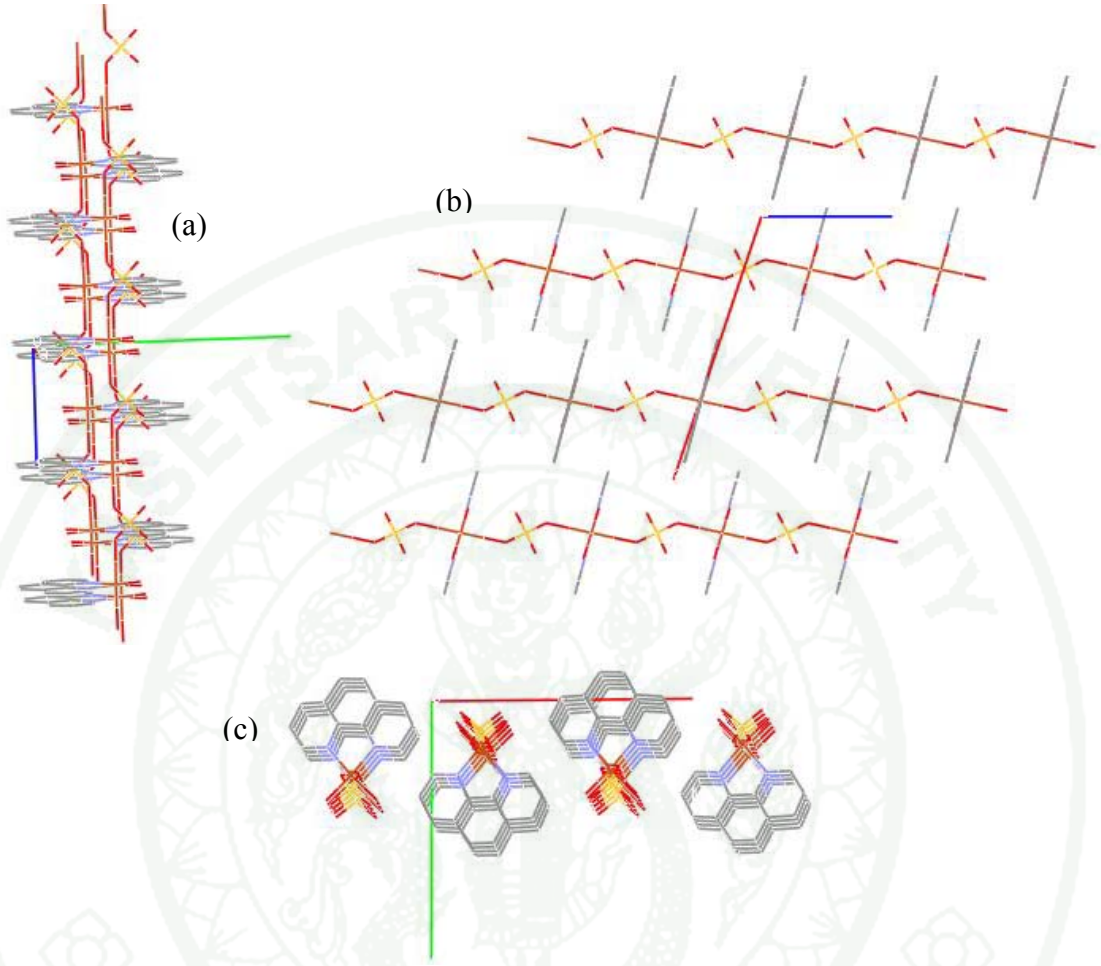

Figure 45 Packing structure of $[Cu(\mu\text{-}SO_4)(phen)(H_2O)_2]_n$ **(6)** view along (a) *a*-axis, (b) *b*-axis and (c) *c*-axis.

1.2 The crystal structure of the manganese(II) complexes

1.2.1 *cis*-$[Mn(phen)_2Cl_2]$ **(11)**

Complex **11** crystallizes in monoclinic system with cell dimensions: a = 9.4651(3) Å, b = 15.1921(6) Å, c = 14.5131(6) Å, $\alpha = \gamma = 90°$, β= 98.9840(10)° with the $P2_1/c$ space group. From 15302 reflections collected, which included all duplicate and equivalent reflections, 6007 independent reflections were obtained by averaging. Of those, 5312 reflections whose intensity were greater than

2σ(I) were used in the structure solution and least-square refinements. The program, SHELXTL 97 (sheldrick, G.M. 1997), was used for structure solution and structure refinement. All hydrogen atoms were located in a diffraction Fourier map and refined isotropically. The Goodness-of-fit on F^2 (S) was S = 1.066 and final R value was 0.0286. Crystal data and structure refinement are shown in Table 11. The atomic position (x, y, z) with equivalent isotropic thermal (Ueq) parameters and the anisotropic thermal (Uij) parameter expressions are shown in Appendix B and C. Bond lengths and bond angles are summarized in Appendix D and E, respectively.

The crystal structure of **11** consists of two phenanthroline ligands and two chloride ion forming the distorted octahedron around Mn(II) as shown in Figure 46. All ligands are in cis position. The square plane is occupied by two nitrogen donors of a phenanthroline (N3, N4), one nitrogen donor (N1) of the other phenanthroline molecule and a chloride atom (Cl1). The second chloride atom (Cl2) and the other nitrogen atom (N2) of phenanthroline are at the axial positions. Two phenanthroline planes are almost perpendicular. The packing of this mononuclear complex are shown in Figure 47. There is extended π-π stacking of the conjugated ring systems, characterized by the interplanar distance of 3.557 Å (Figure 48). Since there is no water in the lattice of complex **11**, hence no hydrogen bonds are formed.

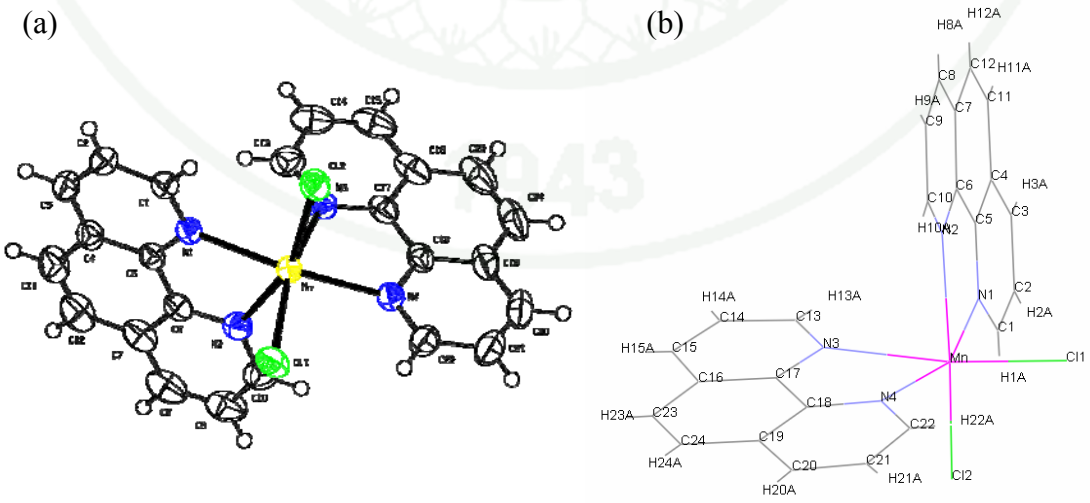

Figure 46 (a) ORTEP view and (b) schematic view of *cis*-$[Mn(phen)_2Cl_2]$ **(11)** showing the numbering scheme.

Table 11 Crystal data and structure refinement for *cis*-$[Mn(phen)_2Cl_2]$ **(11)**

Formula	$[Mn(C_{12}H_8N_2)_2(Cl)_2]$	
Empirical formula	C24 H16 Cl2 Mn N4	
Formula weight	486.25	
Temperature	293(2) K	
Wavelength	0.71073 Å	
Radiation type	Fine-focus sealed tube	
Radiation source	K-alpha molybdenum	
Crystal system	Monoclinic	
Space group	$P2_1/c$	
Unit cell dimensions	a = 9.4651(3) Å	α = 90°
	b = 15.1921(6) Å	β = 98.984(1)°
	c = 14.5131(6) Å	γ = 90°
Volume	2061.30(13) $Å^3$	
Z	4	
Density (calculated)	1.567 Mg/m^3	
Absorption coefficient	0.920 mm^{-1}	
F(000)	988	
θ range for data collection	1.95 to 30.51°	
No. of reflections collected	15302	
No. of independent reflections	6007 [R_{int} = 0.0148]	
No. of reflection > 2σ(I), n	5312	
No. of parameter, p	280	
Absorption correction	None	
Refinement method	Full-matrix least-squares on F^2	
Goodness-of-fit on F^2	S = 1.066	
Final $R_1 = \Sigma\|\|F_0\| - \|F_c\|\| / \Sigma\|F_0\|$	0.0286	
Final $wR_2 = \Sigma w(F_0^2 - F_c^2)^2 / \Sigma w(F_0^2)^2]^{½}$	0.0828	

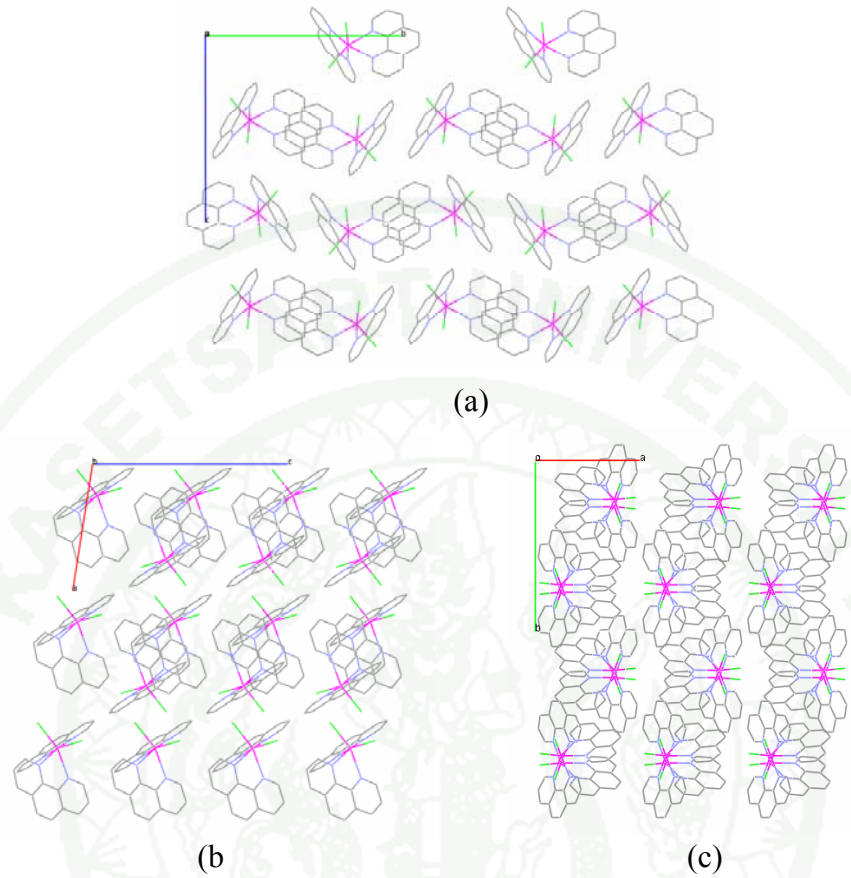

Figure 47 Packing structure of *cis*-[Mn(phen)$_2$Cl$_2$] **(11)** view along (a) *a*-axis, (b) *b*-axis and (c) *c*-axis.

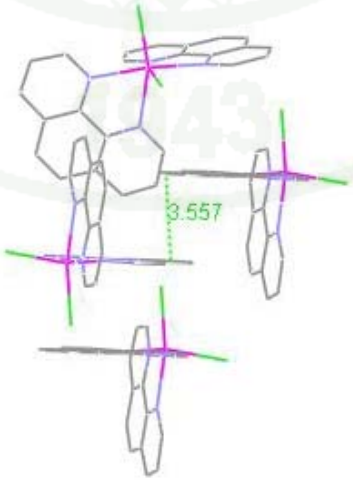

Figure 48 π-π stacking of the conjugated ring systems in *cis*-[Mn(phen)$_2$Cl$_2$] **(11).**

2. HPLC study

Chromatogram of a mixture of copper(II) nitrate trihydrate, phenanthroline and malic acid obtained under the conditions described in the experimental section is shown in Figure 49. Eight fractions of cooking mixture were collected every 3 hours (0, 3, 6, 9, 12,18, 21 and 24 hours) and their chromatograms are shown in Figure 48. The retention time of malate ions at 11.538 min is observed before the mixture was heated. After cooking for 3 hours, two new groups of peaks appear at 9.373, 10.285 and 17.111, 17.334 min. All chromatograms display similar patterns showing two peaks between 9.27-10.086 min. It may be concluded that the conversion of malate ions into oxalate ions started before the reaction time of 3 hours and was completed after 12 hours. It was reported that malate, gallate and tartrate were the least stable among low molecular weight carboxylates. The first two ions began to decompose upon addition of to the 6m NaOH even at room temperature. The major reaction products of most of the decomposing carboxylates were oxalate, acetate and formate. The proposed mechanism is shown in scheme G. Consequently, the oxalate complex of Cu(II) was obtained (complex **1**).

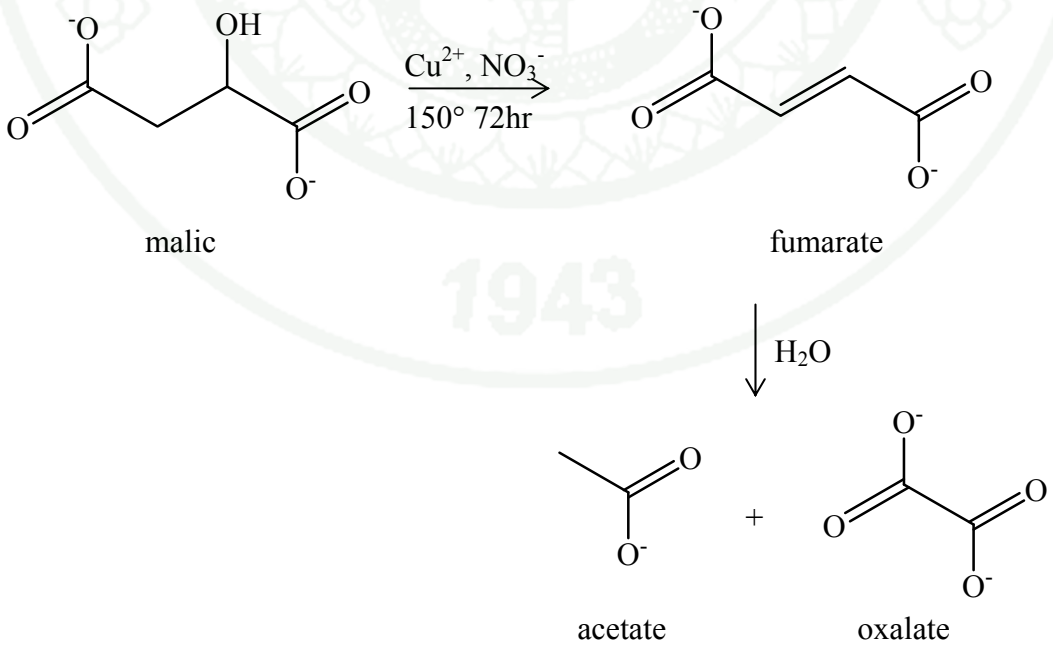

Scheme G The proposed mechanism for the decomposition of malate.

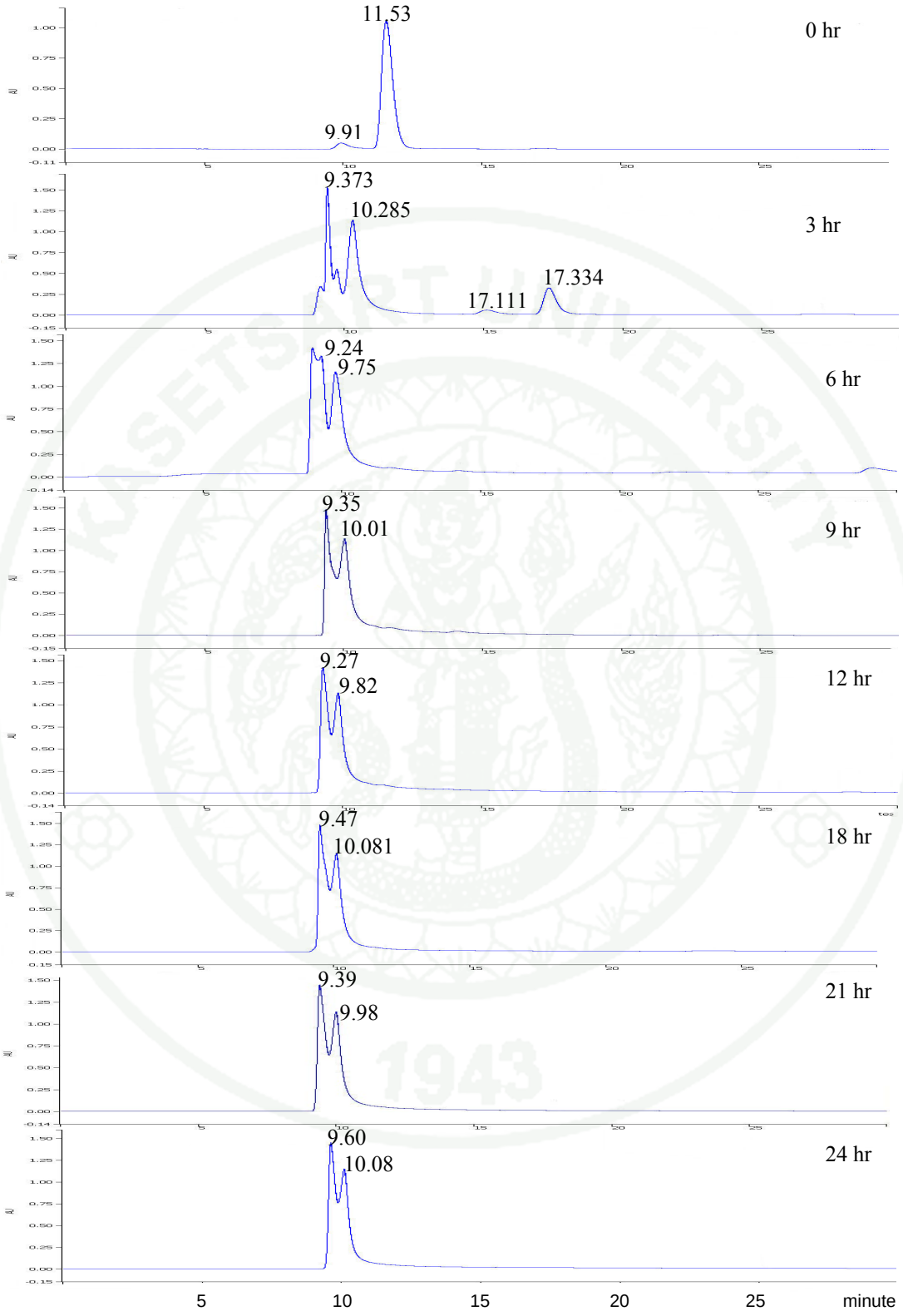

Figure 49 Chromatogram of a mixture of copper(II)nitrate trihydrate, phenanthroline and malic acid.

3. Spectral and Thermal properties

3.1 Fourier Transform Infrared spectroscopy

Total fifteen FTIR spectra were recorded. Some complexes exhibit similar patterns. Therefore the spectra obtained are grouped according to the similarity of pattern into 5 groups (Table 12). The FTIR spectra of four dicarboxylic acids and phenanthroline, which were used as reactant, are shown in Figure 50-54 and are used for comparision with the spectra of the complexes.

Table 12 Grouping of the studied complexes according to the similarity of infrared spectra

Group 1	Complexes containing oxalate and phenanthroline ligands.
	$[Cu(ox)(phen)(H_2O)]\cdot H_2O$ **(1)**
	$[Cu(\mu\text{-}ox)(phen)]_n$ **(3)**
	$[Cu_2(\mu\text{-}ox)_2(phen)_2]_n$ **(4)**
	MnPOxW**(18)**
Group 2	Complex containing succinate and phenanthroline ligands.
	$[Cu_4(\mu\text{-}suc)_2(phen)_4(H_2O)_4](NO_3)_4\cdot 4H_2O$ **(2)**
Group 3	Complex containing sulfate and phenanthroline ligands.
	$[Cu(\mu\text{-}SO_4)(phen)(H_2O)_2]_n$ **(6)**
Group 4	Complexes containing only phenanthroline ligand.
	CuCMa **(7)**
	CuCTa **(8)**
	cis-$[Mn(phen)_2Cl_2]$ **(11)**
	MnPMaW **(15)**
	MnPTaW **(16)**
	MnPSuW **(17)**

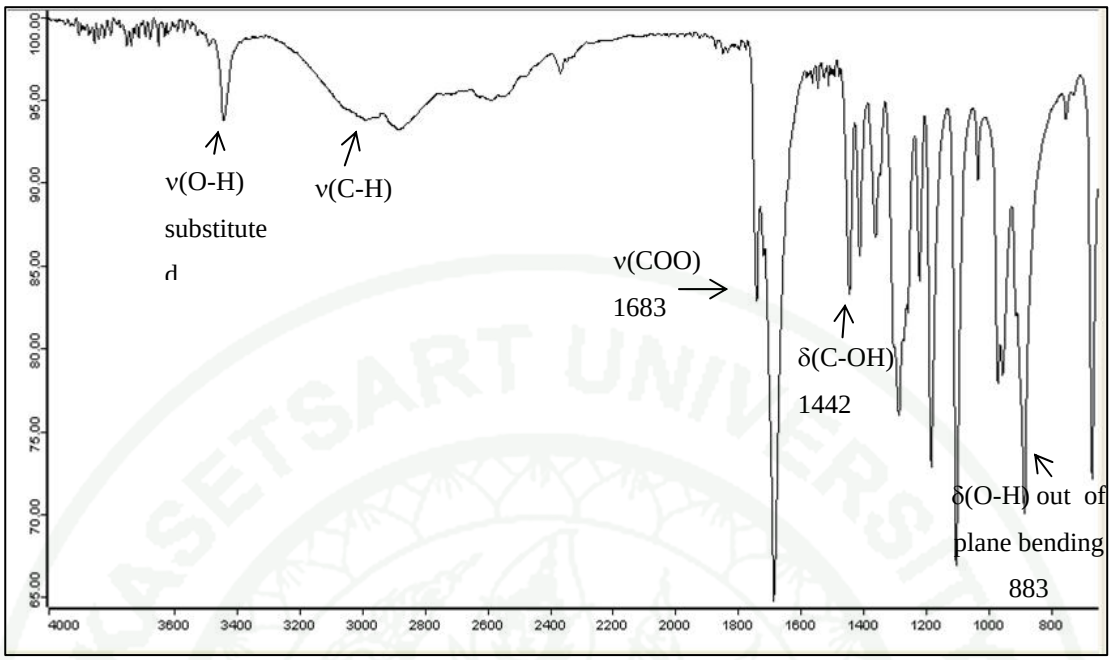

Figure 50 FTIR spectra (ATR technique) of malic acid

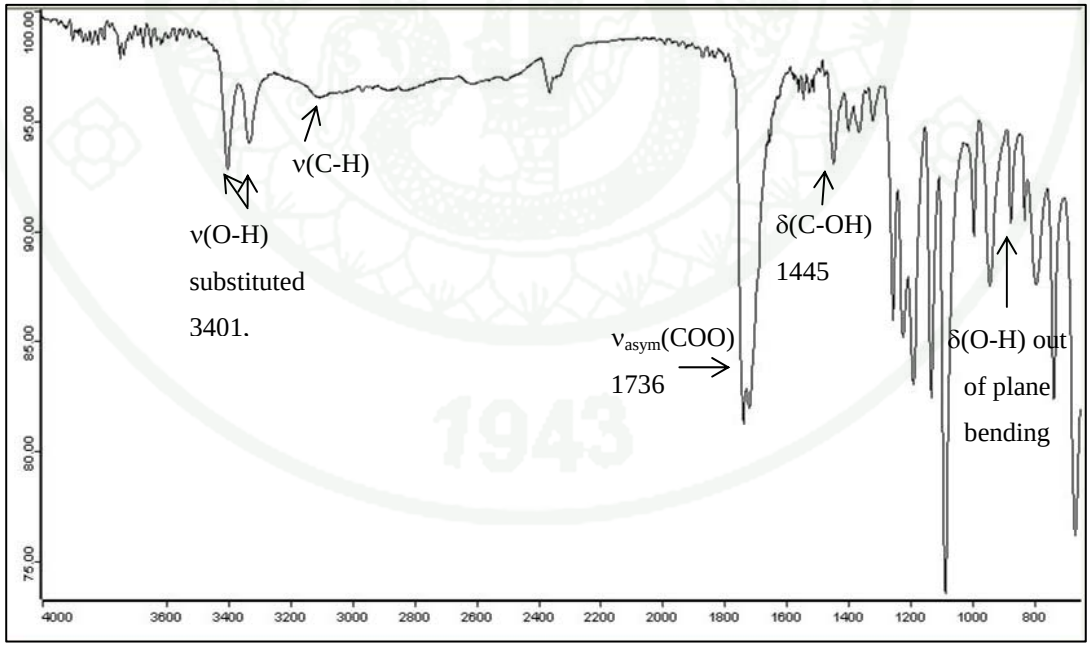

Figure 51 FTIR spectra (ATR technique) of tartaric acid

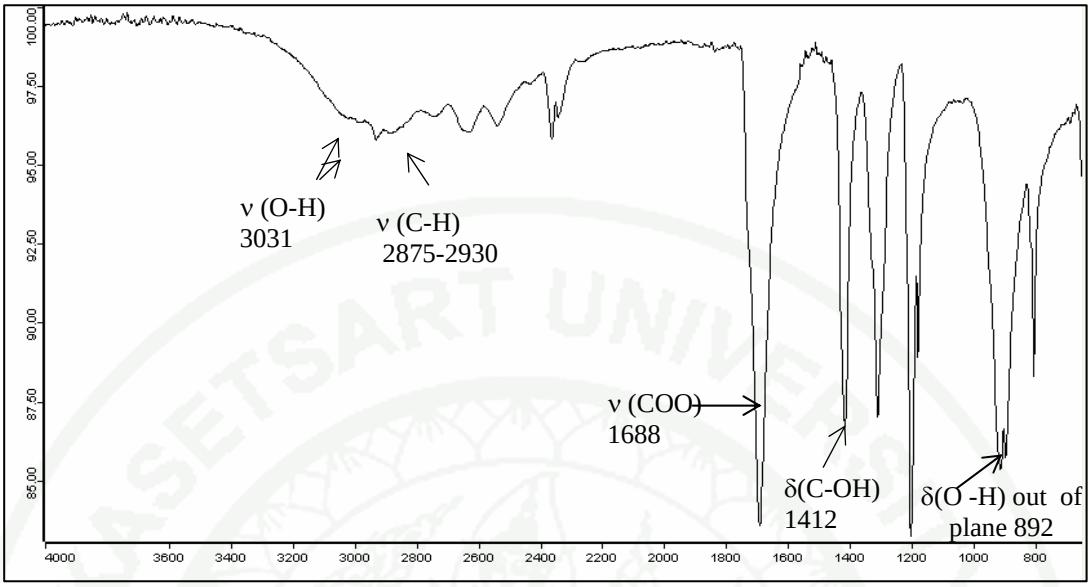

Figure 52 FTIR spectra (ATR technique) of succinic acid.

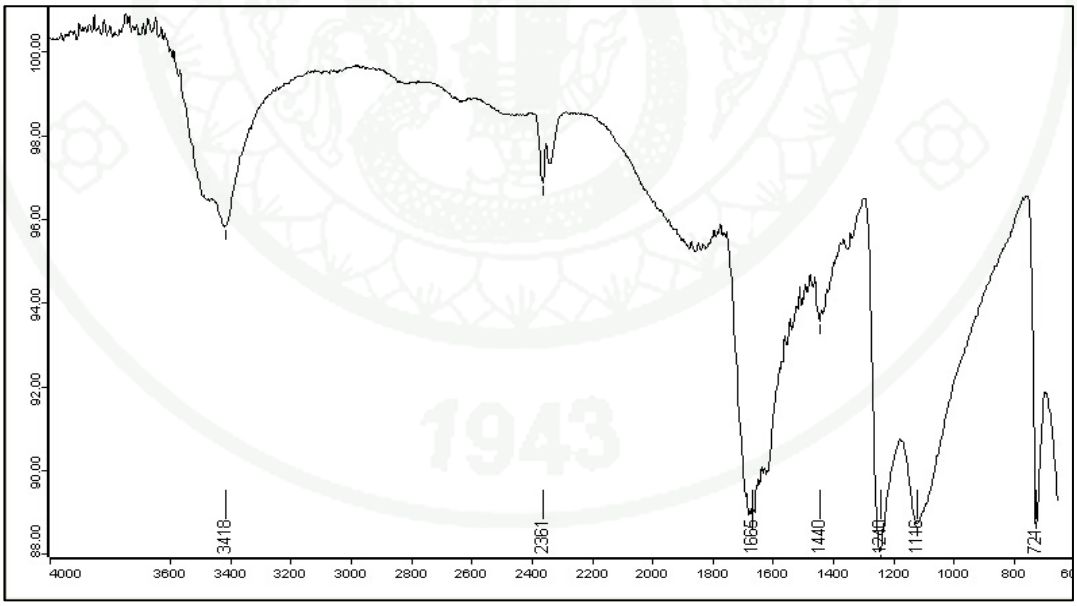

Figure 53 FTIR spectra (ATR technique) of oxalic acid

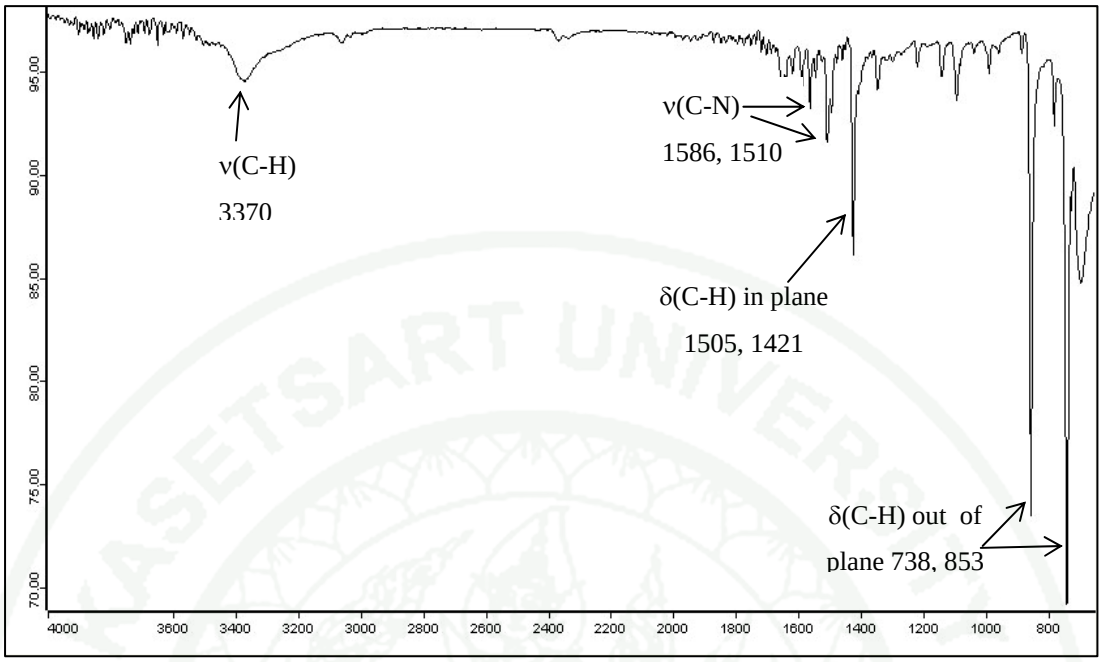

Figure 54 FTIR spectra (ATR technique) of phenanthroline

Group1: The crystal structures of $[Cu(phen)(ox)(H_2O)]\cdot H_2O$ **(1)**, $[Cu(\mu\text{-}ox)(phen)]_n$ **(3)** and $[Cu_2(\mu\text{-}ox)_2(phen)_2]$ **(4)** discussed in section 1 show that oxalate ligands exist as chelate (bidentate) or bis bridge (tetradentate) (Table13). The oxalate ligand in **1** acts as chelate ligand (bidentate ligand) and in **3** and **4** as chelate bridging ligand (tetradentate ligand) between two copper ions. Consequently, complex **1** contains two types of C-O bond which are quite different in bond length (see scheme A-B). For complex **3** and **4**, all four oxygen atoms are coordinated to copper ions thus all C-O bond length are not much different (Scheme I and J). These conclusions are supported by the C-O vibrations observed in their FTIR spectra. Two $\nu(COO)_{asym}$ peaks at 1665 and 1708 cm^{-1} are observed for complex **1** while only one peak at 1660 cm^{-1} was observed for complex **3** and **4**. All assigned peaks involve oxalate and phenanthroline are listed in Table 14 and Figure 55-58.

The spectra of MnPOxW **(18)** displays similar vibrational pattern as complex **1**, **3** and **4** (Figure 58). Consequently, It can be concluded that this compound **(18)** contains oxalate and phenanthroline ligands. Since the crystals of **18** are not suitable for X-ray diffraction experiment, thus no molecular structure is reported.

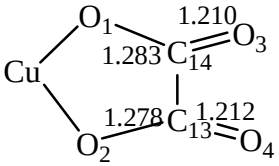

Scheme H

for **1**

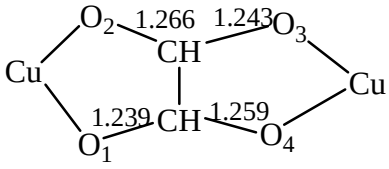

Scheme I

for **3**

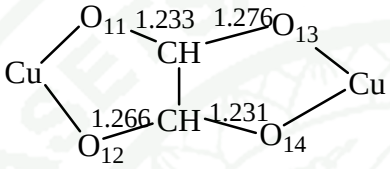

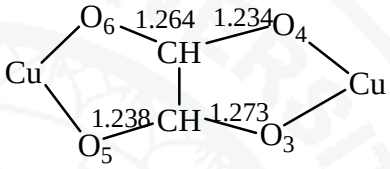

Scheme J

for **4**

Table 13 Coordination modes of oxalate ligand in the studied complexes.

Complex	Coordination mode
$[Cu(phen)(ox)(H_2O)]\cdot H_2O$ **(1)**	chelate (bidentate)
$[Cu(\mu\text{-}ox)(phen)]_n$ **(3)**	bis bridging (tetradentate)
$[Cu_2(\mu\text{-}ox)_2(phen)_2]_n$ **(4)**	bis bridging (tetradentate)

Group 2 : Complex containing succinate and phenanthroline ligands.

The infrared spectrum of **2** displays the vibrational peaks for succinate, phenanthroline and nitrate ligand as shown in Table 15 and Figure 59.

Group 3 : Complex containing sulfate phenanthroline ligands.

The reaction of $CuSO_4$, phenanthroline and tartaric acid results in polymeric sulfate bridge complex $[Cu(\mu\text{-}SO_4)(phen)(H_2O)_2]_n$. Its infrared spectrum exhibit sulfate and phenanthroline peaks. No peaks of tartaric ligand are observed (Figure 60 and Table 16).

Table 14 Vibrational frequencies (cm^{-1}) in the IR spectra of Group 1 Complexes.

Complex	aqua	oxalate			phenanthroline			
		ν_{asym} (COO)	ν_{sym} (COO)	δ(OCO)	ν_{C-H}	ν_{C-N}	δ_{C-H} in plane	δ_{C-H} out of plane
Phen		-	-	-	3077	1550, 1510	1410	730, 855
Oxalic acid	3418	1665	1440, 1240	721	-	-	-	-
$[Cu(ox)(phen)(H_2O)]\cdot H_2O$ (**1**)	3465 (aqua)	1708,1665	1434, 1256	792	3077	1586, 1521	1398	724, 865
$[Cu(\mu\text{-}ox)_2(phen)]$ (**3**)		1661	1426,1294	793	3077	1596, 1518	1343	753, 825
$[Cu_2(\mu\text{-}ox)_2(phen)_2]$ (**4**)		1661	1426,1294	793	3075	1596, 1519	1343	723, 875
MnPOx (**18**)		1668	1423,1313	791	3075	1606, 1518	1343	724, 825
$[Cu_2(\mu\text{-}C_2O_4)_2(bpy)_2(H_2O)(NO_3)_2]$ [1]		1638	1350	820	-	-	-	-
$[Cu(dpyam)_4(\mu\text{-}C_2O_4)_2](ClO_4)_2(H_2O)_3$ [2]		1647	1375	843	-	-	-	-
$[Cu(pya)(C_2O_4)(H_2O)]\cdot(H_2O)$ [3]		1716,1660	1411,1278	843	-	-	-	-
$[Cu_2(bipy)_2(H_2O)(C_2O_4)^*]X_2\cdot[Cu(bipy)(C_2O_4)^{**}]$ [4] X= NO_3^-, BF_4^- or ClO_4^-								
**bidentate		1720, 1670	1410,1280	780	-	-	-	-
*tetradentate		1650, 1645	1350,1315	800	-	-	-	-
$[Cu(ox)(Him)_2]_n$ [5] Him= imidazole		1630	1415	-	-	-	-	-

[1] Tang, J. *et al.*, 2000. **J. Mol. Struc.** 525: 271-275
[2] Youngmee, S. *et al.*, 2003. **Inorg Chim Act**a 353:119-128
[3] Androš, L. *et al.*, 2010. **Polyhedron.** 29:1291-1298
[4] Gleize, D. *et al.* **,** 1992. **J. Chem. Soc., Dalton Trans.** 3209 – 3216
[5] Stamatatos, T. C. *et al.* **,** 2009. **Inorg. Chem. Commu.** 12:402-405

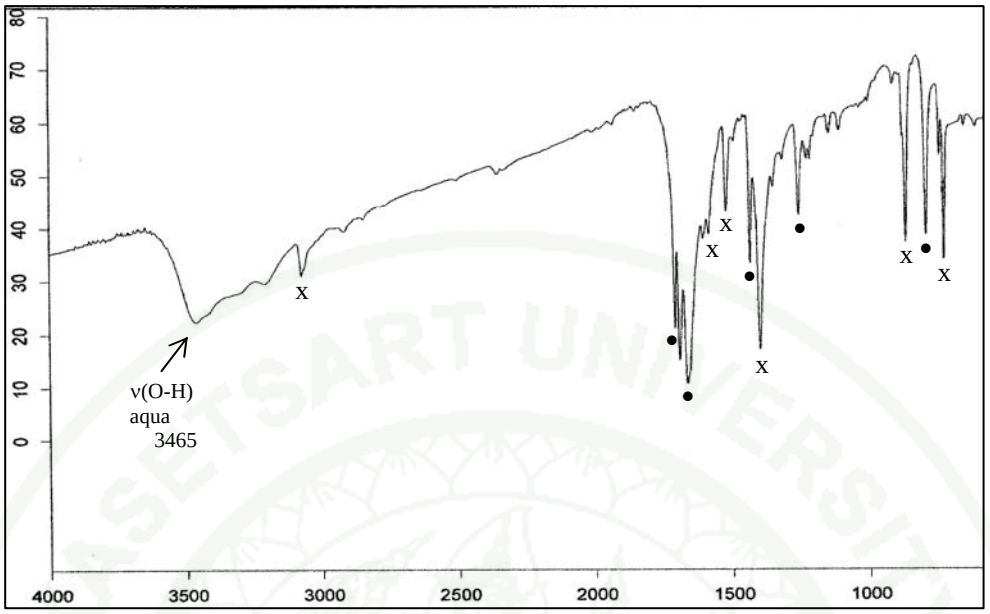

Figure 55 FTIR spectra (ATR technique) of [Cu(ox)(phen)(H_2O)]· H_2O **(1)**.

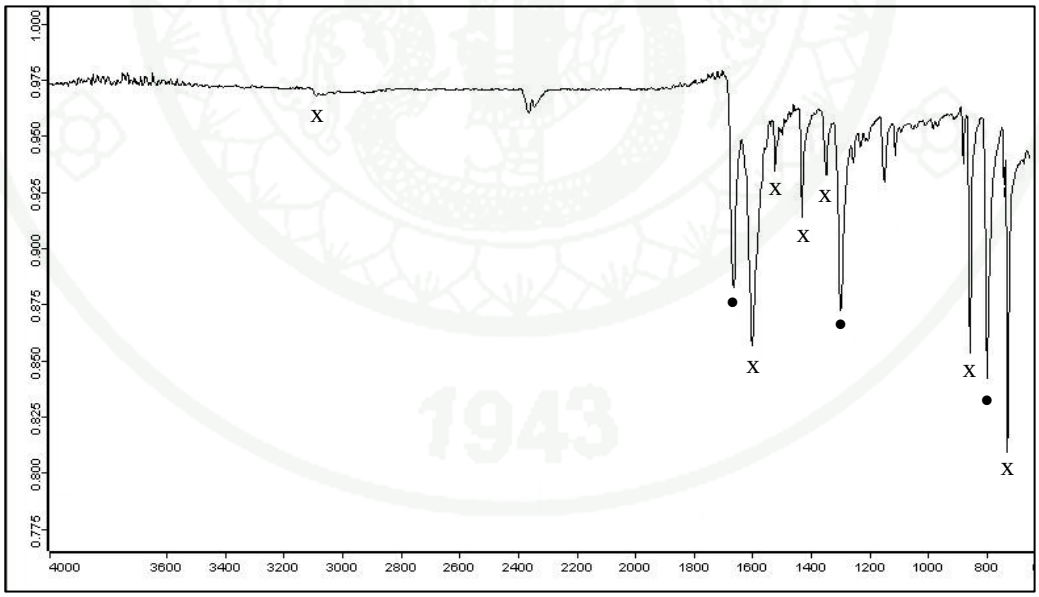

Figure 56 FTIR spectra (ATR technique) of $[Cu(\mu\text{-ox})(phen)]_n$ **(3)**

• : vibrational frequency of oxalate ion

x: vibrational frequency of phenanthroloine

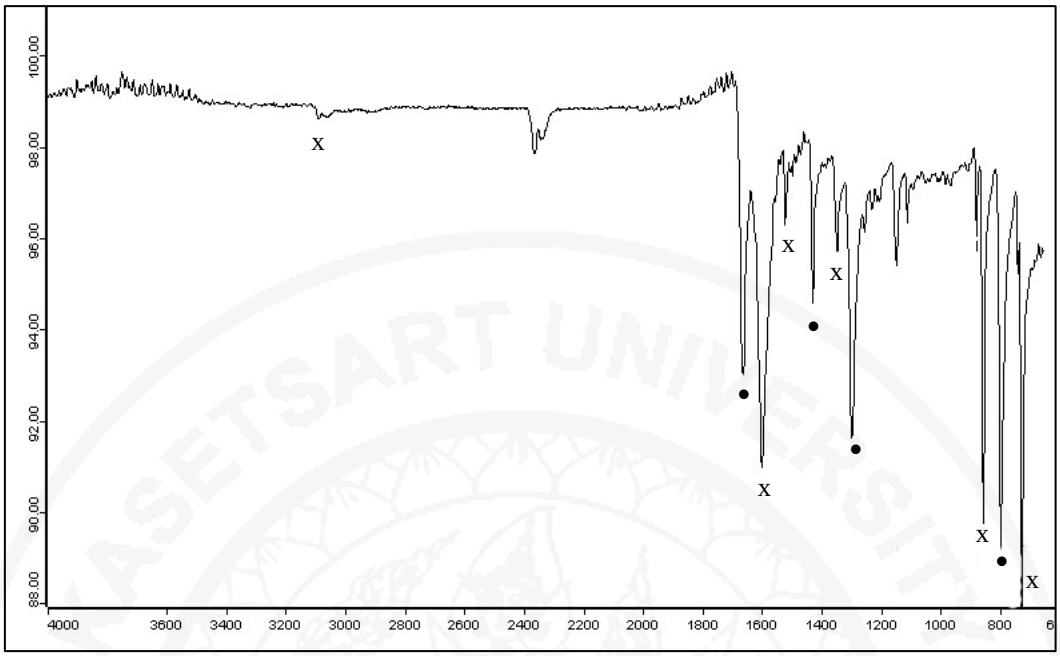

Figure 57 FTIR spectra (ATR technique) of $[Cu_2(\mu\text{-}Ox)_2(phen)_2]_n$ **(4)**

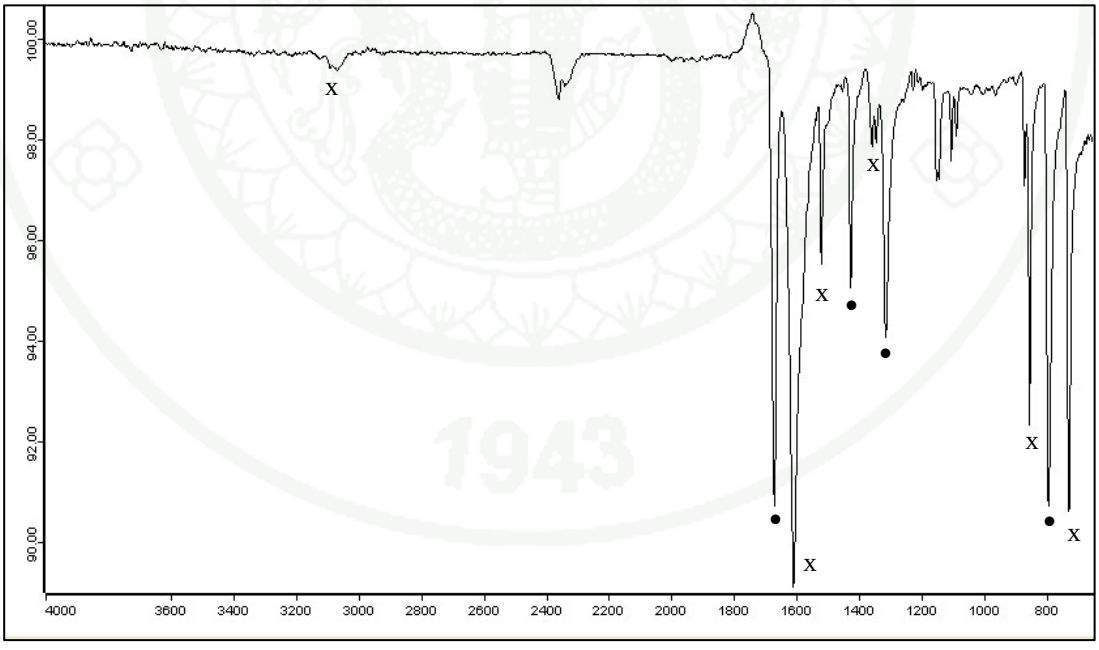

Figure 58 FTIR spectra (ATR technique) of MnPOxW **(18)**

• : vibrational frequency of oxalate ion

x: vibrational frequency of phenanthroloine

Table 15 Vibrational frequencies (cm^{-1}) in the IR spectra of group 2 complex.

Complex	succinate			phenanthroline				nitrate		
	ν_{asym} (COO)	ν_{sym} (COO)	δ(C=O)	ν_{C-H}	ν_{C-N}	δ_{C-H} in plane	δ_{C-H} out of plane	ν_{asym} (NO_2)	ν_{sym} (NO_2)	ν(N=O)
$[Cu_4(\mu\text{-suc})_2(phen)_4(H_2O)_4](NO_3)_4 \cdot 4H_2O$ **(2)**	1648	1427	787	3350	1586, 1519	1406	721, 847	1462	1302	1023
$[Cu_2(phen)_4(\mu\text{-suc})]suc^* \cdot 12.5H_2O$[1]	1608 *1558	1421 *1400			1625	1500	720	-	-	-
$[Cu_2(\mu\text{-}H_2O)(\mu\text{-suc})(phen)_2(NO_3)_2]_n$[2]	1549	1383	1180-1300		-	-	-	1428	1303	1010
$[Cu_2(\mu\text{-}H_2O)(\mu\text{-suc})(bpy)_2(NO_3)_2]_n$[2]	1556	1348	1180-1300		-	-	-	1416	1307	1005
$\{[Cu_4(\mu\text{-suc})_2(bpy)_4(H_2O)_2](ClO_4) \cdot H_2O\}$[2]	1601	1425	1180-1300		-	-	-	-	-	-
$[Cu_8(\mu\text{-suc})_4(phen)_{12}](BF_4)_8 \cdot 8H_2O$[2]	1552	1428	1180-1300		-	-	-	-	-	-

[1]M. Padmanabham *et al*., 2005. **Inorg Chim Acta** 385: 3537-3577

[2]D. Ghoshal *et al*., 2004. **Dalton Trans** 1687-1695

*vibrational frequencies for succinate counter ion

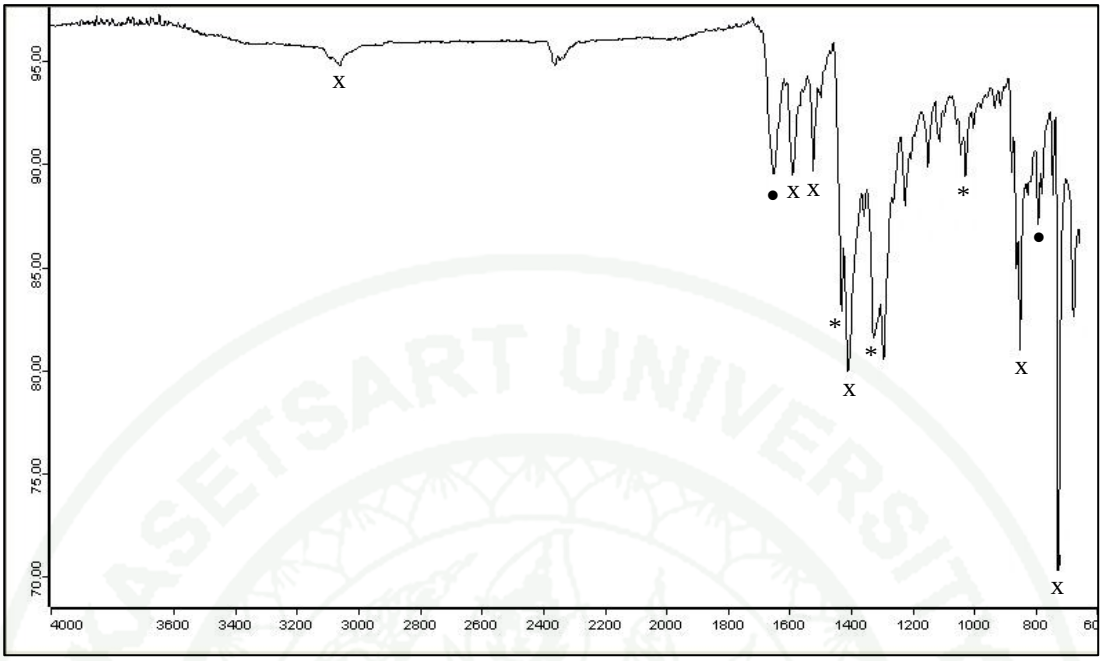

Figure 59 FTIR spectra of $[Cu_4(\mu\text{-}suc)_2(phen)_4(H_2O)_4](NO_3)_4 \cdot 4H_2O$ **(2)**

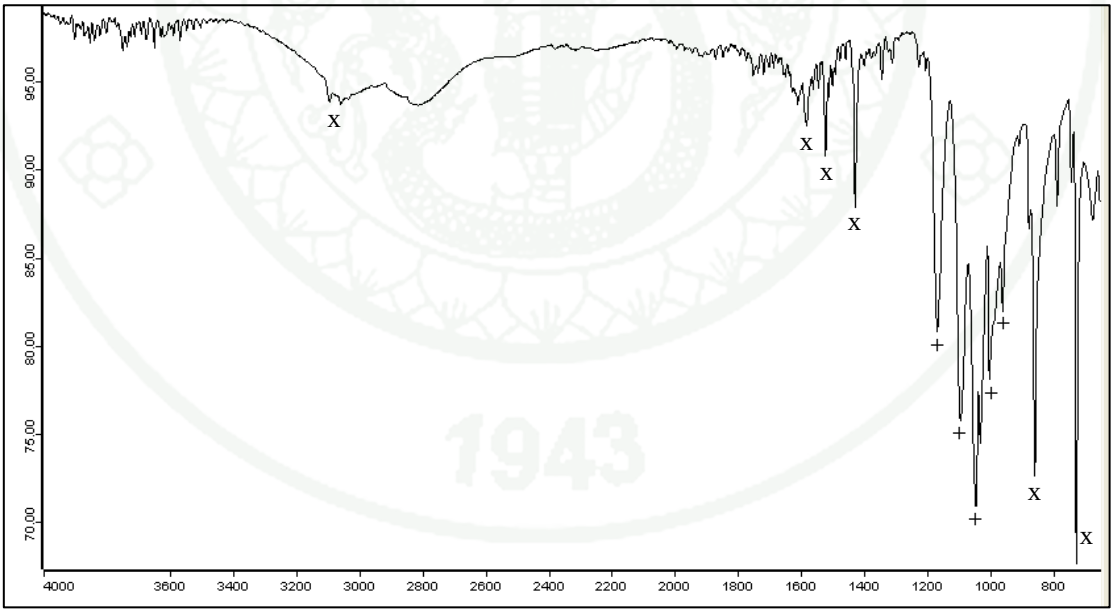

Figure 60 FTIR spectra (ATR technique) of $[Cu(\mu\text{-}SO_4)(phen)(H_2O)_2]_n$ **(6)**

• : vibrational frequency of succinate ion + : vibrational frequency of sulfate ion

x: vibrational frequency of phenanthroloine * : vibrational frequency of nitrate ion

Table 16 Vibrational frequencies (cm^{-1}) in the IR spectra of group 3 complexes.

Complex	sulfate			phenanthroline	
	ν_{asym} (SO)	ν_{sym} (SO)	ν_{C-H}	ring stretching	ring deformation
$[Cu(\mu\text{-}SO_4)(phen)(H_2O)_2]_n$ **(6)**	1165, 1092, 1043	999, 958	3075	1579, 1520, 1425	856, 723
$[Cu(SO_4)(tpm)(H_2O)] \cdot 2H_2O$[1]	1467, 1442, 1116	-	-	-	-
$[Cu(SO_4)(bpm)(H_2O)] \cdot 2H_2O$[1]	1304, 1113	-	-	-	-
$[Cu(SO_4)(bpqa)(H_2O)] \cdot 4H_2O$[1]	1279, 1157	-	-	-	-
$[Cu(phen)(SO_4)]$[2]	1255, 1202, 1161	1003	-	1580, 1509, 1425	718
$[Cu(phen)(SO_4)(H_2O)_2]$[2]	1241, 1227, 1045	1007, 928	-	1584, 1517, 1428	721

[1]P.J. Arnold *et al*, 2001. **J. Chem. Soc. Dalton. Trans** 736-746

[2]R.Olar *et al*, 2008. **J.Thermal Analysis and Calorimetry**, 92 (1): 245-251

Group 4 : Complexes containing only phenanthroline ligand.

The infrared spectra of either copper or manganese complexes in this group show only the vibrational frequencies of phenanthroline molecule (Figure 61-62 and Table 17). Complex **7** was obtained from the hydrothermal reaction of $CuCl_2$, malic acid and phenanthroline giving green crystals which is not suitable for X-ray Diffraction experiment. The spectrum shows neither malate nor oxalate peaks. Thus the malate ion did not coordinate to copper or convert into oxalate ion as in the case of using $Cu(NO_3)_2{\cdot}3H_2O$. Similar observation was found when using tartrate ligand (equation 1-4).

$Cu(NO_3)_2{\cdot}3H_2O$ + 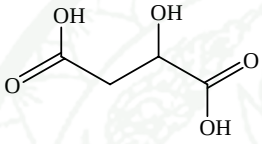 + $C_{12}H_8N_2$ ⟶ $[Cu(ox)(phen)(H_2O)]{\cdot}H_2O$ **(1)** ----(1)

malic acid phen green rod crystal

$Cu(NO_3)_2{\cdot}3H_2O$ + 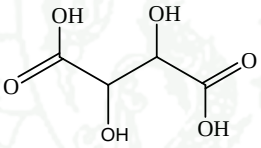 + $C_{12}H_8N_2$ ⟶ $[Cu(\mu\text{-}ox)(phen)]_n$ **(3)** ----(2)

tartaric acid phen green plate

$CuCl_2$ + 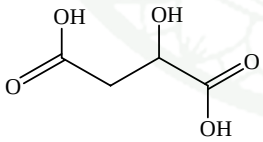 + $C_{12}H_8N_2$ ⟶ CuCMa **(7)** ----(3)

malic acid phen green crystal

$CuCl_2$ + 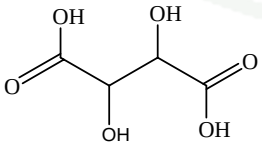 + $C_{12}H_8N_2$ ⟶ CuCTa **(8)** ----(4)

tartaric acid phen green crystal

According to the infrared spectra, complex **7** and **8** must contain at least phenanthroline ligand but contain no dicarboxylic acids.

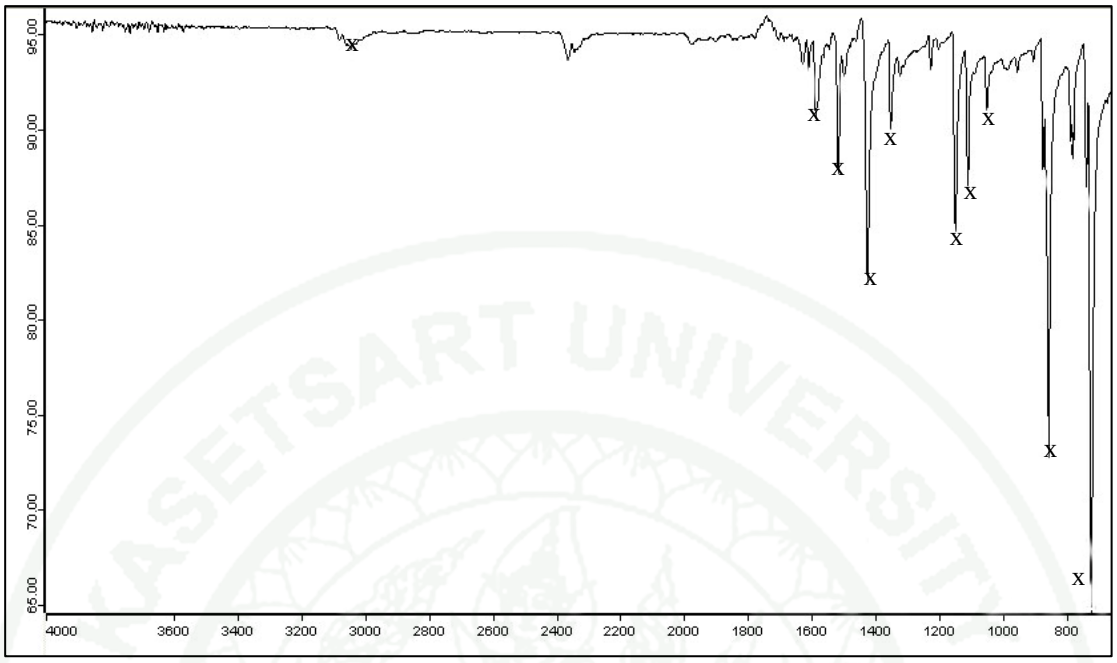

Figure 61 FTIR spectra (ATR technique) of CuCMa **(7)**

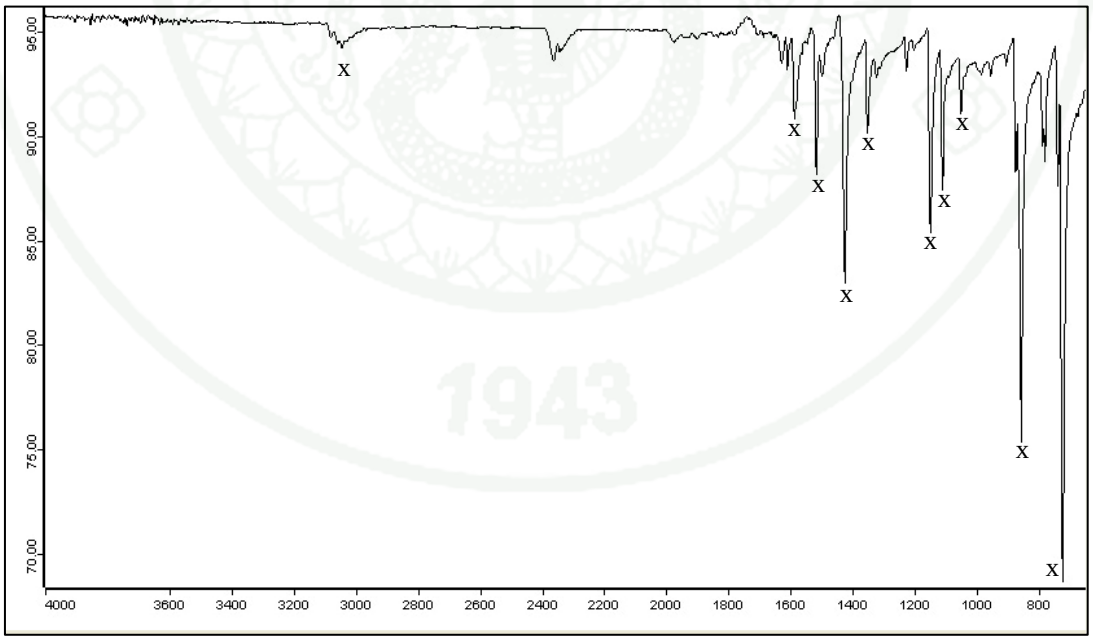

Figure 62 FTIR spectra (ATR technique) of CuCTa **(8)**

x: vibrational frequency of phenanthroloine

Table 17 Vibrational frequencies (cm^{-1}) in the IR spectra of group 4 complexes.

Complex	phenanthroline		
	ν_{C-H}	ring stretching	ring deformation
Phen[1]	3370	1621, 1585, 1505, 1422, 1344, 1217, 1183, 1091	852, 738
CuCMa **(7)**	3044	1585, 1515, 1422, 1349, 1146, 1108, 1047	854, 736
CuCTa **(8)**	3044	1607, 1515, 1422,1349, 1146, 1108, 1047	853, 736
MnPSu **(11)**	3051	1713, 1577, 1509, 1420, 1344, 1226, 1179, 1142	843, 725
MnPMaW **(15)**	3051	1621, 1579, 1493, 1420, 1342, 1226, 1134, 1097	811, 728
MnPTaW **(16)**	3051	1620, 1509, 1420, 1342, 1226, 1134, 1097	811, 728
MnPSuW **(17)**	3051	1621, 1588, 1509, 1420, 1344, 1142, 1092	852, 728

[1]R. G. Inskeep. 1962. **J. Inorg. Nucl. Chem.** (24): 763-776

Similarly, the infrared spectra of complex **11**, **15**, **16** and **17** (Figure 63-66) exhibit only peaks of phenanthroline ligand. No other ligand peaks were observed. These four complexes were obtained as either yellow crystal or yellow precipitate with similar percentage of carbon, hydrogen and nitrogen (Table3). It can be concluded that they have same molecular formula. Complex **11** crystallized as yellow rod and its crystal structure is given in Figure 46. Therefore complex **15** - **17** should have similar structures which consist of a manganese ion coordinating to two phenanthroline and two chloride ligands.

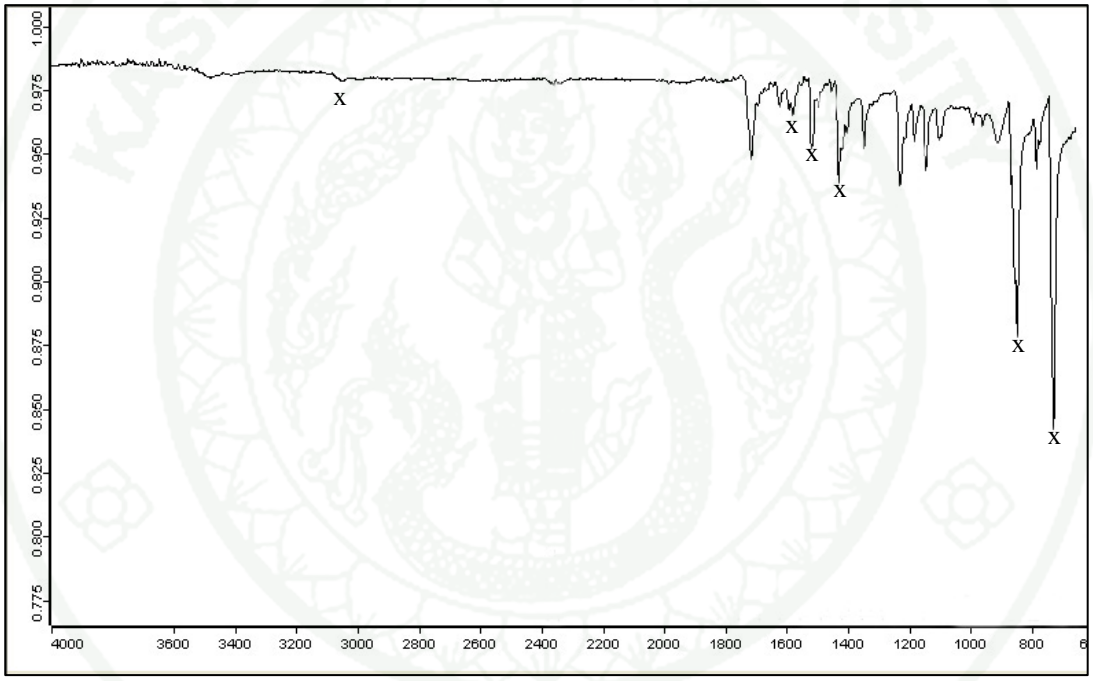

Figure 63 FTIR spectra (ATR technique) of MnPSu **(11)**

x: vibrational frequency of phenanthroloine

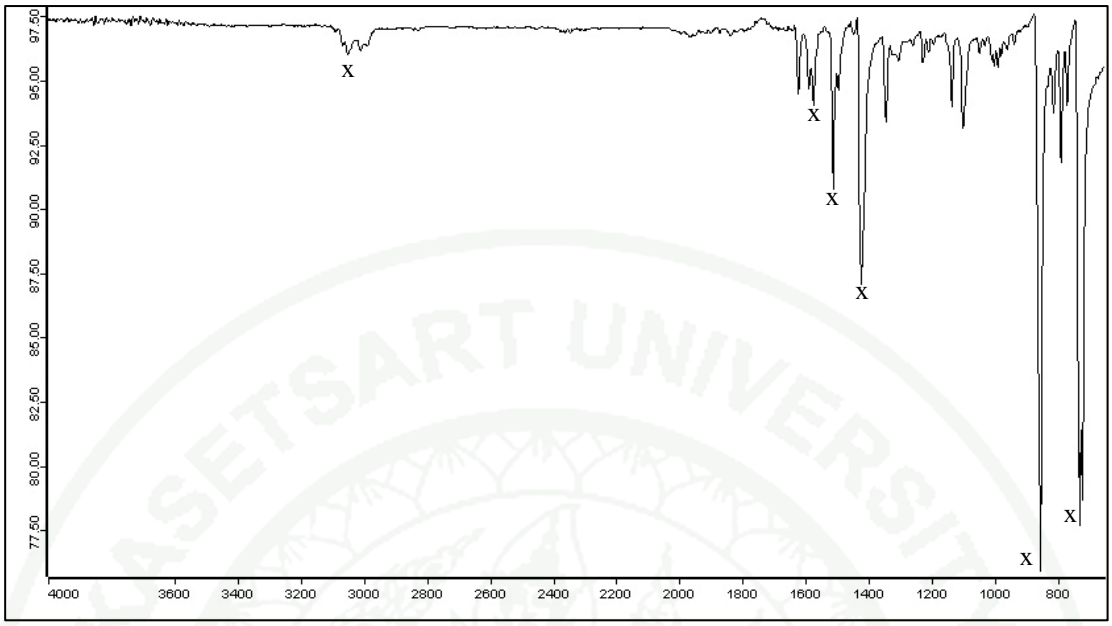

Figure 64 FTIR spectra (ATR technique) of MnPMaW**(15)**

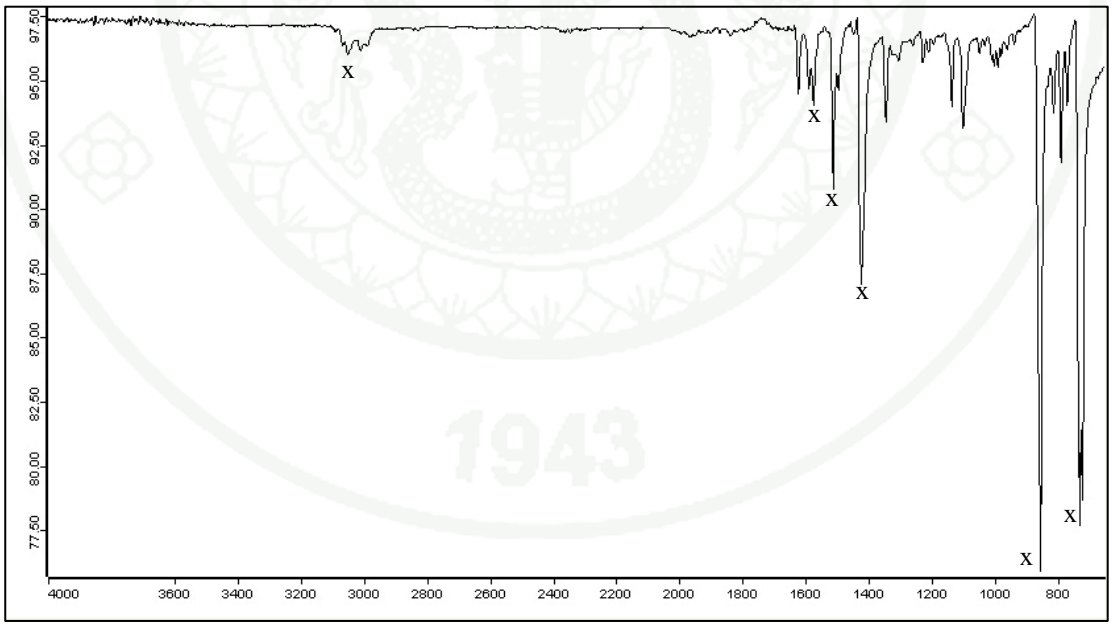

Figure 65 FTIR spectra (ATR technique) of MnPTaW**(16)**

x: vibrational frequency of phenanthroloine

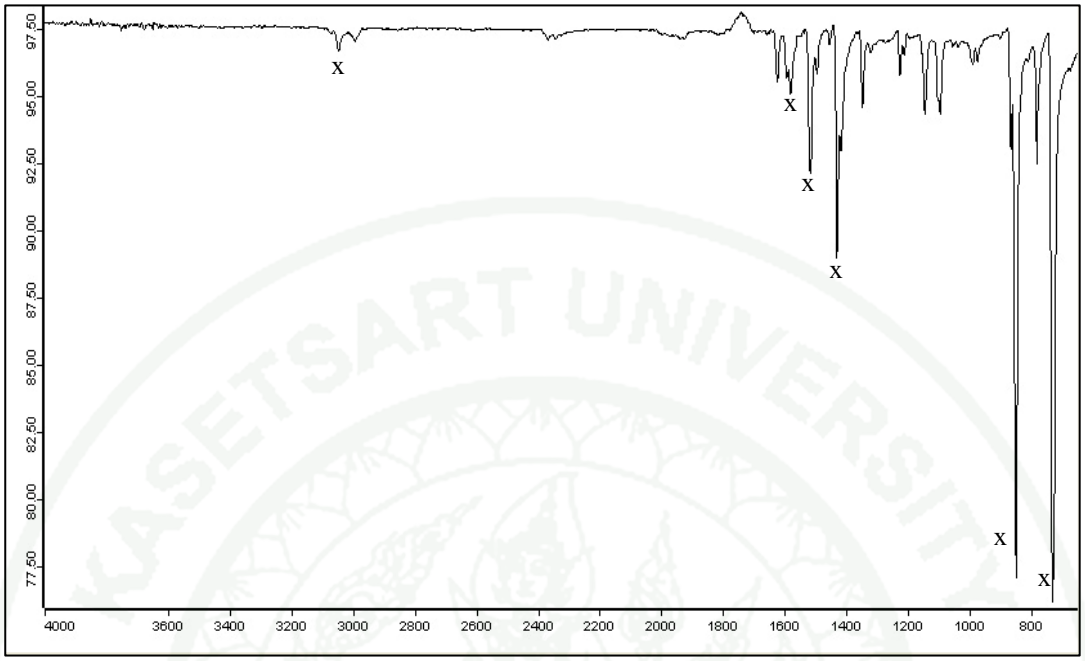

Figure 66 FTIR spectra (ATR technique) of MnPSuW**(17)**

x: vibrational frequency of phenanthroloine

3.2 Electronic spectroscopy

3.2.1 Electronic spectra of the octahedral Cu(II) complexes

In general, the six-coordinated Cu^{2+} complexes are almost always distorted from a regular octahedral structure with the axial ligands of the octahedron further away from the metal ion than the equatorial ligands due to Jahn-Teller distortion. The absorption spectra of Cu^{2+} complexes are broadened by this geometrical distortion from octahedral geometry. The tetragonal distortion is usually assumed to be the most common example of Cu^{2+} coordination. The energy levels of an axially elongated octahedron are shown in Scheme K.

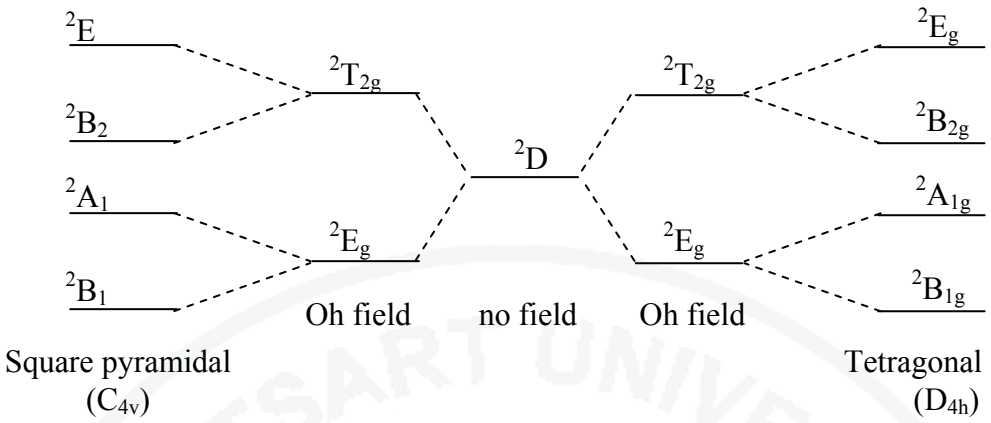

Scheme K Tetragonal field and square pyramidal field

Three possible d-d transitions in tetragonal field are assigned as

$^2B_{1g} \rightarrow {}^2A_{1g}$ ν_1

$^2B_{1g} \rightarrow {}^2B_{2g}$ ν_2

$^2B_{1g} \rightarrow {}^2E_g$ ν_3

They occur in the range 12000-17000 (ν_1), 15500-18000 (ν_2) and 17000-20000 cm^{-1} (ν_3) (Sathyanarayana, 2001). In general, these three bands are nearly superimposed to produce a broad and unsymmetric absorption band. In this study d-d bands in all cases are unresolvable. The electronic spectra of complex **3**, **4** and **6** exhibit a very broad and unsymmetric band in the visible region (630-685 nm) with very low absorptivities and more intense band in UV region at below 380 nm as shown in Figure 67. The former band result from the d-d transition of Cu(II) ion in octahedral crystal field. The latter can be assigned to LMCT of π(phen)→Cu(II) ($d_{x^2-y^2}, d_{z^2}$) transition and internal ligand π →π* transition.

The λ_{max} in UV-Vis spectra of Cu(II) complexes with octahedral geometry are listed in Table 18. Among complex **3**, **4** and **6**, the λ_{max} of **6** shifts to lower energy because the crystal field strength decrease. It is due to the weak field sulfate ligand.

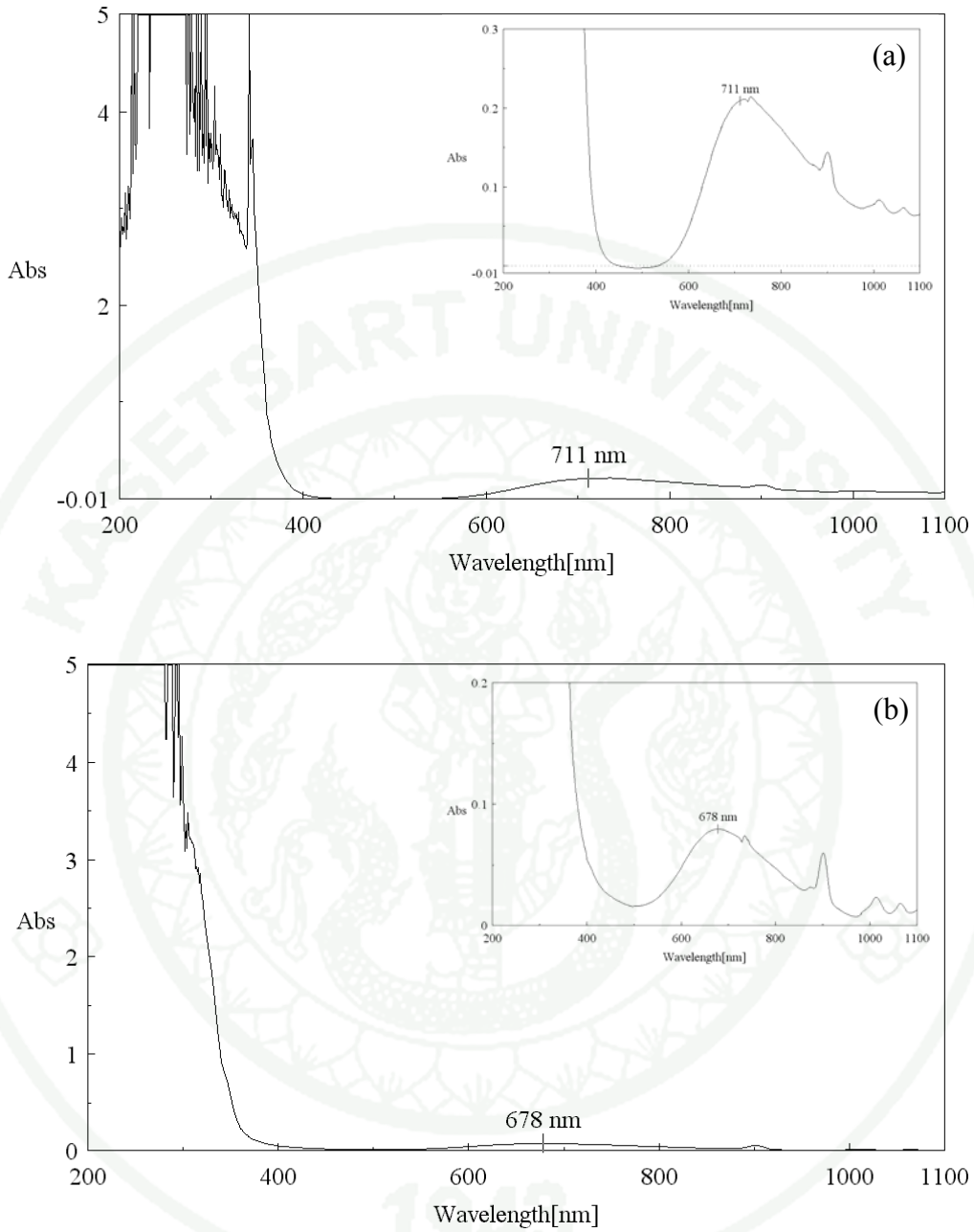

Figure 67 The electronic spectra of (a) $[Cu(Phen)(ox)(H_2O)]\cdot H_2O$ **(1)** and (b) $[Cu_4(\mu\text{-}suc)_2(phen)_4(H_2O)_4](NO_3)_4\cdot 4H_2O$ **(2)**.

3.2.2 Electronic spectra of the square pyramidal Cu(II) complexes

For square pyramidal complexes, the d-d bands observed in the region 9000-10000; 11500-16000 and 15000-19000 cm^{-1} have been ascribed to the

transitions $^2B_1 \rightarrow {}^2A_1$, $^2B_1 \rightarrow {}^2B_2$ and $^2B_1 \rightarrow {}^2E$, respectively (Sathyanarayana, 2001). The electronic spectra of complex **1** and **2** are shown in Figure 68. They display three bands at 9862-9881, 11099 and 14065-14749 cm^{-1}. The λ_{max} of the highest intensity bands are listed in Table 18. In addition, they display more intense band in UV-Vis region at below 400 nm (25000 cm^{-1}), which can be assigned to charge transfer transition.

Table 18 λ_{max} of Cu(II) complexes.

complex	geometry	λ_{max} nm	λ_{max} cm^{-1}
$[Cu(ox)(Phen)\ (H_2O)]\cdot H_2O$ **(1)**	square pyramid	711	14084
$[Cu_4(\mu\text{-suc})_2(phen)_4(H_2O)_4](NO_3)_4 \cdot 4H_2O$ **(2)**	square pyramid	678	14749
$[Cu(\mu\text{-ox})_2(phen)]_n$ **(3)**	octahedron	630	15873
$[Cu_2(\mu\text{-ox})_2(phen)_2]_n$ **(4)**	octahedron	630	15873
$[Cu(\mu\text{-}SO_4)(phen)\ (H_2O)_2]_n$ **(6)**	octahedron	684	14619
$[Cu_4(dpym)_2(OCOC_2H_5)_2(\mu\text{-}O_2(C_2H_5)_6(H_2O)_2]$- $[Cu_2(\mu\text{-}O_2CC_2H_5)_4(H_2O)_2]\cdot(DMF)_2$[1]	trigonal - bipyramid	721	13860
$[Cu_6(phen)_2(H_2O)_2(\mu\text{-}O_2CC_2H_5)_{12}$[1]	square pyramid	724	13800
$[Cu_2(BIBM)_2(C_2O_4)_2]$[2]	octahedron	591	16900
$[Cu_2(dpyam)_2(\mu\text{-}C_2O_4)](Cl)_2]$[3]	square pyramid	726	13770
$[Cu_2(dpyam)_2(\mu\text{-}C_2O_4)](CF_3SO_3)_2]_n$[3]	octahedron	634	15770
$[Cu(bpy)(C_2O_4)(H_2O)]\cdot H_2O$[4]	square pyramid	634	15770
$[Cu(phen)(C_2O_4)(H_2O)]\cdot H_2O$[5]	square pyramid	628	15920
$[Cu(ox)(DMSO)_2]_n$[6]	octahedron	980	10200
		769	13000
		617	16200

[1]Youngmee *et al.*, 2008. **Inorg. Chem. Commun.** 11: 57-62.

[2] Núñez *et al.*, 2001. **Inorg. Chim. Acta.** 318: 8-14.

[3]Youngmee *et al.*, 2006. **Inorg. Chem. Commun**. 9: 973-977.

[4]Androš *et al.*, 2010. **Polyhedron.** 29: 1291-1298.

[5]Chen *et al.*, 2001. **Inorg. Chem.** 40: 2652–2659.

[6]Tuszkanow *et al.*, 2009. **Inorg. Chem. Comm.** 12: 484-486.

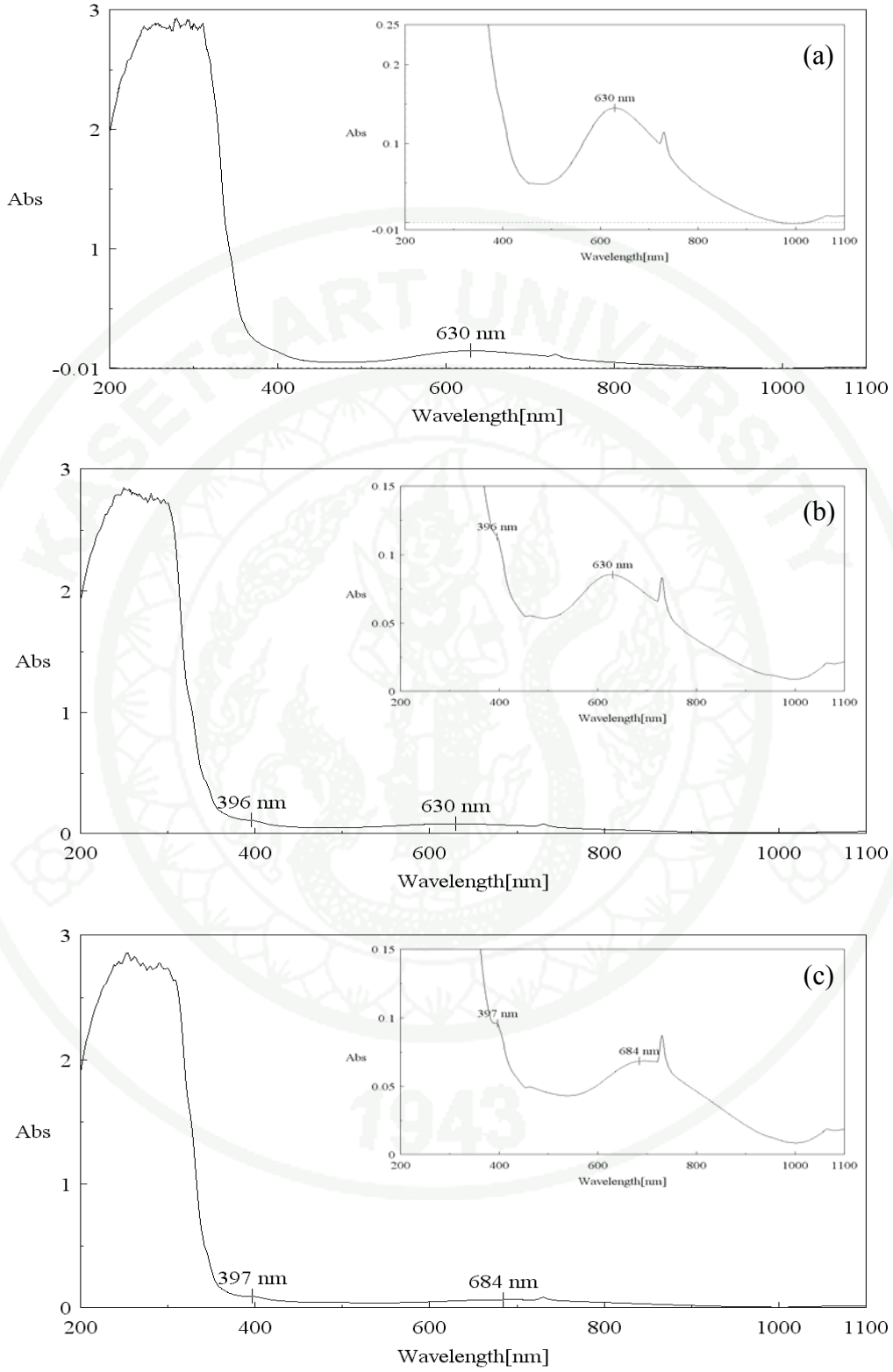

Figure 68 The electronic spectra of (a) $[Cu(\mu\text{-ox})(phen)]_n$ **(3)** (b) $[Cu_2(\mu\text{-ox})_2(phen)_2]_n$ **(4)** and (c) $[Cu(\mu\text{-}SO_4)(phen)(H_2O)_2]_n$ **(6)**.

3.2.3 Electronic spectra of *cis*-$[Mn(phen)_2Cl_2]$ **(11)**

The electronic spectrum of this complex exhibits no peak in the visible region and very intense band in the UV region below 400 nm as shown in Figure 69. The ground state term of high spin octahedrally coordinated Mn^{2+} complex is $^6A_{1g}$. There are on other terms of sextet spin multiplicity (Tanabe-Sugano Diagram) and hence there are no spin allowed d-d transition. It can be concluded that this complex is a high-spin d^5 complexes.

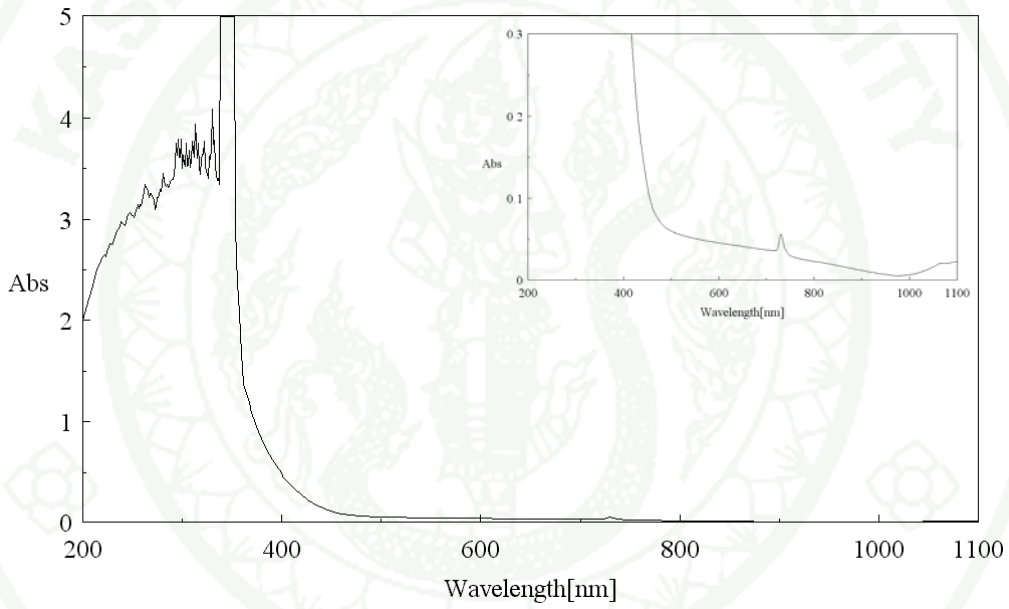

Figure 69 The electronic spectra of *cis*-$[Mn(phen)_2Cl_2]$ (**11**).

3.3 Thermal properties

The thermal analysis of four crystalline complexes **1**, **3**, **4** and **6** has been determined on powder samples in the nitrogen atmosphere from room temperature to 800°C. The TGA result of **1** is shown in Figure 70 reveals that a gradual weight loss of 9.203% from 80 to 120°C corresponds to the release of water molecules. No obviously separate temperature ranges are available for the elimination of solvated or coordinated water molecules. This may be attributed to the fact that the solvated molecules take part in the formation of many types of hydrogen bonds. The observed weight loss (9.203%) is close to the calculated value (9.79%). After the dehydration, the weight of the sample kept constant. When the temperature comes up to about 160°C, the second weight loss corresponding to the decomposition of oxalate ligand was observed. The observed weight loss of 20.82% is in agreement with the calculated value (23.93%). At 210-560°C, the decomposition of phenanthroline occurred and its weight loss of 45.19% is in agreement with the calculated value (48.94%).

The TGA curves of $[Cu(\mu\text{-ox})(phen)]_n$ **(3)** is shown in Figure 71. The first weight loss at 170-200°C corresponds to the decomposition of oxalate ligand. The observed weight loss of 25.39% is close to the calculated value (26.53%). At 200°C the decomposition of phenanthroline molecule started. At 750°C the decomposition was not complete yet, thus the observed weight loss of 46.64% is lower than that calculated value (54.26%).

The TGA curves of $[Cu_2(\mu\text{-ox})_2(phen)_2]_n$ **(4)** consists of two weight losses as shown in Figure 72. The first weight loss at 190-260°C corresponds to the decomposition of oxalate ligand. The observation weight loss of 23.98 % is in agreement with the calculated value (26.53%). The decomposition of phenanthroline molecule began at 260°C and was complete at 550°C, The observed weight loss of 46.46% is lower than the calculated value (54.26%).

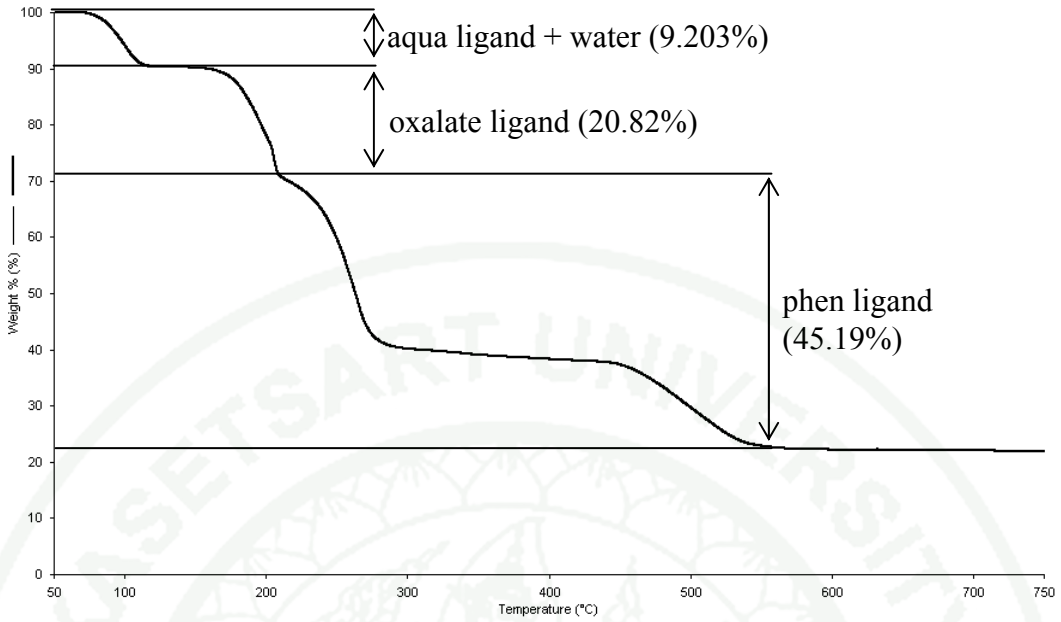

Figure 70 The TGA curve of $[Cu(ox)(phen)(H_2O)]\cdot H_2O$ **(1)**.

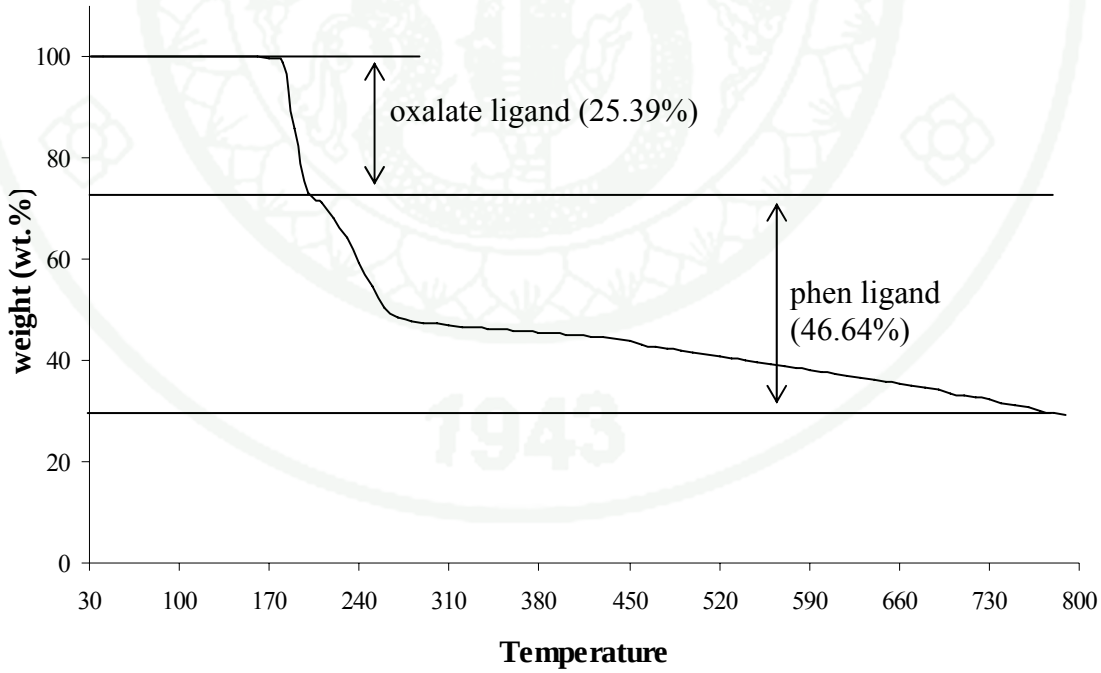

Figure 71 The TGA curve of $[Cu(\mu\text{-}ox)(phen)]_n$ **(3)**.

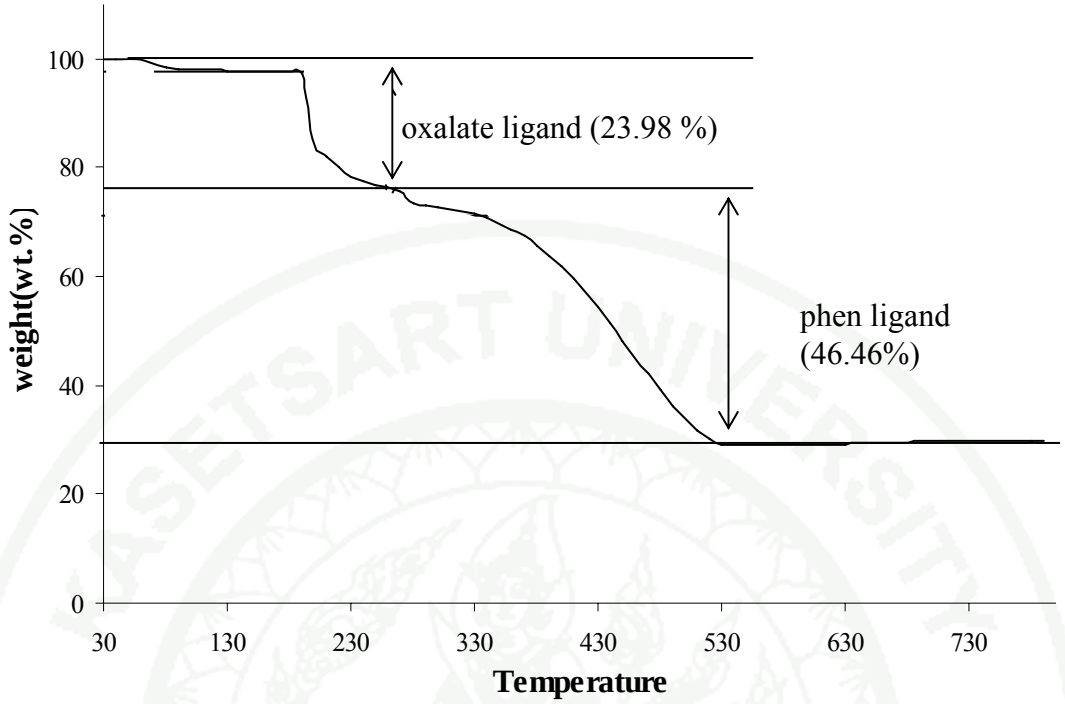

Figure 72 The TGA curves of $[Cu_2(\mu\text{-}ox)_2(phen)_2]_n$ **(4)**

The TGA curves of $[Cu(\mu\text{-}SO_4)(phen)(H_2O)]_n$ **(6)** shown in Figure 73 reveals three distinct weight losses. The first weight loss at 125-180°C corresponds to the release of water molecules. The observed weight loss of 18.24% is lower than the observed weight loss of 9.68%. The large amount of released water may be due to the moisture absorped in the sample. After the dehydration, the weight of sample kept constant until the temperature comes up to 330°C causing the decomposition of sulfate ions with 22.53% weight loss. The phenanthroline decomposed at 332-650°C with 44% weight loss which is in agreement with the calculated value (45.72%).

The decomposition and weight loss of all crystalline complexes are summarized in Table 19.

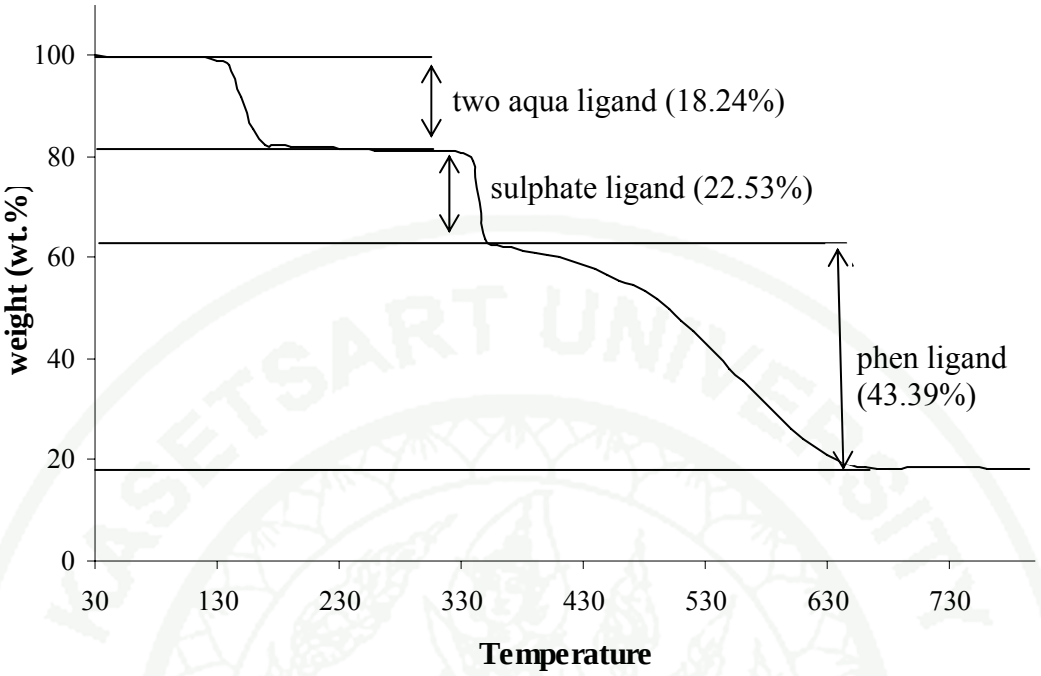

Figure 73 The TGA curve of $[Cu(\mu\text{-}SO_4)(phen)(H_2O)_2]_n$ **(6)**.

Table 19 Decomposition and weight loss of crystalline complexes.

Temperature (°C)	decomposition	weight loss	
		observed	calculated
$[Cu(ox)(phen)(H_2O)]\cdot H_2O$ **(1)**			
80-120	H_2O	9.203	9.79
160-210	oxalate	20.82	23.93
210-560	phen	45.19	48.94
$[Cu(\mu\text{-}ox)(phen)]_n$ **(3)**			
176-200	oxalate	25.39	26.53
200-750	phen	46.64	54.26
$[Cu_2(\mu\text{-}ox)_2(phen)_2]_n$ **(4)**			
190-260	oxalate	23.98	26.53
260-550	phen	46.46	54.26
$[Cu(\mu\text{-}SO_4)(phen)(H_2O)_2]_n$ **(6)**			
125-180	H_2O	18.24	9.68
330-332	SO_4^{2-}	22.53	25.82
332-650	phen	43.39	45.72

CONCLUSIONS

Under solvothermal condition at 150°C 72 and 24 hr, reaction of $Cu(NO_3)_2 \cdot 3H_2O$ with malic or tartaric acid and phenanthroline yield copper-oxalato complexes with different structures.

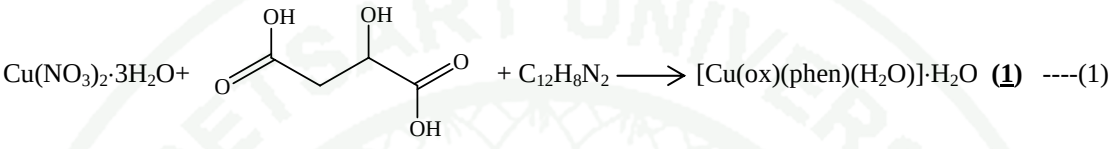

malic acid phen green rod crystal

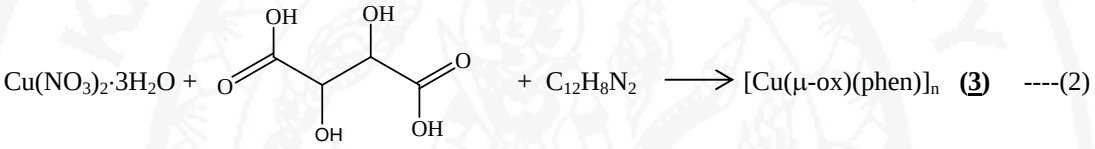

tartaric acid phen green plate

The oxalate ligand in the former is bidentate (chelate) while in the latter is tetradentate (bis-bridge). Similar condition was used for the reaction with succinic acid yielding $[Cu_4(\mu\text{-suc})_2(phen)_4(H_2O)_4](NO_3)_4 \cdot 4H_2O$. It is interesting to note that when $CuSO_4 \cdot 5H_2O$ and $CuCl_2 \cdot 2H_2O$ are used in the reactions with malic acid or tartaric acid, the compounds obtained in both cases **5**-**6** and **7**-**8** are isostructure and contain neither malate nor tartrate ligands. Their infrared spectra and elemental analysis results are similar. The CuSMa **(5)** and **6** give identical crystal structures with the formula of $[Cu(\mu\text{-}SO_4)(phen)(H_2O)_2]_n$.

The above result and discussion show that the anions of copper salts play a role on the formation of the complexes at this solvothermal condition. The $Cu(NO_3)_2 \cdot 3H_2O$ cause the cleavage of hydroxydicarboxylate (malate and tartrate) into oxalate (scheme G).

The HPLC experiment reveals that a conversion of malate into oxalate ion occurred during the course of reaction. In the case of $CuCl_2 \cdot 2H_2O$ and $CuSO_4 \cdot 5H_2O$,

chloride and sulfate ions are more favorable for coordination to copper than carboxylate oxygen.

Only $MnCl_2 \cdot 4H_2O$ was used for the reaction with succinic, malic and tartaric acid. The results obtained are yellow crystal and yellow precipitate in yellow solution. Only one batch involving succinic acid gave yellow rod crystals **11** which are suitable for collecting X-ray Diffraction data. The molecular structure of **11** is *cis*-$[Mn(phen)_2Cl_2]$. The FTIR spectra of **11**, **15**, **16** and **17** have similar pattern indicating similar structure.

The solvothermal reaction of $Cu(NO_3)_2 \cdot 3H_2O$ and oxalic acid was performed in order to compare with the structure of **1** and **3**. The structure of this oxalato complex **4** is polymeric chain of dinuclear copper oxalato complex, while the complex **3** is polymeric chain of mononuclear copper oxalato complex.

The results and observations from this study are summarized as follows

1. Six of twenty-two prepared compounds crystallized as single crystals with blue, green or yellow colors. Six crystalline complexes consist of the following molecular formula:

(1) $[Cu(ox)(phen)(H_2O)] \cdot H_2O$

(2) $[Cu_4(\mu\text{-}suc)_2(phen)_4(H_2O)_4](NO_3)_4 \cdot 4H_2O$

(3) $[Cu(\mu\text{-}ox)(phen)]_n$

(4) $[Cu_2(\mu\text{-}ox)_2(phen)_2]_n$

(6) $[Cu(\mu\text{-}SO_4)(phen)(H_2O)_2]_n$

(11) *cis*-$[Mn(phen)_2Cl_2]$

2. Under solvothermal conditions at 150°C 24 hr and 72 hr, the effect of anions of copper salt on the reactions of Cu(II) ions, phenanthroline and hydroxydicarboxylate anions was observed. $Cu(NO_3)_2 \cdot 3H_2O$ cleavaged malate and tartrate into oxalate resulting in copper oxalate complexes. The molecular structures of the oxalate

complexes obtained reveals different coordination mode of oxalate. For $CuSO_4 \cdot 5H_2O$ and $CuCl_2 \cdot 2H_2O$, no copper oxalate complexes were obtained.

3. The elemental analysis and infrared spectral study reveal the possible structures of powder complexes as follow

(1) CuSMa **(5)** and **6** have similar structure as $[Cu(\mu\text{-}SO_4)(phen)(H_2O)_2]_n$.

(2) CuCMa **(7)** and CuCTa **(8)** have structures as $[Cu(phen)_2Cl_2]$.

(3) MnPMaW **(15)**, MnPTaW **(16)**, MnPSuW **(17)** and **11** have similar structure as *cis*-$[Mn(phen)_2Cl_2]$.

(4) The possible structure of MnPOx **(18)** is $[Mn(\mu\text{-}ox)(phen)]_n$

4. The hydroxycarboxylates with four carbon backbone are cleft in the presence of $Cu(NO_3)_2 \cdot 3H_2O$ into oxalate anions but non-hydroxycarboxylates are not cleft.

LITTERATURE CITES

Androš, L., M. Jurić, P. Planinić, D. Žilić, B. Rakvin and K. Molčanov. 2010. New mononuclear oxalate complexes of copper(II) with 2D and 3D architectures: Synthesis, crystal structures and spectroscopic characterization. **Polyhedron.** 29: 1291-1298.

Ang, S. G. and B. W. Sun. 2005. Crystal Structure and Characterization of Organic−Inorganic Hybridized Molecules with Molecular Zipper Structures and Two-Dimensional Grid Networks. **Cryst. Growth Des.** 5 (1) : 383-386.

_____, _____ and S. Gao. 2004. Synthesis, crystal structurea and magnetic properties of one- and two-dimensional copper (II) complexes bridged by succinate. **Inorg. Chem. Commun.** 7: 795-798.

Arnold, P. J., S. C. Davies, J. R. Dilworth, M. C. Durrant,D. V. Griffiths, D. L. Hughes, R. L. Richards and P. C. Sharpe. 2001. **J. Chem. Soc., Dalton Trans.** 736–746.

Boonmak, J., S. Youngme, T. Chotkhun, C. Engkagul, N. Chaichit, G. A. V. Albada and J. Reedijk. Polynuclear copper (II) carboxylates with 2,2'-bipyridine or 1,10-phenanthroline: Synthesis, characterization, X-ray and magnetism. 2008. **Inorg. Chem. Commum.** 11: 1231-1235.

Calatayud, L. M., I. Castro, J. Sletten, F. Lloret and M. Julve. 2000. Syntheses, crystal structures and magnetic properties of chromatosulfato-, and oxalate-bridged dinuclear copper (II) complexes. **Inorg. Chim. Acta.** 300-302 : 846-854.

Cann M. S. , M. M. Cann , R. M. T. Casey, M. Jackman **,** M. Devereux and V. McKee. 1998**.** Syntheses and X-ray crystal structures of *cis*- [$Mn(bipy)_2C1_2$]-

$2H_20\cdot$ EtOH and *cis*- [Mn $(phen)_2C1_2$](bipy -- 2,2'-bipyddine; phen = 1,10-phenanthroline); catalysts for the disproportionation of hydrogen peroxide. **Inorg. Chim. Acta** 279: 24-29**.**

Castillo, O., A. Luque, S. Iglesias, C. G. Miralles and P. Román. 2001. A novel one-dimensional oxalate-bridged copper (II) complex with 2,2'-bipyridine. **Inorg. Chem. Comm.** 4 : 640-642.

_____, I. Muga, A. Lugue, J. M., G. Zorrilla,J. Sertucha, P. Vitoria and P. Román. 1999. Synthesis, chemical characterization, X-ray crystal structure and magnetic properties of oxalate-bridged copper(II) binuclear complexes with 2,2′-bipyridine and dirthylenetriamine as peripheral ligands. **Polyhedron.** 18: 1235-1245.

Chaudhury, A., S. Neeraj, S. Natarajan and C.N.R. Rao. 2000. An Unusual Open-Framework Cobalt(ii) Phosphate with a Channel Structure That Exhibits Structural and Magnetic Transitions. **Angew. Chem., Int. Ed.** 39: 3091-3093.

Chen, X. F., P. Cheng, X. Liu, B. Zhao, D. Z. Liao, S. P. Yan, and Z. H. Jiang. 2001. Two-dimensional Coordination Polymers of Copper(II) with Oxalate:. Lattice Water Control of Structure. **Inorg. Chem.** 40: 2652–2659.

Deacon, G. B. and R. J. Phillip. 1980. Relationships between the carbon-oxygen stretching frequencies of carboxilato complexes and the type of carboxylate coordination. **Coord. Chem. Rev.** 33: 227-250.

Demir, S., V. T. Yilmaz. B. Sariboga, O. Buyukgungor, J. Mrozinski. 2010. Metal(II) nicotinamide complexes containing succinato, succinate and succinic acid: synthesis, crystal structures, magnetic, thermal, antimicrobial and fluorescent properties. **J. Inorg Organomet Polym.** 20: 220–228.

Du, M., Y. M. Guo and X. H. Bu. 2002. A novel oxalate-bridged dinuclear copper (II) complex with diazamesocyclic terminal ligand: crystal structure, spectroscopy and magnetism. **Inorg. Chim. Acta.** 335 : 136-140.

Duangthongyou, T., S. Jirakulpattana, C. Phakawatchai, M. Kurmoo, S. Siripaisarn-pipat. 2010. Comparison of crystal structures and magnetic properties of two Co(II) complexes containing different dicarboxylic acid ligands Original **Polyhedron**. 29:1156-1162.

Eddaoudi, M., H. Li and O. M. Yaghi. 2000. Highly porous and stable metal-organic frameworks. Structure design and sorption properties. **J. Am. Chem. Soc.** 122(7): 1391-1397.

Fujita, M., Y. J. Kwon, S. Washizu and K. Ogura. 1994. Preoaration, clathration ability, and catalysis of a two-dimensional square net work material composed of cadmium (II) and 4,4'-bipyridine. **J. Am. Chem. Soc.** 116(3): 1151-2.

Ghoshal, D., T. K. Maji, G. Mostafa, S. Sain, T. H. Lu, J. Ribas, E. Zangrado and N. R. Chaudhuri. 2004. Polymeric network of copper (II) succinate and aromatic N-N donor ligands: synthesis, crystal structure, magnetic behavior and the effect of weak interactions on their crystal packing. **Dalton Trans.** 1687-1695.

_____, A. K. Ghosh, G. Mostafa, J. Ribas, N. R. Chaudhuri. 2007. Succinato-bridged copper(II) supramolecular 3D framework: Synthesis, crystal structure and magnetic property. **Inorganica Chimica Acta,** 360 (5) :1771-1775.

Gleizes, A., M. Julve, M. Verdaguer, J. A. Real, J. Faus and X. Solans. 1992. Two different (oxalato)(bipyridine)copper(II) complexes in one single crystal. Crystal structures and magnetic properties of $[Cu_2(bipy)_2(H_2O)_2(C_2O_4)]X_2 \cdot [Cu(bipy)(C_2O_4)]$(X = NO_3^-, BF_4^- or ClO_4^-). **J. Chem. Soc., Dalton Trans.**, 3209 – 3216.

Gkioni, C., A. K. Boudalis, Y. Sanakis and C. P. Raptopoulou. 2007.Weak ferromagnetism in 1D coordination polymers: Syntheses, crystal structures, spectroscopic and magnetic properties of $[Cu(L)(Memal)]_n$ ($Memal^{2-}$ = the dianion of methylmalonic acid, L = 1,10-phenanthroline, 2,2′-bipyridine). **Polyhedron**. 26: 2536-2542.

Hennigar, T. L., D. C.MacQuarrie, P. Losier, R. D.Rogers and M. J. Zaworotko. 1997. Supramolecular isomerism in coordination polymers conformational freedom of ligands in $[Co(NO_3)_2(1,2\text{-bis}(4\text{-pyridyl})\ \text{ethane})_{1.5}]_n$. **Angew. Chem., In Ed in English**, 36(9): 972-973.

Inkeep, R. G. J. 1962. Infra-red spectra of metal complex ions below 600 cm^{-1}. **Inorg. Nucl. Chem.** 24 :763-766.

Janiak, C. 2000. A critical account on π-π stacking in metal complexes with aromatic nitrogen-containing ligands. **J. Chem. Soc., Dalton Trans.** 2000: 3885–3896.

Jin, S., D. WangII, H. Cao, Z. ZhengI, X. Lv and S. Huang. 2009. Crystal structure of aqua-ammine-(μ-succinato)copper(II) dihydrate, $Cu(H_2O)(NH_3)(C_4H_4O_4) \cdot 2H_2O$. **Z. Kristallogr.** 224: 391-392.

Julve, M., M. Verdaguer, A. Gleizes, M. P. Levisalles and O. Kahn. 1984. Design of μ-oxalato copper (II) binuclear complexes exhibiting expected magnetic properties. **Inorg. Chem.** 23: 3808-3818.

Ke, X. J., D. S. Li, J. Zhao, Q. F.He and C.Li. 2009. Aqua(2,2′-bipyrimidine-K^2N,N') (succinato-K^2O^1,O^4)copper(II) dihydrate . **Acta Cryst. E.** 65: 527.

Kitiphaisalnont, P., S. Siripaisarnpipat and N. Chaichit. 2009. Di-μ-succinato-tetrakis [aqua phenanthrolinecopper(II)]tetranitrate tetrahydrate. **Acta. Cryst. E.** 65 : 1284.

Kundu, P., M. K. Saha, S. Sen and S. Mitra. 1996. Thermally included electron transfer reaction of heteromrtallic dinuclear complex in the solid state. **Polyhedron.** 15(3): 415-420.

Li, J., Y. H. Xing, H. Y. Zhao, Z. P. Li, C. G. Wang, X. Q. Zeng, M. F. Ge and S. Y. Niu. 2009. Constructions of a set of hydrogen-bonded supramolecules from reactions of transition metals with 3,5-dimethylpyrazole and different dicarboxylate ligands. **Inorg. Chim. Acta.** 362: 2788.

Liu, C. B., H. L. Wen and S. S. Tan. 2006. First examples of ternary lanthanide succinate complexes: hydro-solvothermal syntheses and structures of lanthanide coordination polymers of succinic acid and 1,10-phenanthroline. **J. Mol. Struc.** 794 : 190-195.

Machold, T., E. Macedi, D.W. Laird, P.M. May and G.T. Hefter. 2009. Decomposition of Bayer process organics: Low-molecular-weight carboxylates. **Hydrometal lurgy.** 99 : 51–57.

Mao, H., C. Zhang, G. Li, H. Zhang, H. Hou, L. Li, Q. Wu, Y. Zhu and E. Wang. 2004. New types of the flexible self-assembled metal-organic coordination polymers constructed by aliphatic dicarboxylates and rigid bidentate nitrogen ligands. **Dalton Trans.** 3918-3925.

Martin, D. P., R. M. Supkowski and R. L. LaDuca. 2008. Layered metal succinate/ bis(4-pyridylmethyl)piperazine coordination polymers featuring mutual inclined interpenetration Original Research Article. **Polyhedron.** 27 : 2545-2550.

McCann, M., F. Humphreys and V. McKee. 1997. Transition metal complexes of dibenzoyl-L-tartaric acid (db-L-tarH_2) and L-tartaric (L-tarH_2); X-ray crystal structure of {[Cu(L-tar)(phen)]·6H_2O}n (phen = 1,10-phenanthroline). **Polyhedron.** 16: 3655-3661.

Moulton, B. and M. J. Zaworotko. 2001. From molecules to crystal engineering. Supramolecular isomerism and polymorphism in network solids. **Chem. Rev.** 101(6): 1629-1658.

Mukherjee, P. S., S. Dalai, N. R. Chaudhuri, E. Zangrando and F. Lloret. 2001. The first metamagnetic one-dimensional molecular material with nickel(II) and end-to-end azido bridges. **Chem. Commun.** 16: 1444-1445.

Lutz, M., S. Smeets and P. Parois. 2010. Catena-Poly[[bis(ethylenediamine)-copper(II)]-μ-sulfato] **Acta Cryst. E.** 66: 671-672.

Núñez, H., J. J. Timor, J. S. Carrió, L. Soto and E. Escrivà. 2001. Synthesis, crystal structure, spectroscopic characterization and magnetic properties of $[Cu_2(BIBM)_2(C_2O_4)_2]\cdot 4H_2O$ (BIBM = bis (2-imidazolyl) bis (methoxy carbonyl) methylmethane). **Inorg. Chim. Acta.** 318: 8-14.

Olar, R., M. Badea1, O.Carp, D.Marinescu1, V. Lazar, C. Balotescu and A. Dumbrava. 2008. Synthesis, characterization and thermal behavior of some thiosulfato and sulfato copper(II) cimplexes antibac terial activity. 92: 245-251.

Padmanabha, M., S. M. Kumary, X. Huang and J. Li. 2005. Succinate bridged dimeric Cu(II) containing sandwiched non-coordinating succinate dianion: Crystal structure, spectroscopic and thermal studies of $[(phen)_2Cu(\mu\text{-}L)Cu(phen)_2]L \cdot 12.5H_2O$ (H_2L = succinic acid; phen = 1,10-phenanthroline). **Inorg. Chim. Acta.** 358: 3537-3544.

Pajunen, A., S. Pajunen, J. Kivikoski and J. Valkone. 1996. catena-Poly[[(dieth ylene triamine.N,N',N''). copper(II)]-/z-succinato-O,O':O'']**. Acta Cryst. C.** 52: 2689-2691.

Reineke, T. M., M. Eddaoudi, M. Fehr, D. Kelley and O. M. Yaghi. 1999. From condensed lanthanide coordination solids to microporous frameworks having accessible metal sites. **J. Am. Chem. Soc.** 121(8): 1651-1657.

Ribas, J., M. Monfort, C. Diaz, C. Bastos and X. Solans. 1994. Ferromagnetic nickel(II) polynuclear complexes with end-on azido as bridging ligand. The first nickel(II)-azido one-dimensional ferromagnetic systems. **Inorg. Chem.** 33: 484-489.

Ruiz ,T. P., C. M. Lozano, V. Tomás, J. Mart´ın. 2004. High-performance liquid chromatographic separation and quantification of citric, lactic, malic, oxalic and tartaric acids using a post-column photochemical reaction and chemiluminescence detection. **Journal of Chromatography A**, 1026: 57–64.

Sathyanarayana, D. N . 2001. **Electronic Absorption Spectroscopy**. Universities Press, Indea.

Seo, J. S., D. Whang, H. Lee, S. I. Jun, J. Oh, Y. J. Jeon and K. Kim. 2000. A homochiral metal-organic porous material for enantioselective separation and catalysis. **Nature** 404(6781): 982-986.

Shyu, E. and R.L. LaDuca. 2009. Divalent metal succinate/perchlorate coordination polymers incorporating a kinked hydrogen-bonding capable diimine: Chains, layers and a (5,6)-connected binodal network featuring alternating rectangular and hexagonal grids. **Polyhedron.** 28 (4): 826-834

Smékal, Z., Z. Trávníček, F. Lloret and J. Marek, 1999. Synthesis and characterization of binuclear μ-oxalato nickel (II), copper (II) and zinc (II) complexes with 3,3'-diamino-*N*-methyl-dipropylamine or *trans*-1,2-diamino cyclohexane. **Polyhedron.** 18 : 2787-2793.

Sieroń, L. and M. B. Strzyżewska. 2000. Bis(m-succinato-*O,O′:O″,O‴*)bis-[bis(2-amino-1,3-benzothiazole-N^3)-copper(II)]. **Acta Cryst C** 56:19-21.

Stamatatos, T. C., S.P. Perlepes, C.P. Raptopoulou, V.Psycharis, C. S. Patrickios, A. J. Tasiopoulos, A. K. Boudalis. 2009. Initial use of 1,1′-oxalyldiimidazole for inorganic synthesis: Decomposition of the ligand as a means to the preparation of an imidazole- and oxalate(-2)-containing, 1D copper(II) complex. **Inorg. Chem. Comm.** 12: 402-405.

Su, J., Y. Wang, S. Yang, G. Li, F. Liao and J. Lin. 2007. New series of indium formates: Hydrothermal synthesis, structure and coordination modes. **Inorg. Chem.** 46(20): 8403-8409.

Tang, J., E. Gao, W. Bu, D. Liao, S. Yan, Z. Jiang and G. Wang. 2000. Synthesis and crystal structure of oxalate-bridged dicopper (II) complex with hydrogen bonds $[Cu_2(\mu\text{-}C_2O_4)(bpy)_2(H_2O)_2(NO_3)_2]$. **J. Mol. Struc.** 525: 271-275.

Tojal, J. G., M. K. Urtiaga, R. Cortés, L. Lezama, M. I. Arriortua and T. Rojo. 1994. Synthesis, Structure, Spectroscopic and Magnetic Properties of two Copper(II) Dimers containing Pyridine-2-carbaldehyde Thiosemicarbazonate (L), $[\{CuL(X)\}_2]$ (X = Cl or Br). **J. Chem. Soc. Dalton Trans.** 1687-1695.

Tuszkanow, M. P., M. Daszkiewicz, G. Maciejewska, M. C.Golonka. 2009.Decom position of allantoin in the presence of Cu(II) ions resulting in the formation of a coordination polymer containing oxalate species. **Inorg. Chem. Comm.** 12: 484-486.

Vučković, G., M. A. Nikolić, T. Lis, J. Mroziński, M. Korabik and D.D. Radanović. 2008. X-ray analyses, spectroscopic and magnetic properties of $[Cu_4(succinato)\ (tpmc)_2](ClO_4)_6{\cdot}2C_2H_5OH{\cdot}4H_2O$ and $[Cu_2(C_6H_5COO)tpmc](ClO_4)_3\cdot 0.5\ CH_3OH{\cdot}0.5H_2O$ complexes. **J. Mol. Struc.** 872: 135-144.

Wang, M., B. Hu, X.T. Deng and C. G. Wang. 2007. μ-oxalato-κ^4–*O,O′:O‴*-bis[chloro1,10-phenanthroline-κ^2*N,N′*)(copper)(II)]. **Acta Cryst. E**.63: 710–711.

Wang, Z., H. Wang, X. L. Wang, S. Liang and J.Y. Han.2006 catena-Poly[[bis (imida zole-κ*N*)copper(II)]-μ-succinato-κ^2*O:O′*] **Acta Cryst. E**.62: 1972–1973.

Wojtczak, W. A., M. J. Hampden-Smith and E. N. Duesler. 1998. Synthesis, characterization, and thermal behavior of polydentate ligand adducts of barium trifluoroacetate. **Inorg. Chem.** 37(8): 1781-1790.

Xu, X., Y. Ma and E. Wang. 2007. Different aliphatic dicarboxylates affected assemble of new coordination polymers constructed from flexible–rigid mixed ligands. **J. Sol. Stat. Chem.** 180:3136-3145.

Ying, E.-B., Y.-Q. Zheng, et al. 2004. Syntheses, crystal structures and properties of two Cu(II) coordination polymers: $Cu(C_3N_2H_4)_2(HL)_2$ and $Cu(C_3N_2H_4)_2L$ with $C_3N_2H_4$=imidazole, H_2L=adipic acid. **J. Mol. Struc.** 693(1-3): 73-80.

Yaghi, O. M., G. Li and H. Li. 1995. Selective binding and removal of guests in a microporous metal-organic framework. **Nature** 378(6558): 703-6.

Youngmee, S., A. Cheansirisomboon, C. Danvirutai, C. Pakawatchai and N. Chaichit. 2008. Polynuclear paddle-wheel copper (II) propionate with di-2-pyridylamine or 1,10-phenanthroline: Preparation, characterization and X-ray structure. **Inorg. Chem. Commun.** 11: 57-62.

_____, _____, _____, _____, _____, C. Engkagul, Gerard A. V. Albada, J. S. Costa and J. Reedijk. 2008. Three new polynuclear tetracarboxylato-bridged copper(II) complexes: Syntheses, X-ray structure and magnetic properties. **Polyhedron**. 27: 1875.

Youngmee, S., A. Cheansirisomboon, C. Danvirutai, C. Pakawatchai, G. A. V. Albada and J. Reeijk. 2006. Two new oxalate-bridged dinuclear copper (II) complexes with di-2-pyridylamine: crystal structures, spectroscopic and magnetic properties. **Inorg. Chem. Commun.** 9: 973-977.

Youngmee, S., G. A. V. Albada, N. Chaichit, P. Gunnasoot, P. Kongsaeree, I. Mutikainen, O. Roubeau, J. Reeijk and U. Turpeinen. 2003. Synthesis, Spectroscopic characterization, X-ray crystal structure and magnetic properties of oxalate-bridged copper(II) dinuclear complexes with di-2-pyridylamine. **Inorg. Chim. Acta.** 353: 119-128.

Youngmee, S., N. Wannarit, C. Pakawatchai, N. Chaichit, E. Somsook, U. Turpeinen and I. Mutikainen. 2007. Structural diversities and spectroscopic properties of bis and tris (1,10-phenanthroline) copper (II) complexes. **Polyhedron.** 26 : 1459-1468.

Zhang, H. X., B. S. Kang, Z. Y. Zhou, A. S. C. Chan, K. B. Yu, Z. N. Chen and C. Ren. 2001. Assemblies based on trans-oxamidato-bridged copper(II) building blocks and the spacer succinate. **Inorg. Chem. Commun.** 4: 695-698.

Zhang, L., W. M. Bu, S. P. Yan, Z. H. Jiang, D. Z. Liao and G. L. Wang. 2000. Weaker magnetic interactions of oxalate-copper (II) binuclear compounds: synthesis, spectroscopy, crystal structure and magneticsm. **Polyhedron**. 19: 1105-1110.

Zheng, Y. Q., W. H. Liu and J. L. Lin. 2002. Two succinato-bridged Zinc(II) phenan throline complexes: $[Zn(phen)L_{2/2}](H_2L)$ and $[(phen)_2Zn(m\text{-}L)Zn\ (phen)_2]L \cdot 11H_2O$ with H_2L = succinic acid. **Z. Anorg. Allg. Chem.** 628: 620-624.

Zhou, Z.-H., J.-M. Yang and H.-L. Wan. 2005. Diamine substitution reactions of tetrahydrate succinato nickel, cobalt, and zinc coordination polymers. **Crystal Growth & Design** 5(5): 1825-1830.

APPENDICES

Appendix A

Single bond covalent radii used in SHELHX program

APPENDIX A

Single bond covalent radii used in SHELHX program

C	0.770	H	0.320
N	0.700	O	0.660
Cu	1.280	Mn	1.370

Appendix B

Atomic coordinated and equivalent isotropic
displacement parameters of Cu(II) and Mn(II) complexes

Appendix Table B1 Atomic coordinates ($x10^4$) and equivalent isotropic displacement parameters ($Åx10^3$) for $[Cu(ox)(phen)(H_2O)]\cdot H_2O$ (**1**)

	x	y	z	U(eq)
Cu(1)	6436(1)	4808(1)	1542(1)	31(1)
O(1)	5103(2)	3552(1)	1979(1)	38(1)
O(2)	5921(2)	6147(1)	2274(1)	42(1)
O(3)	3543(2)	3588(2)	2835(1)	56(1)
O(4)	4608(2)	6220(2)	3232(1)	64(1)
O(5)	8774(2)	4098(2)	2310(1)	55(1)
O(6)	11099(2)	5764(2)	3236(1)	51(1)
N(1)	6546(2)	3585(1)	623(1)	31(1)
N(2)	7332(2)	6207(1)	914(1)	31(1)
C(1)	6146(2)	2266(2)	499(1)	40(1)
C(2)	6364(3)	1560(2)	-169(1)	44(1)
C(3)	7032(2)	2220(2)	-710(1)	40(1)
C(4)	7476(2)	3614(2)	-591(1)	32(1)
C(5)	8206(2)	4403(2)	-1111(1)	37(1)
C(6)	8585(2)	5746(2)	-967(1)	37(1)
C(7)	8289(2)	6430(2)	-285(1)	32(1)
C(8)	8669(2)	7817(2)	-92(1)	39(1)
C(9)	8394(3)	8349(2)	590(1)	42(1)
C(10)	7722(2)	7518(2)	1085(1)	39(1)
C(11)	7611(2)	5674(2)	241(1)	27(1)
C(12)	7194(2)	4250(2)	86(1)	27(1)
C(13)	5032(2)	5635(2)	2701(1)	38(1)
C(14)	4487(2)	4123(2)	2503(1)	35(1)

Appendix Table B2 Atomic coordinates ($x10^4$) and equivalent isotropic displacement parameters ($Åx10^3$) for $[Cu_4(\mu\text{-suc})_2(C_{12}H_8N_2)_4\ (H_2O)_4](NO_3)_4 \cdot 4H_2O$ (**2**)

	x	y	z	U(eq)
Cu(1)	2870(1)	459(1)	2594(1)	28(1)
Cu(2)	4541(1)	924(1)	703(1)	28(1)
O(1)	5954(3)	549(1)	1565(3)	40(1)
O(2)	4661(3)	129(1)	2689(3)	38(1)
O(3)	6118(4)	1113(1)	-618(3)	43(1)
O(4)	1350(5)	129(1)	3799(4)	58(1)
O(5)	2091(3)	215(1)	939(3)	37(1)
O(6)	3553(4)	514(1)	-390(3)	40(1)
O(7)	-1911(12)	2391(4)	691(10)	191(2)
O(8)	-1382(12)	2708(4)	2187(10)	191(2)
O(9)	-3494(12)	2700(4)	1619(9)	191(2)
O(10)	-18(6)	620(2)	6390(5)	80(1)
O(11)	-1232(6)	1133(2)	5928(5)	80(1)
O(12)	-996(6)	714(2)	4439(5)	80(1)
O(13)	8466(5)	645(1)	-1270(4)	53(1)
O(14)	6181(10)	1896(2)	-1023(7)	105(2)
N(1)	1424(3)	915(1)	2426(3)	28(1)
N(2)	3661(3)	746(1)	4221(3)	30(1)
N(3)	2987(3)	1323(1)	-8(3)	31(1)
N(4)	5046(3)	1345(1)	2033(3)	29(1)
N(5)	-754(7)	817(2)	5574(6)	80(1)
N(6)	-2256(16)	2581(4)	1483(12)	191(2)
C(1)	277(4)	985(1)	1527(4)	35(1)
C(2)	-628(5)	1320(1)	1556(5)	44(1)
C(3)	-343(5)	1588(1)	2536(5)	44(1)
C(4)	829(4)	1516(1)	3524(4)	36(1)
C(5)	1192(6)	1767(1)	4627(5)	50(1)
C(6)	2326(6)	1680(1)	5539(4)	52(1)
C(7)	3218(5)	1330(1)	5464(4)	40(1)

Appendix Table B2 (Continued)

	x	y	z	U(eq)
C(8)	4391(6)	1214(2)	6398(4)	51(1)
C(9)	5138(6)	872(2)	6231(4)	51(1)
C(10)	4754(5)	644(1)	5126(4)	40(1)
C(11)	2887(4)	1082(1)	4393(3)	30(1)
C(12)	1680(4)	1176(1)	3420(3)	29(1)
C(13)	1976(5)	1298(1)	-1039(4)	41(1)
C(14)	944(5)	1602(2)	-1369(5)	50(1)
C(15)	946(5)	1931(1)	-612(5)	50(1)
C(16)	2019(5)	1964(1)	489(4)	40(1)
C(17)	2115(6)	2291(1)	1378(5)	51(1)
C(18)	3176(6)	2307(1)	2398(6)	53(1)
C(19)	4237(5)	1993(1)	2661(4)	39(1)
C(20)	5367(6)	1984(1)	3722(5)	48(1)
C(21)	6289(5)	1665(1)	3902(4)	45(1)
C(22)	6097(4)	1347(1)	3049(4)	35(1)
C(23)	4138(4)	1664(1)	1835(4)	30(1)
C(24)	3028(4)	1651(1)	740(3)	30(1)
C(25)	5830(4)	238(1)	2196(3)	29(1)
C(26)	7229(4)	-12(1)	2433(3)	31(1)
C(27)	2562(4)	269(1)	-151(3)	28(1)
C(28)	1862(4)	28(1)	-1284(4)	32(1)

Appendix Table B3 Atomic coordinates ($x10^4$) and equivalent isotropic displacement parameters ($Åx10^3$) for $[Cu(\mu\text{-ox})(phen)]_n$ (**3**)

	x	y	z	U(eq)
Cu(1)	1278(1)	968(1)	7656(1)	29(1)
O(1)	3363(2)	1369(2)	6729(1)	35(1)
O(2)	2204(2)	2439(2)	8422(1)	36(1)
O(3)	-814(2)	1300(2)	8570(1)	37(1)
O(4)	170(2)	2177(2)	6777(1)	37(1)
N(1)	532(2)	-690(2)	6944(1)	34(1)
N(2)	2199(2)	-399(2)	8559(1)	31(1)
C(1)	-264(3)	-816(3)	6119(2)	45(1)
C(2)	-734(4)	-2037(3)	5760(2)	54(1)
C(3)	-383(3)	-3151(3)	6269(2)	48(1)
C(4)	480(3)	-3077(2)	7139(2)	39(1)
C(5)	976(3)	-4184(2)	7712(4)	50(1)
C(6)	1812(4)	-4036(2)	8528(2)	47(1)
C(7)	2276(3)	-2758(2)	8857(2)	37(1)
C(8)	3169(3)	-2528(3)	9688(2)	45(1)
C(9)	3572(3)	-1279(3)	9935(2)	48(1)
C(10)	3065(3)	-227(3)	9343(2)	41(1)
C(11)	1809(2)	-1649(2)	8311(2)	31(1)
C(12)	919(2)	-1810(2)	7446(2)	30(1)
C(13)	4027(2)	2299(2)	7122(2)	28(1)
C(14)	3425(2)	2874(2)	8122(2)	28(1)

Appendix Table B4 Atomic coordinates ($x10^4$) and equivalent isotropic displacement parameters ($Åx10^3$) for $[Cu_2(\mu\text{-}ox)_2(phen)_2]_n$ (**4**)

	x	y	z	U(eq)
Cu(1)	8644(1)	3059(1)	5621(1)	30(1)
Cu(2)	13644(1)	6125(1)	5621(1)	30(1)
Cu(3)	6199(1)	8059(1)	622(1)	31(1)
Cu(4)	1199(1)	11125(1)	622(1)	30(1)
O(1)	6542(4)	3489(4)	6554(3)	36(1)
O(2)	7703(4)	4563(4)	4859(3)	36(1)
O(3)	9741(4)	4300(4)	6509(3)	38(1)
O(4)	10727(4)	3430(4)	4714(3)	37(1)
O(5)	11546(4)	5753(4)	6555(3)	36(1)
O(6)	12705(4)	4686(4)	4861(3)	36(1)
N(1)	7718(5)	1724(4)	4733(3)	33(1)
N(2)	9378(5)	1434(5)	6339(4)	35(1)
N(3)	12716(5)	7521(4)	4724(3)	32(1)
N(4)	14391(5)	7814(5)	6345(4)	36(1)
N(5)	5445(5)	6439(5)	1343(4)	36(1)
N(6)	7111(5)	6721(4)	-269(3)	33(1)
N(7)	438(5)	12815(5)	1345(4)	36(1)
N(8)	2114(5)	12526(4)	-274(3)	32(1)
C(1)	6854(7)	1906(6)	3938(5)	43(1)
C(2)	6349(7)	848(7)	3369(5)	51(2)
C(3)	6745(7)	-394(7)	3592(5)	45(2)
C(4)	7641(6)	-632(6)	4430(4)	39(1)
C(5)	8089(8)	-1907(7)	4762(6)	49(2)
C(6)	8959(9)	-2056(7)	5581(7)	51(2)
C(7)	9428(6)	-951(6)	6151(5)	40(1)
C(8)	10291(7)	-1009(8)	7015(5)	50(2)
C(9)	10651(8)	102(8)	7516(6)	56(2)
C(10)	10185(7)	1308(7)	7171(5)	47(1)
C(11)	9006(6)	319(5)	5841(4)	30(1)
C(12)	8096(6)	474(5)	4980(4)	32(1)

Appendix Table B4 (Continued)

	x	y	z	U(eq)
C(13)	11861(6)	7357(6)	3938(4)	40(1)
C(14)	11345(7)	8409(7)	3356(5)	48(2)
C(15)	11751(7)	9643(7)	3604(5)	46(2)
C(16)	12635(6)	9883(6)	4430(4)	38(1)
C(17)	13101(7)	11153(6)	4757(5)	45(1)
C(18)	13941(10)	11303(8)	5577(6)	53(2)
C(19)	14432(6)	10203(6)	6158(5)	41(1)
C(20)	15294(7)	10272(7)	7017(5)	52(2)
C(21)	15647(8)	9163(8)	7530(6)	55(2)
C(22)	15188(7)	7937(7)	7164(5)	47(1)
C(23)	13994(6)	8933(5)	5834(4)	30(1)
C(24)	13108(6)	8781(5)	4978(4)	33(1)
C(25)	10894(6)	4822(5)	6157(4)	28(1)
C(26)	11486(6)	4250(5)	5155(4)	29(1)
C(27)	15883(6)	4436(5)	6160(4)	27(1)
C(28)	16479(6)	5004(5)	5158(4)	30(1)
C(29)	4646(6)	6302(7)	2169(5)	47(1)
C(30)	4159(7)	5096(8)	2517(6)	56(2)
C(31)	4528(7)	3972(7)	2015(5)	49(2)
C(32)	5403(6)	4053(6)	1143(5)	41(1)
C(33)	5886(9)	2932(7)	572(7)	50(2)
C(34)	6739(8)	3098(6)	-242(6)	47(2)
C(35)	7189(6)	4365(6)	-572(4)	38(1)
C(36)	8077(7)	4601(7)	-1401(5)	46(2)
C(37)	8493(7)	5846(7)	-1637(5)	51(2)
C(38)	7979(6)	6904(7)	-1062(5)	42(1)
C(39)	6722(6)	5467(5)	-26(4)	31(1)
C(40)	5831(6)	5316(5)	838(4)	30(1)
C(41)	-342(7)	12949(7)	2164(5)	46(1)
C(42)	-820(8)	14162(7)	2521(5)	55(2)

Appendix Table B4 (Continued)

	x	y	z	U(eq)
C(43)	-461(7)	15271(7)	2016(5)	49(2)
C(44)	385(6)	15195(6)	1155(5)	42(1)
C(45)	897(8)	16305(8)	576(6)	48(2)
C(46)	1731(7)	16163(6)	-239(6)	48(2)
C(47)	2191(6)	14884(6)	-570(4)	38(1)
C(48)	3078(7)	14650(7)	-1404(5)	45(2)
C(49)	3470(7)	13406(7)	-1645(5)	49(2)
C(50)	2975(7)	12352(7)	-1054(5)	43(1)
C(51)	1719(6)	13774(5)	-23(4)	32(1)
C(52)	833(6)	13939(5)	830(4)	31(1)
C(53)	3350(6)	9255(5)	161(4)	29(1)
C(54)	3934(6)	9828(5)	1165(4)	28(1)
C(55)	-1667(6)	9993(6)	165(4)	31(1)
C(56)	8941(6)	9423(5)	1163(4)	28(1)
O(7)	14740(4)	4949(4)	6504(3)	39(1)
O(8)	15728(4)	5824(4)	4712(3)	38(1)
O(14)	3274(4)	10755(4)	1552(3)	37(1)
O(15)	82(4)	9947(4)	1506(3)	38(1)
O(11)	4094(4)	8427(4)	-281(3)	37(1)
O(12)	5081(4)	9300(4)	1508(3)	38(1)
O(10)	7110(4)	9567(4)	-131(3)	38(1)
O(9)	8278(4)	8497(4)	1552(3)	37(1)
O(16)	-901(4)	10824(4)	-284(3)	38(1)
O(13)	2119(4)	9691(4)	-140(3)	37(1)

Appendix Table B5 Atomic coordinates ($x10^4$) and equivalent isotropic displacement parameters ($Åx10^3$) for $[Cu(\mu\text{-}SO_4)(phen)(H_2O)_2]_n$ (**6**)

	x	y	z	U(eq)
Cu(1)	2013(1)	2007(1)	5083(1)	25(1)
S	2013(2)	1394(1)	86(3)	24(1)
O(5)	1053(3)	1035(3)	5012(5)	28(1)
N(1)	1116(4)	3098(3)	4947(7)	25(1)
O(6)	3007(3)	1027(3)	5131(6)	29(1)
O(3)	1640(4)	1974(3)	1391(6)	34(1)
N(2)	2921(4)	3103(3)	5217(7)	27(1)
O(2)	1253(3)	764(3)	-1203(6)	28(1)
O(1)	2795(3)	751(3)	1342(6)	33(1)
C(4)	1009(5)	4851(4)	4938(9)	36(2)
C(7)	2958(5)	4856(4)	5201(9)	30(1)
C(1)	205(5)	3078(5)	4840(10)	35(1)
C(10)	3823(5)	3065(5)	5308(10)	36(1)
C(11)	2481(4)	3964(3)	5146(7)	23(1)
C(12)	1508(4)	4001(4)	5005(8)	25(1)
C(8)	3983(6)	4790(5)	5374(14)	43(2)
C(3)	118(6)	4793(5)	4861(12)	42(2)
C(2)	-331(5)	3906(4)	4797(11)	40(1)
C(9)	4355(6)	3919(6)	5402(11)	52(2)
C(6)	2503(5)	5730(4)	5130(9)	37(1)
C(5)	1588(6)	5749(4)	5019(10)	46(2)
O(4)	2376(4)	1994(3)	-1244(6)	35(1)

Appendix Table B6 Atomic coordinates ($x10^4$) and equivalent isotropic displacement parameters ($Åx10^3$) for *cis*-$[Mn(phen)_2(Cl)_2]$ (**11**)

	x	y	z	U(eq)
Cl(1)	8133(1)	1302(1)	3305(1)	46(1)
N(1)	6181(1)	1419(1)	5315(1)	32(1)
N(4)	8285(1)	3534(1)	3824(1)	38(1)
C(5)	4764(1)	1344(1)	4980(1)	32(1)
N(2)	5164(1)	2276(1)	3715(1)	36(1)
N(3)	6732(1)	3528(1)	5241(1)	38(1)
C(18)	8098(1)	4311(1)	4251(1)	38(1)
C(6)	4226(1)	1796(1)	4125(1)	34(1)
C(17)	7256(1)	4309(1)	5000(1)	38(1)
C(4)	3831(1)	832(1)	5428(1)	39(1)
C(22)	9068(2)	3532(1)	3137(1)	47(1)
C(2)	5842(2)	464(1)	6578(1)	44(1)
C(13)	5954(2)	3522(1)	5923(1)	48(1)
C(3)	4413(2)	385(1)	6248(1)	44(1)
C(10)	4678(2)	2662(1)	2909(1)	48(1)
C(1)	6692(1)	986(1)	6086(1)	38(1)
C(7)	2768(1)	1706(1)	3747(1)	44(1)
C(16)	7008(2)	5104(1)	5452(1)	49(1)
C(19)	8690(2)	5110(1)	3995(1)	51(1)
C(12)	1846(2)	1193(1)	4228(1)	56(1)
C(8)	2302(2)	2134(1)	2891(1)	55(1)
C(11)	2353(2)	775(1)	5027(1)	53(1)
C(9)	3253(2)	2606(1)	2473(1)	58(1)
C(21)	9713(2)	4295(1)	2850(1)	58(1)
C(15)	6171(2)	5062(1)	6167(1)	58(1)
C(20)	9532(2)	5076(1)	3276(1)	60(1)
C(14)	5644(2)	4277(1)	6403(1)	56(1)
C(23)	7625(2)	5899(1)	5169(1)	63(1)
C(24)	8428(2)	5905(1)	4482(2)	65(1)
Mn	7546(1)	2291(1)	4513(1)	32(1)
Cl(2)	9587(1)	2163(1)	5767(1)	47(1)

Appendix C

Anisotropic thermal parameters for Cu(II) and Mn(II) complexes

Appendix Table C1 Anisotropic displacement parameters ($Å^2 \times 10^3$) for [Cu-(ox)(phen)(H_2O)]·H_2O (**1**)

	U_{11}	U_{22}	U_{33}	U_{23}	U_{13}	U_{12}
Cu(1)	39(1)	30(1)	28(1)	-1(1)	17(1)	-2(1)
O(1)	46(1)	33(1)	40(1)	1(1)	23(1)	-4(1)
O(2)	59(1)	34(1)	41(1)	-5(1)	25(1)	-2(1)
O(3)	60(1)	70(1)	46(1)	10(1)	29(1)	-9(1)
O(4)	93(1)	56(1)	55(1)	-14(1)	43(1)	8(1)
O(5)	51(1)	35(1)	70(1)	4(1)	-4(1)	2(1)
O(6)	50(1)	41(1)	64(1)	-1(1)	18(1)	3(1)
C(1)	50(1)	33(1)	45(1)	-2(1)	24(1)	-6(1)
C(2)	53(1)	32(1)	52(1)	-9(1)	23(1)	-5(1)
C(3)	44(1)	41(1)	39(1)	-11(1)	17(1)	0(1)
C(4)	31(1)	40(1)	26(1)	-1(1)	9(1)	3(1)
C(5)	39(1)	50(1)	26(1)	3(1)	14(1)	5(1)
C(6)	37(1)	51(1)	27(1)	10(1)	13(1)	0(1)
C(7)	30(1)	39(1)	26(1)	8(1)	6(1)	-1(1)
C(8)	42(1)	40(1)	35(1)	13(1)	7(1)	-7(1)
C(9)	52(1)	33(1)	39(1)	3(1)	6(1)	-10(1)
C(10)	51(1)	34(1)	32(1)	-1(1)	10(1)	-5(1)
C(11)	28(1)	32(1)	23(1)	4(1)	7(1)	0(1)
C(12)	28(1)	31(1)	24(1)	2(1)	9(1)	1(1)
C(13)	47(1)	39(1)	31(1)	2(1)	14(1)	10(1)
C(14)	36(1)	43(1)	27(1)	7(1)	11(1)	3(1)
N(2)	36(1)	30(1)	27(1)	1(1)	11(1)	-2(1)
N(1)	36(1)	30(1)	31(1)	-1(1)	15(1)	-3(1)

Appendix Table C2 Anisotropic displacement parameters ($Å^2 \times 10^3$) for $[Cu_4(\mu\text{-}ox)_2(phen)_4(H_2O)_4](NO_3)_4 \cdot 4H_2O$ (**2**)

	U_{11}	U_{22}	U_{33}	U_{23}	U_{13}	U_{12}
Cu(1)	28(1)	31(1)	25(1)	-5(1)	2(1)	1(1)
Cu(2)	29(1)	24(1)	29(1)	-1(1)	0(1)	1(1)
O(1)	39(1)	30(1)	51(2)	6(1)	-2(1)	7(1)
O(2)	36(1)	40(1)	40(1)	1(1)	8(1)	10(1)
O(3)	41(2)	47(2)	44(2)	6(1)	14(1)	3(1)
O(4)	72(2)	43(2)	63(2)	-1(2)	33(2)	-14(2)
O(5)	37(1)	44(2)	30(1)	-12(1)	5(1)	-3(1)
O(6)	48(2)	34(1)	37(1)	-8(1)	2(1)	-11(1)
O(7)	146(4)	276(7)	139(4)	-78(4)	-43(3)	73(4)
O(8)	146(4)	276(7)	139(4)	-78(4)	-43(3)	73(4)
O(9)	146(4)	276(7)	139(4)	-78(4)	-43(3)	73(4)
O(10)	89(2)	73(2)	78(2)	-1(1)	-2(1)	5(1)
O(11)	89(2)	73(2)	78(2)	-1(1)	-2(1)	5(1)
O(12)	89(2)	73(2)	78(2)	-1(1)	-2(1)	5(1)
O(13)	62(2)	51(2)	48(2)	-2(2)	16(2)	7(2)
O(14)	169(7)	59(3)	89(4)	7(3)	23(5)	-35(4)
N(1)	27(1)	32(1)	25(1)	-2(1)	2(1)	-2(1)
N(2)	33(1)	33(1)	24(1)	-1(1)	0(1)	-2(1)
N(3)	29(1)	33(1)	31(1)	3(1)	0(1)	1(1)
N(4)	28(1)	26(1)	32(1)	0(1)	1(1)	0(1)
N(5)	89(2)	73(2)	78(2)	-1(1)	-2(1)	5(1)
N(6)	146(4)	276(7)	139(4)	-78(4)	-43(3)	73(4)
C(1)	28(2)	42(2)	33(2)	-3(1)	-4(1)	-4(1)
C(2)	30(2)	53(2)	48(2)	4(2)	-6(2)	4(2)
C(3)	34(2)	38(2)	60(3)	3(2)	5(2)	8(2)
C(4)	38(2)	30(2)	40(2)	-3(1)	6(2)	3(1)
C(5)	64(3)	33(2)	55(3)	-13(2)	10(2)	6(2)
C(6)	76(3)	41(2)	40(2)	-18(2)	4(2)	1(2)
C(7)	52(2)	38(2)	27(2)	-7(1)	0(2)	-6(2)
C(8)	67(3)	55(3)	28(2)	-8(2)	-8(2)	-9(2)

Appendix Table C2 (Continued)

	U_{11}	U_{22}	U_{33}	U_{23}	U_{13}	U_{12}
C(9)	57(3)	60(3)	31(2)	1(2)	-14(2)	-1(2)
C(10)	44(2)	45(2)	31(2)	5(2)	-5(2)	2(2)
C(11)	36(2)	32(2)	23(1)	-2(1)	3(1)	-4(1)
C(12)	29(2)	30(2)	28(2)	-3(1)	4(1)	0(1)
C(13)	39(2)	51(2)	31(2)	1(2)	-3(2)	1(2)
C(14)	43(2)	65(3)	40(2)	10(2)	-10(2)	4(2)
C(15)	44(2)	48(2)	54(3)	15(2)	-6(2)	12(2)
C(16)	40(2)	32(2)	48(2)	11(2)	3(2)	5(2)
C(17)	56(3)	28(2)	68(3)	6(2)	1(2)	12(2)
C(18)	62(3)	24(2)	72(3)	-7(2)	4(2)	4(2)
C(19)	42(2)	25(2)	48(2)	-3(2)	4(2)	-4(1)
C(20)	53(2)	40(2)	49(2)	-12(2)	-1(2)	-9(2)
C(21)	41(2)	50(2)	40(2)	-8(2)	-7(2)	-8(2)
C(22)	30(2)	39(2)	34(2)	1(1)	-2(1)	-1(1)
C(23)	31(2)	24(1)	35(2)	2(1)	2(1)	-2(1)
C(24)	30(2)	27(2)	34(2)	5(1)	4(1)	1(1)
C(25)	33(2)	28(2)	25(1)	-6(1)	-3(1)	7(1)
C(26)	33(2)	33(2)	25(2)	-2(1)	-4(1)	8(1)
C(27)	25(1)	28(2)	29(2)	-7(1)	-2(1)	5(1)
C(28)	27(2)	35(2)	32(2)	-10(1)	-2(1)	1(1)

Appendix Table C3 Anisotropic displacement parameters ($Å^2 \times 10^3$) for $[Cu(\mu\text{-ox})(phen)]_n$ (**3**)

	U_{11}	U_{22}	U_{33}	U_{23}	U_{13}	U_{12}
Cu(1)	30(1)	29(1)	29(1)	4(1)	-2(1)	1(1)
O(1)	36(1)	34(1)	35(1)	-6(1)	1(1)	-4(1)
O(2)	37(1)	37(1)	34(1)	-3(1)	10(1)	-4(1)
O(3)	36(1)	41(1)	34(1)	13(1)	3(1)	1(1)
O(4)	36(1)	43(1)	32(1)	12(1)	8(1)	9(1)
N(1)	32(1)	37(1)	33(1)	2(1)	-4(1)	0(1)
N(2)	34(1)	31(1)	29(1)	3(1)	-1(1)	-1(1)
C(1)	47(1)	51(2)	38(1)	3(1)	-12(1)	-2(1)
C(2)	52(2)	67(2)	43(2)	-10(1)	-10(1)	-6(2)
C(3)	48(1)	50(2)	45(2)	-13(1)	0(1)	-10(1)
C(4)	36(1)	40(1)	41(1)	-4(1)	4(1)	-3(1)
C(5)	60(2)	30(1)	59(2)	-2(2)	9(2)	-3(1)
C(6)	56(2)	31(1)	54(2)	7(1)	6(1)	6(1)
C(7)	39(1)	36(1)	38(1)	10(1)	6(1)	8(1)
C(8)	49(2)	48(1)	37(1)	16(1)	-4(1)	11(1)
C(9)	53(2)	57(2)	34(1)	8(1)	-14(1)	1(1)
C(10)	45(1)	42(1)	35(1)	5(1)	-10(1)	-3(1)
C(11)	29(1)	33(1)	30(1)	3(1)	6(1)	5(1)
C(12)	30(1)	31(1)	30(1)	2(1)	4(1)	1(1)
C(13)	30(1)	27(1)	26(1)	-2(1)	-2(1)	1(1)
C(14)	32(1)	26(1)	28(1)	2(1)	2(1)	5(1)

Appendix Table C4 Anisotropic displacement parameters ($Å^2 \times 10^3$) for $[Cu_2(\mu\text{-}ox)_2(phen)_2]_n$(**4**)

	U_{11}	U_{22}	U_{33}	U_{23}	U_{13}	U_{12}
Cu(1)	31(1)	30(1)	30(1)	-4(1)	-1(1)	0(1)
Cu(2)	32(1)	30(1)	29(1)	5(1)	-2(1)	1(1)
Cu(3)	31(1)	30(1)	30(1)	-4(1)	2(1)	1(1)
Cu(4)	32(1)	29(1)	29(1)	4(1)	1(1)	0(1)
O(1)	36(2)	36(2)	36(2)	6(2)	2(2)	3(2)
O(2)	37(2)	38(2)	33(2)	3(2)	9(2)	5(2)
O(3)	37(2)	43(2)	34(2)	-12(2)	9(2)	-10(2)
O(4)	35(2)	43(2)	33(2)	-11(2)	2(2)	0(2)
O(5)	40(2)	33(2)	37(2)	-5(2)	3(2)	-6(2)
O(6)	38(2)	40(2)	31(2)	-2(2)	6(2)	-2(2)
N(1)	38(2)	33(2)	29(2)	-3(2)	1(2)	2(2)
N(2)	34(2)	39(3)	33(2)	-4(2)	-6(2)	1(2)
N(3)	37(2)	34(2)	26(2)	3(2)	-4(2)	0(2)
N(4)	34(2)	37(3)	36(3)	1(2)	-4(2)	0(2)
N(5)	32(2)	36(3)	40(3)	-2(2)	4(2)	1(2)
N(6)	35(2)	36(2)	27(2)	-2(2)	3(2)	2(2)
N(7)	31(2)	43(3)	34(2)	1(2)	4(2)	2(2)
N(8)	35(2)	35(2)	26(2)	5(2)	2(2)	1(2)
C(1)	51(3)	42(3)	35(3)	-2(2)	-8(2)	3(3)
C(2)	55(4)	61(4)	38(3)	-13(3)	-14(3)	3(3)
C(3)	52(4)	52(4)	32(3)	-13(3)	-3(3)	-11(3)
C(4)	37(3)	36(3)	43(3)	-8(2)	6(2)	-7(2)
C(5)	58(4)	33(3)	54(4)	-5(3)	8(3)	-6(3)
C(6)	72(5)	23(3)	58(5)	7(3)	12(3)	9(3)
C(7)	34(3)	44(3)	42(3)	5(3)	6(2)	2(2)
C(8)	52(4)	50(4)	47(4)	14(3)	1(3)	9(3)
C(9)	56(4)	65(5)	47(4)	14(3)	-15(3)	6(3)
C(10)	53(4)	51(4)	39(3)	-5(3)	-12(3)	-1(3)
C(11)	33(3)	30(3)	28(3)	-4(2)	6(2)	-3(2)
C(12)	31(2)	34(3)	32(3)	-4(2)	9(2)	-3(2)

Appendix Table C4 (Continued)

	U_{11}	U_{22}	U_{33}	U_{23}	U_{13}	U_{12}
C(13)	43(3)	41(3)	34(3)	7(2)	-7(2)	0(2)
C(14)	52(4)	57(4)	34(3)	10(3)	-13(3)	0(3)
C(15)	52(4)	51(4)	35(3)	17(3)	-2(3)	14(3)
C(16)	38(3)	37(3)	37(3)	12(2)	5(2)	9(2)
C(17)	51(4)	37(3)	47(4)	8(3)	8(3)	9(3)
C(18)	74(5)	33(4)	52(5)	-6(3)	14(4)	-1(3)
C(19)	41(3)	39(3)	45(3)	-2(3)	7(2)	-1(2)
C(20)	55(4)	50(4)	51(4)	-17(3)	-1(3)	-11(3)
C(21)	50(4)	64(5)	51(4)	-11(3)	-11(3)	-3(3)
C(22)	49(3)	51(4)	40(3)	3(3)	-12(3)	-3(3)
C(23)	32(3)	29(3)	30(3)	5(2)	2(2)	0(2)
C(24)	29(2)	33(3)	36(3)	3(2)	5(2)	4(2)
C(25)	29(2)	30(3)	25(2)	0(2)	-1(2)	1(2)
C(26)	34(3)	25(3)	29(3)	1(2)	0(2)	3(2)
C(27)	33(3)	28(3)	21(2)	4(2)	-3(2)	-3(2)
C(28)	36(3)	28(3)	26(3)	-1(2)	-1(2)	-7(2)
C(29)	49(3)	54(4)	36(3)	-7(3)	12(2)	-5(3)
C(30)	52(4)	69(5)	45(4)	11(3)	14(3)	-4(3)
C(31)	55(4)	42(3)	50(4)	14(3)	-5(3)	-10(3)
C(32)	33(3)	48(3)	43(3)	9(3)	-5(2)	-3(2)
C(33)	56(5)	28(4)	67(5)	4(3)	-15(4)	0(3)
C(34)	54(4)	31(3)	58(4)	-3(3)	-6(3)	8(3)
C(35)	40(3)	38(3)	35(3)	-10(2)	-3(2)	11(2)
C(36)	54(4)	50(4)	35(3)	-17(3)	3(3)	14(3)
C(37)	58(4)	57(4)	37(3)	-10(3)	14(3)	2(3)
C(38)	41(3)	49(4)	37(3)	-7(3)	9(2)	0(3)
C(39)	32(2)	33(3)	28(3)	-3(2)	-9(2)	2(2)
C(40)	34(3)	30(3)	27(3)	0(2)	-5(2)	4(2)
C(41)	51(4)	47(4)	40(3)	1(3)	14(3)	1(3)
C(42)	58(4)	65(5)	42(4)	-11(3)	8(3)	7(3)

Appendix Table C4 (Continued)

	U_{11}	U_{22}	U_{33}	U_{23}	U_{13}	U_{12}
C(43)	56(4)	47(4)	45(4)	-14(3)	-4(3)	13(3)
C(44)	35(3)	43(3)	46(3)	-7(3)	-5(2)	5(2)
C(46)	55(4)	34(3)	55(4)	3(3)	-7(3)	-8(3)
C(47)	39(3)	39(3)	37(3)	14(2)	-5(2)	-10(2)
C(48)	46(3)	52(4)	38(3)	16(3)	1(2)	-12(3)
C(49)	54(4)	54(4)	39(3)	8(3)	14(3)	-1(3)
C(50)	48(3)	45(3)	37(3)	1(3)	10(2)	1(3)
C(51)	29(2)	32(3)	33(3)	4(2)	-7(2)	-6(2)
C(52)	33(3)	29(3)	29(3)	1(2)	-8(2)	1(2)
C(53)	31(3)	29(3)	27(3)	4(2)	1(2)	-6(2)
C(54)	28(2)	29(3)	28(3)	-4(2)	-1(2)	0(2)
C(55)	31(3)	30(3)	32(3)	-4(2)	2(2)	6(2)
C(56)	31(3)	28(3)	24(2)	5(2)	2(2)	3(2)
O(7)	34(2)	46(2)	36(2)	13(2)	9(2)	10(2)
O(8)	38(2)	39(2)	38(2)	14(2)	3(2)	3(2)
O(14)	37(2)	36(2)	39(2)	-8(2)	1(2)	3(2)
O(15)	37(2)	42(2)	35(2)	13(2)	-12(2)	-10(2)
O(11)	38(2)	40(2)	33(2)	-9(2)	-3(2)	2(2)
O(12)	38(2)	45(2)	32(2)	-11(2)	-8(2)	7(2)
O(10)	39(2)	41(2)	32(2)	3(2)	-11(2)	-2(2)
O(9)	41(2)	33(2)	36(2)	6(2)	-4(2)	-4(2)
O(16)	37(2)	41(2)	35(2)	13(2)	-2(2)	-1(2)
O(13)	41(2)	38(2)	33(2)	-2(2)	-12(2)	4(2)

Appendix Table C5 Anisotropic displacement parameters ($Å^2 \times 10^3$) for $[Cu(\mu\text{-}SO_4)(phen)(H_2O)_2]_n$ **(6)**.

	U_{11}	U_{22}	U_{33}	U_{23}	U_{13}	U_{12}
Cu(1)	25(1)	18(1)	34(1)	0(1)	13(1)	-1(1)
S	32(1)	19(1)	24(1)	1(1)	15(1)	-2(1)
O(5)	39(2)	28(2)	20(2)	-3(1)	14(1)	-9(2)
N(1)	24(2)	23(2)	29(2)	-2(2)	11(2)	-4(2)
O(6)	28(2)	19(2)	42(2)	1(1)	12(2)	2(1)
O(3)	40(2)	34(2)	32(2)	-5(2)	17(2)	7(2)
N(2)	27(3)	27(2)	30(2)	-2(2)	13(2)	-4(2)
O(2)	30(2)	25(2)	32(2)	1(1)	12(2)	-3(2)
O(1)	45(3)	28(2)	28(2)	0(2)	15(2)	11(2)
C(4)	55(4)	25(2)	25(3)	3(2)	9(2)	19(2)
C(7)	32(3)	29(2)	29(3)	1(2)	12(2)	-2(2)
C(1)	31(3)	39(3)	40(3)	2(2)	18(2)	-2(2)
C(10)	23(3)	41(3)	46(3)	6(3)	11(2)	0(2)
C(11)	36(2)	12(2)	22(2)	-2(1)	10(2)	-9(2)
C(12)	21(2)	35(2)	23(2)	-3(2)	11(2)	-3(2)
C(8)	40(4)	42(3)	47(4)	-1(2)	15(3)	-19(3)
C(3)	41(4)	47(4)	36(3)	-1(2)	11(2)	26(3)
C(2)	23(2)	47(3)	53(4)	1(3)	16(3)	14(3)
C(9)	36(3)	77(5)	47(4)	3(3)	19(3)	-11(4)
C(6)	48(4)	29(2)	32(3)	3(2)	9(2)	-17(2)
C(5)	78(5)	15(2)	40(3)	1(2)	11(3)	-2(2)
O(4)	55(3)	26(2)	30(2)	-2(2)	21(2)	-16(2)

Appendix Table C6 Anisotropic displacement parameters ($Å^2 \times 10^3$) for *cis*-$[Mn(phen)_2Cl_2]$ **(11)**.

	U_{11}	U_{22}	U_{33}	U_{23}	U_{13}	U_{12}
Cl(1)	37(1)	53(1)	48(1)	-16(1)	8(1)	-5(1)
N(1)	31(1)	32(1)	33(1)	-1(1)	3(1)	-4(1)
N(4)	38(1)	39(1)	36(1)	3(1)	3(1)	-7(1)
C(5)	30(1)	31(1)	35(1)	-5(1)	6(1)	-2(1)
N(2)	39(1)	33(1)	36(1)	0(1)	3(1)	2(1)
N(3)	45(1)	33(1)	36(1)	-3(1)	5(1)	1(1)
C(18)	38(1)	33(1)	39(1)	6(1)	-8(1)	-7(1)
C(6)	30(1)	31(1)	38(1)	-6(1)	2(1)	3(1)
C(17)	41(1)	31(1)	38(1)	-2(1)	-8(1)	0(1)
C(4)	35(1)	40(1)	45(1)	-8(1)	14(1)	-7(1)
C(22)	42(1)	59(1)	40(1)	8(1)	6(1)	-8(1)
C(2)	56(1)	41(1)	34(1)	4(1)	7(1)	-8(1)
C(13)	57(1)	45(1)	42(1)	-6(1)	12(1)	4(1)
C(3)	51(1)	42(1)	43(1)	-3(1)	20(1)	-12(1)
C(10)	60(1)	42(1)	40(1)	3(1)	2(1)	5(1)
C(1)	39(1)	39(1)	34(1)	2(1)	1(1)	-6(1)
C(7)	32(1)	43(1)	54(1)	-11(1)	-4(1)	7(1)
C(16)	54(1)	35(1)	50(1)	-9(1)	-18(1)	6(1)
C(19)	48(1)	41(1)	55(1)	15(1)	-16(1)	-14(1)
C(12)	27(1)	64(1)	76(1)	-13(1)	3(1)	-1(1)
C(8)	47(1)	51(1)	59(1)	-11(1)	-16(1)	14(1)
C(11)	32(1)	61(1)	68(1)	-9(1)	16(1)	-10(1)
C(9)	71(1)	50(1)	45(1)	1(1)	-15(1)	14(1)
C(21)	45(1)	80(1)	48(1)	23(1)	2(1)	-16(1)
C(15)	67(1)	51(1)	51(1)	-20(1)	-8(1)	18(1)
C(20)	50(1)	61(1)	62(1)	28(1)	-12(1)	-23(1)
C(14)	64(1)	61(1)	43(1)	-14(1)	6(1)	16(1)
C(23)	75(1)	31(1)	72(1)	-6(1)	-21(1)	-1(1)
C(24)	69(1)	32(1)	81(1)	11(1)	-26(1)	-14(1)
Mn	33(1)	31(1)	33(1)	-1(1)	6(1)	-5(1)
Cl(2)	38(1)	55(1)	45(1)	4(1)	-2(1)	-11(1)

Appendix D

Bond length of Cu(II) and Mn(II) complexes

Appendix Table D1 Bond lengths [Å] for [Cu(ox)(phen)(H_2O)]·H_2O **(1)**

Distance	Value, Å	Distance	Value, Å
Cu(1)-O(1)	1.936(2)	Cu(1)-O(2)	1.942(1)
Cu(1)-N(1)	2.015(1)	Cu(1)-N(2)	2.004(1)
Cu(1)-O(5)	2.223(2)	O(1)-C(14)	1.283(2)
O(2)-C(13)	1.278(2)	O(3)-C(14)	1.210(2)
O(4)-C(13)	1.212(2)	C(1)-N(1)	1.326(2)
C(1)-C(2)	1.402(2)	C(2)-C(3)	1.370(3)
C(3)-C(4)	1.403(3)	C(4)-C(12)	1.404(2)
C(4)-C(5)	1.435(2)	C(5)-C(6)	1.348(3)
C(6)-C(7)	1.436(2)	C(7)-C(8)	1.403(3)
C(7)-C(11)	1.402(2)	C(8)-C(9)	1.367(3)
C(9)-C(10)	1.398(2)	C(11)-C(12)	1.433(2)
C(10)-N(2)	1.327(2)	C(11)-N(2)	1.354(2)
C(12)-N(1)	1.357(2)	C(13)-C(14)	1.549(3)

Appendix Table D2 Bond lengths [Å] for $[Cu_4(\mu\text{-suc})_2(phen)_4(H_2O)_4](NO_3)_4 \cdot 4H_2O$ **(2)**

Distance	Value, Å	Distance	Value, Å
Cu(1)-O(2)	1.948(3)	Cu(1)-O(5)	1.966(3)
Cu(1)-O(4)	2.240(3)	Cu(1)-N(1)	2.015(3)
Cu(1)-N(2)	2.011(3)	Cu(1)-Cu(2)	3.032(6)
Cu(2)-O(1)	1.946(3)	Cu(2)-O(3)	2.160(3)
Cu(2)-O(6)	1.952(3)	Cu(2)-N(3)	2.025(3)
Cu(2)-N(4)	2.007(3)	N(1)-C(1)	1.331(4)
N(1)-C(12)	1.362(4)	N(2)-C(10)	1.326(5)
N(2)-C(11)	1.360(5)	N(3)-C(13)	1.327(5)
N(3)-C(24)	1.358(5)	N(4)-C(22)	1.334(5)
N(4)-C(23)	1.359(4)	O(1)-C(25)	1.258(5)
O(2)-C(25)	1.264(5)	O(3)-H(4)	0.730(7)
O(3)-H(16)	0.700(6)	O(4)-H(24)	0.818(1)
O(4)-H(23)	0.818(1)	O(5)-C(27)	1.259(4)
O(6)-C(27)	1.260(5)	O(7)-N(6)	1.114(1)
O(8)-N(6)	1.099(1)	O(9)-N(6)	1.199(1)
O(10)-N(5)	1.216(8)	O(11)-N(5)	1.231(8)
O(12)-N(5)	1.224(8)	O(13)-H(13C)	0.750(8)
O(13)-H(13D)	0.700(7)	O(14)-H(14B)	0.819(1)
O(14)-H(14C)	0.820(8)	C(1)-C(2)	1.399(6)
C(2)-C(3)	1.371(7)	C(3)-C(4)	1.406(6)
C(4)-C(12)	1.398(5)	C(4)-C(5)	1.437(6)
C(5)-C(6)	1.342(7)	C(6)-C(7)	1.441(6)
C(7)-C(11)	1.401(5)	C(7)-C(8)	1.405(6)
C(8)-C(9)	1.364(7)	C(9)-C(10)	1.396(6)
C(11)-C(12)	1.432(5)	C(13)-C(14)	1.405(6)
C(14)-C(15)	1.369(7)	C(15)-C(16)	1.415(6)
C(16)-C(17)	1.443(7)	C(16)-C(24)	1.403(5)
C(17)-C(18)	1.344(7)	C(18)-C(19)	1.436(6)
C(19)-C(20)	1.411(6)	C(19)-C(23)	1.407(5)
C(20)-C(21)	1.364(7)	C(21)-C(22)	1.400(6)
C(23)-C(24)	1.426(5)	C(25)-C(26)	1.510(5)
C(26)-C(28)#1	1.510(5)	C(27)-C(28)	1.513(4)
C(28)-C(26)#1	1.510(5)		

Appendix Table D3 Bond lengths [Å] for $[Cu(\mu\text{-ox})(phen)]_n$ **(3)**

Distance	Value, Å	Distance	Value, Å
Cu(1)-O(4)	1.976(2)	Cu(1)-O(1)	2.309(2)
Cu(1)-N(2)	2.020(2)	Cu(1)-N(1)	2.047(2)
O(1)-C(13)	1.239(3)	O(2)-C(14)	1.266(3)
O(3)-C(14)#1	1.243(3)	O(4)-C(13)#	11.259(3)
N(1)-C(1)	1.327(3)	N(1)-C(12)	1.365(3)
N(2)-C(10)	1.323(3)	N(2)-C(11)	1.359(3)
C(1)-C(2)	1.396(4)	C(2)-C(3)	1.357(4)
C(3)-C(4)	1.406(4)	C(4)-C(12)	1.407(3)
C(4)-C(5)	1.432(4)	C(5)-C(6)	1.338(6)
C(6)-C(7)	1.433(4)	C(7)-C(11)	1.406(3)
C(7)-C(8)	1.397(4)	C(8)-C(9)	1.360(4)
C(9)-C(10)	1.406(4)	C(11)-C(12)	1.422(3)
C(13)-O(4)#2	1.259(3)	C(13)-C(14)	1.555(3)
C(14)-O(3)#2	1.243(3)		

Appendix Table D4 Bond lengths [Å] for $[Cu_2(\mu\text{-ox})_2(phen)_2]_n$ **(4)**

Distance	Value, Å	Distance	Value, Å
Cu(1)-N(1)	1.989(5)	Cu(1)-N(2)	2.027(5)
Cu(1)-O(1)	2.335(4)	Cu(1)-O(2)	2.031(4)
Cu(1)-O(3)	1.999(4)	Cu(1)-O(4)	2.292(4)
Cu(2)-N(3)	2.044(4)	Cu(2)-N(4)	2.084(5)
Cu(2)-O(5)	2.323(4)	Cu(2)-O(6)	1.975(4)
Cu(2)-O(7)	1.957(4)	Cu(2)-O(8)	2.283(4)
Cu(3)-N(5)	2.033(5)	Cu(3)-N(6)	1.989(5)
Cu(3)-O(9)	2.315(4)	Cu(3)-O(10)	2.017(4)
Cu(3)-O(11)	2.305(4)	Cu(3)-O(12)	2.009(4)
Cu(4)-N(7)	2.088(5)	Cu(4)-N(8)	2.043(4)
Cu(4)-O(13)	1.966(4)	Cu(4)-O(14)	2.301(4)
Cu(4)-O(15)	1.970(4)	Cu(4)-O(16)	2.292(4)
O(1)-C(27)#1	1.253(6)	O(2)-C(28)#1	1.271(7)
O(3)-C(25)	1.273(6)	O(4)-C(26)	1.234(7)
O(5)-C(25)	1.238(6)	O(6)-C(26)	1.264(6)
N(1)-C(1)	1.337(7)	N(1)-C(12)	1.359(7)
N(2)-C(10)	1.339(8)	N(2)-C(11)	1.357(7)
N(3)-C(13)	1.319(7)	N(3)-C(24)	1.372(7)
N(4)-C(22)	1.320(8)	N(4)-C(23)	1.376(7)
N(5)-C(29)	1.332(7)	N(5)-C(40)	1.371(7)
N(6)-C(38)	1.338(7)	N(6)-C(39)	1.365(7)
N(7)-C(41)	1.314(8)	N(7)-C(52)	1.383(7)
N(8)-C(50)	1.317(7)	N(8)-C(51)	1.361(7)
C(1)-C(2)	1.393(9)	C(2)-C(3)	1.348(10)
C(3)-C(4)	1.408(9)	C(4)-C(12)	1.404(8)
C(4)-C(5)	1.432(9)	C(5)-C(6)	1.361(1)
C(6)-C(7)	1.421(1)	C(7)-C(8)	1.400(9)
C(7)-C(11)	1.411(8)	C(8)-C(9)	1.351(1)
C(9)-C(10)	1.379(1)	C(11)-C(12)	1.428(8)
C(13)-C(14)	1.406(8)	C(14)-C(15)	1.349(1)
C(15)-C(16)	1.389(9)	C(16)-C(24)	1.407(8)

Appendix Table D4 (Continued)

Distance	Value, Å	Distance	Value, Å
C(16)-C(17)	1.427(9)	C(17)-C(18)	1.346(1)
C(18)-C(19)	1.435(1)	C(19)-C(20)	1.394(9)
C(19)-C(23)	1.419(8)	C(20)-C(21)	1.360(1)
C(21)-C(22)	1.402(1)	C(23)-C(24)	1.410(8)
C(25)-C(26)	1.555(6)	C(27)-O(1)#2	1.253(6)
C(27)-O(7)	1.256(6)	C(27)-C(28)	1.557(6)
C(28)-O(8)	1.236(7)	C(28)-O(2)#2	1.271(7)
C(30)-C(31)	1.366(1)	C(31)-C(32)	1.416(9)
C(32)-C(40)	1.404(8)	C(32)-C(33)	1.439(1)
C(33)-C(34)	1.350(1)	C(34)-C(35)	1.423(9)
C(35)-C(39)	1.402(8)	C(35)-C(36)	1.396(9)
C(36)-C(37)	1.360(1)	C(37)-C(38)	1.401(9)
C(39)-C(40)	1.421(8)	C(41)-C(42)	1.392(1)
C(42)-C(43)	1.356(1)	C(43)-C(44)	1.389(9)
C(44)-C(52)	1.409(8)	C(44)-C(45)	1.447(1)
C(45)-C(46)	1.338(1)	C(46)-C(47)	1.435(9)
C(47)-C(48)	1.398(9)	C(47)-C(51)	1.414(7)
C(48)-C(49)	1.353(1)	C(49)-C(50)	1.408(8)
C(51)-C(52)	1.408(8)	C(53)-O(11)	1.233(7)
C(53)-O(13)	1.276(6)	C(53)-C(54)	1.555(6)
C(54)-O(14)	1.231(6)	C(54)-O(12)	1.266(6)
C(55)-O(16)	1.253(7)	C(55)-O(10)#1	1.264(6)
C(55)-C(56)#1	1.557(6)	C(56)-O(9)	1.236(6)
C(56)-O(15)#2	1.259(6)	C(56)-C(55)#2	1.557(6)
O(15)-C(56)#1	1.259(6)	O(10)-C(55)#2	1.264(6)

Appendix Table D5 Bond lengths [Å] for $[Cu(\mu\text{-}SO_4)(phen)(H_2O)_2]_n$ **(6)**

Distance	Value, Å	Distance	Value, Å
Cu(1)-O(5)	1.955(4)	Cu(1)-O(6)	2.002(4)
Cu(1)-N(1)	2.001(5)	Cu(1)-N(2)	2.018(5)
S-O(3)	1.456(5)	S-O(4)	1.477(5)
S-O(2)	1.489(5)	S-O(1)	1.510(5)
N(1)-C(1)	1.335(9)	N(1)-C(12)	1.377(7)
N(2)-C(10)	1.326(9)	N(2)-C(11)	1.355(7)
C(1)-C(2)	1.394(9)	C(3)-C(2)	1.394(1)
C(4)-C(3)	1.315(1)	C(4)-C(12)	1.387(8)
C(4)-C(5)	1.505(1)	C(6)-C(5)	1.342(5)
C(7)-C(6)	1.382(1)	C(7)-C(8)	1.496(1)
C(8)-C(9)	1.327(1)	C(10)-C(9)	1.414(1)
C(7)-C(11)	1.422(8)	C(11)-C(12)	1.422(3)

Appendix Table D6 Bond lengths [Å] for *cis*-[$Mn(phen)_2Cl_2$] **(11)**

Distance	Value, Å	Distance	Value, Å
Cl(1)-Mn	2.4379(4)	Cl(2)-Mn	2.4463(4)
N(1)-Mn	2.2913(1)	N(2)-Mn	2.3682(1)
N(3)-Mn	2.3444(1)	N(4)-Mn	2.2962(1)
N(1)-C(1)	1.3226(2)	N(1)-C(5)	1.3581(1)
N(2)-C(6)	1.3570(2)	N(2)-C(10)	1.3246(2)
N(3)-C(13)	1.3227(2)	N(3)-C(17)	1.3536(2)
N(4)-C(18)	1.3573(2)	N(4)-C(22)	1.3325(2)
C(2)-C(1)	1.4005(2)	C(2)-C(3)	1.368(2)
C(4)-C(3)	1.406(2)	C(4)-C (11)	1.4315(2)
C(5)-C(4)	1.4100(2)	C(5)-C(6)	1.4389(2)
C(6)-C(7)	1.4096(2)	C(7)-C(8)	1.410(2)
C(7)-C(12)	1.431(2)	C(8)-C(9)	1.365(3)
C(10)-C(9)	1.400(2)	C(13)-C(14)	1.397(2)
C(15)-C(14)	1.357(3)	C(16)-C(15)	1.402(3)
C(16)-C(23)	1.429(2)	C(17)-C(16)	1.4114(2)
C(18)-C(17)	1.445(2)	C(18)-C(19)	1.4106(2)
C(19)-C(20)	1.409(3)	C(19)-C(24)	1.441(3)
C(12)-C(11)	1.343(3)	C(21)-C(20)	1.361(3)
C(22)-C(21)	1.404(2)	C(23)-C(24)	1.345(3)

Appendix E

Bond angle of Cu(II) and Mn(II) complexes

Appendix Table E1 Bond angle [°] for [Cu(ox)(phen)(H_2O)]·H_2O **(1)**

Angle	Value, °	Angle	Value, °
O(1)-Cu(1)-O(2)	85.17(5)	O(1)-Cu(1)-O(5)	95.11(6)
O(1)-Cu(1)-N(1)	94.98(5)	O(1)-Cu(1)-N(2)	166.81(6)
O(2)-Cu(1)-N(1)	167.74(6)	O(2)-Cu(1)-N(2)	94.81(6)
O(2)-Cu(1)-O(5)	96.74(7)	N(1)-Cu(1)-O(5)	95.46(7)
N(2)-Cu(1)-N(1)	82.25(5)	N(2)-Cu(1)-O(5)	97.99(6)
C(14)-O(1)-Cu(1)	112.68(1)	C(13)-O(2)-Cu(1)	112.42(1)
C(1)-N(1)-Cu(1)	129.64(1)	C(12)-N(1)-Cu(1)	112.04(1)
C(1)-N(1)-C(12)	118.26(1)	C(10)-N(2)-Cu(1)	129.00(1)
C(11)-N(2)-Cu(1)	112.61(1)	C(10)-N(2)-C(11)	118.34(1)
N(1)-C(1)-C(2)	121.77(2)	C(3)-C(2)-C(1)	120.33(2)
C(2)-C(3)-C(4)	119.11(2)	C(3)-C(4)-C(12)	116.97(2)
C(3)-C(4)-C(5)	124.04(2)	C(12)-C(4)-C(5)	118.98(2)
C(6)-C(5)-C(4)	121.06(2)	C(5)-C(6)-C(7)	121.19(2)
C(11)-C(7)-C(8)	116.61(2)	C(11)-C(7)-C(6)	118.91(2)
C(8)-C(7)-C(6)	124.46(2)	C(9)-C(8)-C(7)	119.57(2)
C(8)-C(9)-C(10)	120.06(2)	N(2)-C(10)-C(9)	121.81(2)
N(2)-C(11)-C(7)	123.59(2)	N(2)-C(11)-C(12)	116.47(1)
C(7)-C(11)-C(12)	119.94(1)	N(1)-C(12)-C(4)	123.54(2)
N(1)-C(12)-C(11)	116.56(1)	C(4)-C(12)-C(11)	119.90(1)
O(4)-C(13)-O(2)	126.06(2)	O(4)-C(13)-C(14)	118.94(2)
O(2)-C(13)-C(14)	115.00(1)	O(3)-C(14)-O(1)	125.81(2)
O(1)-C(14)-C(13)	114.54(1)	O(3)-C(14)-C(13)	119.64(2)

Appendix Table E2 Bond angle[°] for $[Cu_4(\mu\text{-suc})_2(phen)_4(H_2O)_4](NO_3)_4 \cdot 4H_2O$ **(2)**

Angle	Value, °	Angle	Value, °
O(2)-Cu(1)-O(4)	102.84(1)	O(2)-Cu(1)-O(5)	90.69(1)
O(2)-Cu(1)-N(1)	164.53(1)	O(2)-Cu(1)-N(2)	91.42(1)
O(5)-Cu(1)-N(1)	95.00(1)	O(5)-Cu(1)-N(2)	175.95(1)
O(5)-Cu(1)-O(4)	95.40(1)	N(1)-Cu(1)-O(4)	90.95(1)
N(2)-Cu(1)-O(4)	87.49(1)	N(2)-Cu(1)-N(1)	82.10(1)
O(2)-Cu(1)-Cu(2)	83.04(9)	O(4)-Cu(1)-Cu(2)	172.09(1)
O(5)-Cu(1)-Cu(2)	79.10(9)	N(1)-Cu(1)-Cu(2)	83.93(8)
N(2)-Cu(1)-Cu(2)	97.73(9)	O(1)-Cu(2)-N(3)	173.84(1)
O(1)-Cu(2)-N(4)	93.81(1)	O(1)-Cu(2)-O(3)	93.07(1)
O(1)-Cu(2)-O(6)	91.46(1)	O(6)-Cu(2)-O(3)	97.50(1)
O(6)-Cu(2)-N(3)	91.23(1)	O(6)-Cu(2)-N(4)	164.98(1)
O(1)-Cu(2)-Cu(1)	72.40(9)	O(3)-Cu(2)-Cu(1)	164.16(1)
O(6)-Cu(2)-Cu(1)	77.09(9)	N(3)-Cu(2)-Cu(1)	102.83(9)
N(4)-Cu(2)-Cu(1)	91.12(9)	N(3)-Cu(2)-O(3)	92.07(1)
N(4)-Cu(2)-O(3)	96.25(1)	N(4)-Cu(2)-N(3)	82.25(1)
C(25)-O(1)-Cu(2)	134.9(3)	C(25)-O(2)-Cu(1)	121.1(2)
Cu(2)-O(3)-H(4)	122(5)	Cu(2)-O(3)-H(16)	125(5)
H(4)-O(3)-H(16)	110(7)	Cu(1)-O(4)-H(24)	144(7)
Cu(1)-O(4)-H(23)	118(5)	H(24)-O(4)-H(23)	98(7)
C(27)-O(5)-Cu(1)	126.8(2)	C(27)-O(6)-Cu(2)	130.2(2)
H(13D)-O(13)-H(13C)	97(7)	H(14B)-O(14)-H(14C)	88(8)
C(1)-N(1)-Cu(1)	129.7(3)	C(1)-N(1)-C(12)	117.8(3)
C(12)-N(1)-Cu(1)	112.5(2)	C(10)-N(2)-C(11)	118.2(3)
C(10)-N(2)-Cu(1)	129.3(3)	C(11)-N(2)-Cu(1)	112.4(2)
C(13)-N(3)-C(24)	119.2(3)	C(13)-N(3)-Cu(2)	129.1(3)
C(24)-N(3)-Cu(2)	111.7(2)	C(22)-N(4)-C(23)	118.2(3)
C(22)-N(4)-Cu(2)	129.3(3)	C(23)-N(4)-Cu(2)	112.4(2)
O(10)-N(5)-O(12)	122.5(7)	O(10)-N(5)-O(11)	117.0(6)
O(12)-N(5)-O(11)	120.4(6)	O(8)-N(6)-O(7)	119.1(16)

Appendix Table E2 (Continued)

Angle	Value, °	Angle	Value, °
O(8)-N(6)-O(9)	112.7(14)	O(7)-N(6)-O(9)	127.8(14)
N(1)-C(1)-C(2)	122.4(4)	N(1)-C(1)-H(1)	118.8
N(2)-C(10)-C(9)	122.3(4)	N(2)-C(10)-H(10)	118.9
N(2)-C(11)-C(7)	123.0(3)	N(2)-C(11)-C(12)	116.7(3)
N(1)-C(12)-C(4)	123.5(3)	N(1)-C(12)-C(11)	116.2(3)
N(3)-C(13)-C(14)	121.4(4)	N(3)-C(13)-H(13)	119.3
N(4)-C(22)-C(21)	122.1(4)	N(4)-C(22)-H(22)	119.0
N(4)-C(23)-C(19)	123.3(3)	N(4)-C(23)-C(24)	116.6(3)
N(3)-C(24)-C(16)	122.8(3)	N(3)-C(24)-C(23)	117.0(3)
O(1)-C(25)-O(2)	125.4(3)	O(1)-C(25)-C(26)	116.4(3)
O(2)-C(25)-C(26)	118.1(3)		

Symmetry transformations used to generate equivalent atoms: #1 -x+1,-y,-z

Appendix Table E3 Bond angle[°] for $[Cu(\mu\text{-ox})(phen)]_n$ **(3)**

Angle	Value, °	Angle	Value, °
O(2)-Cu(1)-O(1)	77.95(6)	O(2)-Cu(1)-O(3)	88.42(7)
O(2)-Cu(1)-N(1)	172.73(8)	O(2)-Cu(1)-N(2)	91.77(8)
O(3)-Cu(1)-O(1)	161.40(5)	O(4)-Cu(1)-O(1)	89.83(6)
O(4)-Cu(1)-O(2)	93.24(7)	O(4)-Cu(1)-O(3)	78.25(6)
O(4)-Cu(1)-N(1)	93.69(8)	O(4)-Cu(1)-N(2)	173.37(7)
N(1)-Cu(1)-O(1)	99.90(7)	N(1)-Cu(1)-O(3)	95.11(8)
N(2)-Cu(1)-O(1)	95.46(7)	N(2)-Cu(1)-O(3)	97.57(7)
N(2)-Cu(1)-N(1)	81.48(8)	C(13)-O(1)-Cu(1)	108.25(1)
C(13)#1-O(4)-Cu(1)	118.07(1)	C(14)-O(2)-Cu(1)	118.26(2)
C(14)#1-O(3)-Cu(1)	108.10(1)	C(1)-N(1)-Cu(1)	130.30(2)
C(12)-N(1)-Cu(1)	111.74(1)	C(10)-N(2)-Cu(1)	129.07(2)
C(11)-N(2)-Cu(1)	112.69(1)	C(1)-N(1)-C(12)	117.90(2)
C(10)-N(2)-C(11)	118.20(2)	N(1)-C(1)-C(2)	122.70(3)
C(3)-C(2)-C(1)	119.6(3)	C(2)-C(3)-C(4)	120.1(3)
C(3)-C(4)-C(12)	116.7(2)	C(3)-C(4)-C(5)	125.2(3)
C(4)-C(12)-C(11)	120.3(2)	C(5)-C(6)-C(7)	121.3(2)
C(6)-C(5)-C(4)	121.8(2)	C(7)-C(11)-C(12)	120.2(2)
C(8)-C(7)-C(6)	124.5(2)	C(8)-C(9)-C(10)	118.9(2)
C(9)-C(8)-C(7)	120.3(2)	C(11)-C(7)-C(6)	118.4(2)
C(11)-C(7)-C(8)	117.1(2)	C(12)-C(4)-C(5)	118.1(3)
N(1)-C(12)-C(4)	122.9(2)	N(1)-C(12)-C(11)	116.76(2)
N(2)-C(10)-C(9)	122.7(2)	N(2)-C(11)-C(7)	122.7(2)
N(2)-C(11)-C(12)	117.1(2)	O(1)-C(13)-O(4)#21	25.0(2)
O(1)-C(13)-C(14)	118.31(2)	O(4)#2-C(13)-C(14)	116.70(2)
O(3)#2-C(14)-O(2)	125.3(2)	O(3)#2-C(14)-C(13)	117.79(2)
O(2)-C(14)-C(13)	116.92(2)		

Symmetry transformations used to generate equivalent atoms:
#1 x-1/2,-y+1/2,z #2 x+1/2,-y+1/2,z

Appendix Table E4 Bond angle [°] for $[Cu_2(\mu\text{-}ox)_2(phen)_2]_n$ **(4)**

Angle	Value, °	Angle	Value, °
N(1)-Cu(1)-O(3)	174.74(2)	N(1)-Cu(1)-N(2)	82.37(2)
O(3)-Cu(1)-N(2)	93.88(2)	N(1)-Cu(1)-O(2)	91.96(2)
O(3)-Cu(1)-O(2)	92.00(2)	N(2)-Cu(1)-O(2)	173.38(2)
N(1)-Cu(1)-O(4)	98.79(2)	O(3)-Cu(1)-O(4)	77.89(2)
N(2)-Cu(1)-O(4)	96.32(2)	O(2)-Cu(1)-O(4)	87.88(2)
N(1)-Cu(1)-O(1)	95.32(2)	O(3)-Cu(1)-O(1)	88.95(2)
N(2)-Cu(1)-O(1)	99.95(2)	O(2)-Cu(1)-O(1)	77.10(2)
O(4)-Cu(1)-O(1)	159.72(2)	O(7)-Cu(2)-O(6)	94.54(2)
O(7)-Cu(2)-N(3)	172.60(2)	O(6)-Cu(2)-N(3)	91.90(2)
O(7)-Cu(2)-N(4)	93.28(2)	O(6)-Cu(2)-N(4)	171.68(2)
N(3)-Cu(2)-N(4)	80.49(2)	O(7)-Cu(2)-O(8)	79.08(2)
O(6)-Cu(2)-O(8)	89.62(2)	N(3)-Cu(2)-O(8)	97.35(2)
N(4)-Cu(2)-O(8)	94.65(2)	O(7)-Cu(2)-O(5)	90.03(2)
O(6)-Cu(2)-O(5)	78.09(2)	N(3)-Cu(2)-O(5)	94.87(2)
N(4)-Cu(2)-O(5)	99.09(2)	O(8)-Cu(2)-O(5)	162.93(2)
N(6)-Cu(3)-O(12)	173.90(2)	N(6)-Cu(3)-O(10)	92.75(2)
O(12)-Cu(3)-O(10)	91.59(2)	N(6)-Cu(3)-N(5)	82.66(2)
O(12)-Cu(3)-N(5)	93.20(2)	O(10)-Cu(3)-N(5)	174.71(2)
N(6)-Cu(3)-O(11)	98.65(2)	O(12)-Cu(3)-O(11)	77.22(1)
O(10)-Cu(3)-O(11)	87.77(2)	N(5)-Cu(3)-O(11)	95.48(2)
N(6)-Cu(3)-O(9)	96.06(2)	O(12)-Cu(3)-O(9)	89.08(2)
O(10)-Cu(3)-O(9)	77.39(2)	N(5)-Cu(3)-O(9)	100.42(2)
O(11)-Cu(3)-O(9)	159.56(2)	O(13)-Cu(4)-O(15)	94.65(2)
O(13)-Cu(4)-N(8)	92.19(2)	O(15)-Cu(4)-N(8)	171.90(2)
O(13)-Cu(4)-N(7)	172.16(2)	O(15)-Cu(4)-N(7)	92.93(2)
N(8)-Cu(4)-N(7)	80.41(2)	O(13)-Cu(4)-O(16)	89.36(2)
O(15)-Cu(4)-O(16)	78.42(2)	N(8)-Cu(4)-O(16)	97.35(2)
N(7)-Cu(4)-O(16)	94.15(2)	O(13)-Cu(4)-O(14)	78.62(2)
O(15)-Cu(4)-O(14)	90.33(2)	N(8)-Cu(4)-O(14)	95.28(2)
N(7)-Cu(4)-O(14)	99.34(2)	O(16)-Cu(4)-O(14)	162.87(2)

Appendix Table E4 (Continued)

Angle	Value, °	Angle	Value, °
C(27)#1-O(1)-Cu(1)	108.4(3)	C(28)#1-O(2)-Cu(1)	118.8(3)
C(25)-O(3)-Cu(1)	117.5(3)	C(26)-O(4)-Cu(1)	109.2(3)
C(25)-O(5)-Cu(2)	107.1(3)	C(26)-O(6)-Cu(2)	119.0(4)
C(1)-N(1)-C(12)	118.3(5)	C(1)-N(1)-Cu(1)	129.0(4)
C(12)-N(1)-Cu(1)	112.6(4)	C(10)-N(2)-C(11)	117.6(5)
C(10)-N(2)-Cu(1)	130.8(4)	C(11)-N(2)-Cu(1)	111.5(4)
C(13)-N(3)-C(24)	117.9(5)	C(13)-N(3)-Cu(2)	128.7(4)
C(24)-N(3)-Cu(2)	113.4(4)	C(22)-N(4)-C(23)	118.6(5)
C(22)-N(4)-Cu(2)	129.9(4)	C(23)-N(4)-Cu(2)	111.4(4)
C(29)-N(5)-C(40)	117.5(5)	C(29)-N(5)-Cu(3)	131.8(4)
C(40)-N(5)-Cu(3)	110.7(4)	C(38)-N(6)-C(39)	118.4(5)
C(38)-N(6)-Cu(3)	128.8(4)	C(39)-N(6)-Cu(3)	112.7(4)
C(41)-N(7)-C(52)	118.2(6)	C(41)-N(7)-Cu(4)	130.5(5)
C(52)-N(7)-Cu(4)	111.3(4)	C(50)-N(8)-C(51)	118.5(5)
C(50)-N(8)-Cu(4)	128.1(4)	C(51)-N(8)-Cu(4)	113.4(4)
N(1)-C(1)-C(2)	121.4(6)	C(3)-C(2)-C(1)	120.9(6)
C(2)-C(3)-C(4)	119.7(6)	C(12)-C(4)-C(3)	116.6(6)
C(12)-C(4)-C(5)	118.6(6)	C(3)-C(4)-C(5)	124.8(6)
C(6)-C(5)-C(4)	121.2(6)	C(5)-C(6)-C(7)	121.2(7)
C(8)-C(7)-C(11)	115.9(6)	C(8)-C(7)-C(6)	125.2(6)
C(11)-C(7)-C(6)	118.9(6)	C(9)-C(8)-C(7)	120.6(7)
C(8)-C(9)-C(10)	120.1(7)	N(2)-C(10)-C(9)	122.3(6)
N(2)-C(11)-C(7)	123.5(6)	N(2)-C(11)-C(12)	116.6(5)
C(7)-C(11)-C(12)	119.9(5)	N(1)-C(12)-C(4)	123.2(5)
N(1)-C(12)-C(11)	116.7(5)	C(4)-C(12)-C(11)	120.2(5)
N(3)-C(13)-C(14)	123.0(6)	C(15)-C(14)-C(13)	118.7(6)
C(14)-C(15)-C(16)	121.1(6)	C(15)-C(16)-C(24)	116.9(6)
C(15)-C(16)-C(17)	125.0(5)	C(24)-C(16)-C(17)	118.1(6)
C(18)-C(17)-C(16)	121.3(6)	C(17)-C(18)-C(19)	122.1(7)
C(20)-C(19)-C(23)	117.1(6)	C(20)-C(19)-C(18)	125.7(6)

Appendix Table E4 (Continued)

Angle	Value, °	Angle	Value, °
C(23)-C(19)-C(18)	117.2(6)	C(21)-C(20)-C(19)	120.5(6)
C(20)-C(21)-C(22)	119.5(6)	N(4)-C(22)-C(21)	122.4(6)
N(4)-C(23)-C(24)	117.7(5)	N(4)-C(23)-C(19)	121.9(6)
C(24)-C(23)-C(19)	120.4(5)	N(3)-C(24)-C(16)	122.4(5)
N(3)-C(24)-C(23)	116.7(5)	C(16)-C(24)-C(23)	120.9(5)
O(5)-C(25)-O(3)	124.2(5)	O(5)-C(25)-C(26)	118.9(4)
O(3)-C(25)-C(26)	116.9(4)	O(4)-C(26)-O(6)	125.9(5)
O(4)-C(26)-C(25)	117.7(4)	O(6)-C(26)-C(25)	116.4(4)
O(1)#2-C(27)-O(7)	124.5(5)	O(1)#2-C(27)-C(28)	118.6(4)
O(7)-C(27)-C(28)	116.9(4)	O(8)-C(28)-O(2)#2	125.2(5)
O(8)-C(28)-C(27)	118.1(4)	O(2)#2-C(28)-C(27)	116.7(4)
N(5)-C(29)-C(30)	123.3(6)	C(31)-C(30)-C(29)	119.7(6)
C(30)-C(31)-C(32)	119.5(6)	C(40)-C(32)-C(31)	116.9(6)
C(40)-C(32)-C(33)	118.9(6)	C(31)-C(32)-C(33)	124.2(6)
C(34)-C(33)-C(32)	120.3(7)	C(33)-C(34)-C(35)	122.1(6)
C(39)-C(35)-C(36)	116.8(6)	C(39)-C(35)-C(34)	118.3(6)
C(36)-C(35)-C(34)	124.9(6)	C(37)-C(36)-C(35)	120.6(5)
C(36)-C(37)-C(38)	119.6(6)	N(6)-C(38)-C(37)	121.7(6)
N(6)-C(39)-C(35)	122.9(5)	N(6)-C(39)-C(40)	116.5(5)
C(35)-C(39)-C(40)	120.6(5)	N(5)-C(40)-C(32)	123.1(6)
N(5)-C(40)-C(39)	117.1(5)	C(32)-C(40)-C(39)	119.8(5)
N(7)-C(41)-C(42)	123.0(7)	C(43)-C(42)-C(41)	119.5(7)
C(42)-C(43)-C(44)	120.1(6)	C(43)-C(44)-C(52)	117.8(6)
C(43)-C(44)-C(45)	125.5(6)	C(52)-C(44)-C(45)	116.6(6)
C(46)-C(45)-C(44)	122.5(7)	C(45)-C(46)-C(47)	120.9(6)
C(48)-C(47)-C(51)	117.0(6)	C(48)-C(47)-C(46)	124.6(5)
C(51)-C(47)-C(46)	118.3(6)	C(49)-C(48)-C(47)	120.0(5)
C(48)-C(49)-C(50)	119.6(6)	N(8)-C(50)-C(49)	122.4(6)
N(8)-C(51)-C(52)	117.5(5)	N(8)-C(51)-C(47)	122.5(5)
C(52)-C(51)-C(47)	120.0(5)	N(7)-C(52)-C(44)	121.3(6)
N(7)-C(52)-C(51)	117.2(5)	C(44)-C(52)-C(51)	121.5(5)
O(11)-C(53)-O(13)	125.1(5)	O(11)-C(53)-C(54)	118.5(4)

Appendix Table E4 (Continued)

Angle	Value, °	Angle	Value, °
O(13)-C(53)-C(54)	116.4(4)	O(14)-C(54)-O(12)	125.5(5)
O(14)-C(54)-C(53)	118.5(4)	O(12)-C(54)-C(53)	116.0(4)
O(16)-C(55)-O(10)#1	125.3(5)	O(16)-C(55)-C(56)#1	117.6(4)
O(10)#1-C(55)-C(56)#1	117.1(4)	O(9)-C(56)-O(15)#2	125.3(5)
O(9)-C(56)-C(55)#2	118.0(4)	O(15)#2-C(56)-C(55)#2	116.7(4)
C(27)-O(7)-Cu(2)	117.5(3)	C(28)-O(8)-Cu(2)	107.4(3)
C(54)-O(14)-Cu(4)	107.8(3)	C(56)#1-O(15)-Cu(4)	118.2(3)
C(53)-O(11)-Cu(3)	108.9(3)	C(54)-O(12)-Cu(3)	118.5(3)
C(55)#2-O(10)-Cu(3)	118.1(3)	C(56)-O(9)-Cu(3)	108.9(3)
C(55)-O(16)-Cu(4)	107.9(3)	C(53)-O(13)-Cu(4)	118.3(3)

Symmetry transformations used to generate equivalent atoms:
#1 x-1,y,z #2 x+1,y,z

Appendix Table E5 Bond angle [°] for $[Cu(\mu\text{-}SO_4)(phen)(H_2O)_2]_n$ **(6)**

Angle	Value, °	Angle	Value, °
O(5)-Cu(1)-O(6)	93.70(7)	O(5)-Cu(1)-N(1)	92.72(2)
O(6)-Cu(1)-N(1)	173.31(2)	O(5)-Cu(1)-N(2)	174.5(2)
O(6)-Cu(1)-N(2)	91.64(2)	N(1)-Cu(1)-N(2)	81.97(7)
O(3)-S-O(1)	109.7(3)	O(3)-S-O(2)	109.8(3)
O(3)-S-O(4)	112.14(1)	O(4)-S-O(2)	107.8(3)
O(4)-S-O(1)	109.5(3)	O(2)-S-O(1)	107.81(9)
C(1)-N(1)-Cu(1)	129.7(4)	C(1)-N(1)-C(12)	115.8(5)
C(12)-N(1)-Cu(1)	114.5(4)	C(10)-N(2)-C(11)	120.5(5)
C(10)-N(2)-Cu(1)	128.8(4)	C(11)-N(2)-Cu(1)	110.6(4)
N(1)-C(1)-C(2)	123.4(6)	N(2)-C(10)-C(9)	120.9(6)
N(2)-C(11)-C(7)	122.2(7)	N(2)-C(11)-C(12)	120.3(5)
N(1)-C(12)-C(4)	123.6(7)	N(1)-C(12)-C(11)	112.5(6)
C(3)-C(4)-C(12)	118.3(6)	C(3)-C(4)-C(5)	127.6(6)
C(12)-C(4)-C(5)	114.1(7)	C(11)-C(7)-C(6)	121.8(7)
C(11)-C(7)-C(8)	116.0(6)	C(6)-C(7)-C(8)	122.2(6)
N(1)-C(1)-C(2)	123.4(6)	N(2)-C(10)-C(9)	120.9(6)
N(2)-C(11)-C(7)	122.2(7)	N(2)-C(11)-C(12)	120.3(5)
C(7)-C(11)-C(12)	117.4(6)	N(1)-C(12)-C(4)	123.6(7)
N(1)-C(12)-C(11)	112.5(6)	C(4)-C(12)-C(11)	123.8(6)
C(9)-C(8)-C(7)	117.9(7)	C(4)-C(3)-C(2)	121.6(6)
C(3)-C(2)-C(1)	117.4(7)	C(8)-C(9)-C(10)	122.5(8)
C(5)-C(6)-C(7)	119.8(6)	C(6)-C(5)-C(4)	123.1(7)

Appendix Table E6 Bond angle [°] for *cis*-[$Mn(phen)_2Cl_2$] **(11)**

Angle	Value, °	Angle	Value, °
N(1)-Mn-N(2)	70.97(4)	N(1)-Mn-N(3)	89.06(4)
N(1)-Mn-N(4)	158.61(4)	N(3)-Mn-N(2)	82.71(4)
N(4)-Mn-N(2)	97.24(4)	N(4)-Mn-N(3)	71.41(4)
N(1)-Mn-Cl(1)	102.65(3)	N(2)-Mn-Cl(1)	87.07(3)
N(3)-Mn-Cl(1)	161.07(3)	N(4)-Mn-Cl(1)	94.26(3)
N(1)-Mn-Cl(2)	91.04(3)	N(2)-Mn-Cl(2)	160.72(3)
N(3)-Mn-Cl(2)	90.31(3)	N(4)-Mn-Cl(2)	97.51(3)
Cl(1)-Mn-Cl(2)	104.120(1)	C(1)-N(1)-Mn	123.84(8)
C(5)-N(1)-Mn	118.01(8)	C(1)-N(1)-C(5)	118.16(1)
C(6)-N(2)-Mn	115.37(8)	C(10)-N(2)-Mn	126.90(1)
C(13)-N(3)-Mn	126.31(9)	C(17)-N(3)-Mn	115.26(9)
C(18)-N(4)-Mn	116.48(8)	C(22)-N(4)-Mn	124.55(1)
C(10)-N(2)-C(6)	117.70(1)	C(13)-N(3)-C(17)	117.99(1)
C(22)-N(4)-C(18)	118.10(1)	N(1)-C(1)-C(2)	123.31(1)
C(3)-C(2)-C(1)	119.13(1)	C(2)-C(3)-C(4)	119.26(1)
C(3)-C(4)-C(5)	117.80(1)	C(3)-C(4)-C(11)	122.96(1)
C(5)-C(4)-C(11)	119.23(1)	N(1)-C(5)-C(4)	122.35(1)
N(1)-C(5)-C(6)	117.78(1)	C(4)-C(5)-C(6)	119.86(1)
N(2)-C(6)-C(7)	123.26(1)	N(2)-C(6)-C(5)	117.84(1)
C(7)-C(6)-C(5)	118.89(1)	C(6)-C(7)-C(8)	116.87(1)
C(6)-C(7)-C(12)	119.78(1)	C(8)-C(7)-C(12)	123.35(1)
C(9)-C(8)-C(7)	119.70(1)	C(8)-C(9)-C(10)	119.15(2)
N(2)-C(10)-C(9)	123.31(2)	C(12)-C(11)-C(4)	121.15(1)
C(11)-C(12)-C(7)	121.06(1)	N(3)-C(13)-C(14)	123.52(2)
C(15)-C(14)-C(13)	118.79(2)	C(14)-C(15)-C(16)	119.97(1)
C(17)-C(16)-C(15)	117.34(1)	C(17)-C(16)-C(23)	118.99(2)
C(15)-C(16)-C(23)	123.67(1)	N(3)-C(17)-C(16)	122.40(1)
N(3)-C(17)-C(18)	117.61(1)	C(16)-C(17)-C(18)	119.99(1)
N(4)-C(18)-C(17)	117.96(1)	N(4)-C(18)-C(19)	122.87(1)
C(19)-C(18)-C(17)	119.17(1)	C(20)-C(19)-C(18)	117.23(2)
C(18)-C(19)-C(24)	119.15(2)	C(20)-C(19)-C(24)	123.62(2)
C(21)-C(20)-C(19)	119.60(1)	C(20)-C(21)-C(22)	119.59(2)
N(4)-C(22)-C(21)	122.59(2)	C(24)-C(23)-C(16)	121.47(2)
C(23)-C(24)-C(19)	121.22(2)		

Appendix F

Least-squares planes (x, y, z in crystal coordinates) and deviations of Cu(II) and Mn(II) complexes

Appendix Table F1 Least-squares planes (x, y, z in crystal coordinates) and deviations of $[Cu(ox)(phen)(H_2O)]\cdot H_2O$ (**1**).

Atom	Distance, Å	Atom	Distance, Å
	Plan 1 : Cu(1), N(1), N(2), O(1), O(2)		
*Cu(1)	0.1737 (0.0006)	*O(1)	-0.0525 (0.0007)
*N(1)	-0.0344 (0.0007)	*O(2)	-0.0370 (0.0008)
*N(2)	-0.0498 (0.0007)		
Rms deviation of fitted atoms = 0.0871			

Equation for calculate of least-squares plane

6.4725 (0.0028) x - 2.7417 (0.0053) y + 6.6894 (0.0083) z = 3.7051 (0.0035)

Appendix Table F2 Least-squares planes (x, y, z in crystal coordinates) and deviations of $[Cu_4(\mu\text{-suc})_2(phen)_4(H_2O)_4](NO_3)_4\cdot 4H_2O$ **(2)**

Atom	Distance, Å	Atom	Distance, Å
	Plan 1 : Cu(1), N(1), N(2), O(2), O(5)		
*Cu(1)	-0.1198 (0.0012)	*O(2)	0.1252 (0.0015)
*N(1)	0.1246 (0.0015)	*O(5)	-0.0590 (0.0014)
*N(2)	-0.0710 (0.0016)		
Rms deviation of fitted atoms = 0.1040			
	Plan 2 : Cu(2), N(3), N(4), O(1), O(6)		
*Cu(2)	0.1307 (0.0013)	*O(1)	0.0366 (0.0015)
*N(3)	0.0461 (0.0016)	*O(6)	-0.1067 (0.0015)
*N(4)	-0.1067 (0.0016)		
Rms deviation of fitted atoms = 0.0931			

Equation for calculate of least-squares plane

plane1: 5.4594 (0.0077) x + 20.4949 (0.0282) y - 5.9632 (0.0091) z = 1.0805 (0.0042)

plane2: 6.4725 (0.0028) x - 2.7417 (0.0053) y + 6.6894 (0.0083) z = 3.7051 (0.0035)

Appendix Table F3 Least-squares planes (x, y, z in crystal coordinates) and deviations of $[Cu(\mu\text{-ox})(phen)]_n$ **(3)**

Atom	Distance, Å	Atom	Distance, Å
	Plan 1 : Cu(1), N(1), N(2), O(2), O(4)		
*Cu(1)	-0.0138 (0.0008)	*O(2)	-0.0545 (0.0008)
*N(1)	-0.0588 (0.0009)	*O(4)	0.0607 (0.0008)
*N(2)	0.0664 (0.0009)		
Rms deviation of fitted atoms = 0. 0542			

Equation for calculate of least-squares plane

- 7.2059 (0.0032) x - 0.0149 (0.0067) y + 8.2160 (0.0060) z = 5.3818 (0.0052)

Appendix Table F4 Least-squares planes (x, y, z in crystal coordinates) and deviations of $[Cu_2(\mu\text{-ox})_2(phen)_2]_n$ **(4)**

Atom	Distance, Å	Atom	Distance, Å
	Plan 1 : Cu(1), N(1), N(2), O(2), O(3)		
*Cu(1)	-0.0022 (0.0018)	*O(2)	-0.0568 (0.0020)
*N(1)	0.0633 (0.0021)	*O(3)	0.0568 (0.0019)
*N(2)	-0.0612 (0.0021)		
Rms deviation of fitted atoms = 0.0533			
	Plan 2 : Cu(2), N(3), N(4), O(6), O(7)		
*Cu(2)	-0.0047 (0.0018)	*O(6)	-0.0574 (0.0020)
*N(3)	0.0646 (0.0021)	*O(7)	0.0589 (0.0019)
*N(4)	-0.0614 (0.0021)		
Rms deviation of fitted atoms = 0.0543			
	Plan 3 : Cu(3), N(5), N(6), O(10), O(12)		
*Cu(3)	0.0134 (0.0018)	*O(10)	0.0541 (0.0019)
*N(5)	0.0585 (0.0020)	*O(12)	-0.0602 (0.0019)
*N(6)	-0.0658 (0.0020)		
Rms deviation of fitted atoms = 0. 0538			

Appendix Table F4 (Continued)

Atom	Distance, Å	Atom	Distance, Å
	Plan 4 : Cu(4), N(7), N(8), O(13), O(15)		
*Cu(4)	0.0150 (0.0018)	*O(13)	0.0536 (0.0019)
*N(7)	0.0580 (0.0020)	*O(15)	-0.0606 (0.0018)
*N(8)	-0.0660 (0.0020)		
Rms deviation of fitted atoms = 0. 0538			

Equation for calculate of least-squares plane

Plane1: 7.2146 (0.0086) x - 0.0169 (0.0149) y - 8.2317 (0.0161) z = 1.6064 (0.0170)

Plane2: 7.2142 (0.0088) x + 0.0029 (0.0149) y - 8.2327 (0.0163) z = 5.2221 (0.0236)

Plane3: 7.2088 (0.0086) x + 0.0258 (0.0144) y + 8.2270 (0.0159) z = 4.9880 (0.0128)

Plane4: 7.2067 (0.0083) x - 0.0188 (0.0143) y + 8.2313 (0.0155) z = 1.3405 (0.0160)

Appendix Table F5 Least-squares planes (x, y, z in crystal coordinates) and deviations of $[Cu(\mu\text{-}SO_4)(phen)(H_2O)_2]_n$ **(6)**

Atom	Distance, Å	Atom	Distance, Å
	Plan 1 : Cu(1), N(1), N(2), O(5), O(6)		
*Cu(1)	0.0043 (0.0022)	*O(5)	0.0257 (0.0009)
*N(1)	-0.0304 (0.0011)	*O(6)	-0.0278 (0.0010)
*N(2)	0.0282 (0.0009)		
Rms deviation of fitted atoms = 0. 0542			

Equation for calculate of least-squares plane

- 0.6854 (0.0093) x - 0.0373 (0.0314) y + 6.7598 (0.0013) z = 3.2864 (0.0061)

Appendix Table F6 Least-squares planes (x, y, z in crystal coordinates) and deviations of *cis*-[$Mn(phen)_2Cl_2$] **(11)**

Atom	Distance, Å	Atom	Distance, Å
	Plan 1 : N(1), N(3), N(4), Cl(1)		
*N(1)	0.0277 (0.0004)	*N(4)	0.0356 (0.0006)
*N(3)	-0.0373 (0.0006)	*Cl(1)	-0.0260 (0.0004)
Rms deviation of fitted atoms = 0.0837			

Equation for calculate of least-squares plane

7.2103 (0.0018) x - 1.9308 (0.0041) y + 7.3800 (0.0034) z = 8.0777 (0.0012)

Appendix G

Publication

Acta Crystallographica Section E
Structure Reports Online
ISSN 1600-5368

Di-μ_4-succinato-tetrakis[aqua-phenanthrolinecopper(II)] tetranitrate tetrahydrate

Panana Kitiphaisalnont,[a] Sutatip Siripaisarnpipat[a]* and Narongsak Chaichit[b]

[a]Department of Chemistry, Kasetsart University, Bangkok 10903, Thailand, and [b]Department of Physics, Thammasat University, Rangsit, Pathumthani 12121, Thailand
Correspondence e-mail: fscists@ku.ac.th

Received 21 September 2009; accepted 29 September 2009

Key indicators: single-crystal X-ray study; T = 293 K; mean σ(C–C) = 0.006 Å; R factor = 0.064; wR factor = 0.191; data-to-parameter ratio = 19.4.

In the title compound, $[Cu_4(C_4H_4O_4)_2(C_{12}H_8N_2)_4(H_2O)_4](NO_3)_4\cdot 4H_2O$, the complete tetracation is generated by crystallographic inversion symmetry. Both unique Cu^{2+} ions are coordinated by an *N*,*N*′-bidentate phenanthroline molecule, two *O*-monodentate bis-bridging succinate dianions and a water molecule, resulting in distorted CuN_2O_3 square-based pyramidal geometries for the metal ions, with the water molecule occupying the apical site. In the crystal, the components are linked by O—H···O hydrogen bonds and aromatic π–π stacking interactions [minimum centroid–centroid separation = 3.537 (2) Å].

Related literature

For related structures, see: McCann *et al.* (1998); Padmanabhan *et al.* (2005); Ghosh *et al.* (2007).

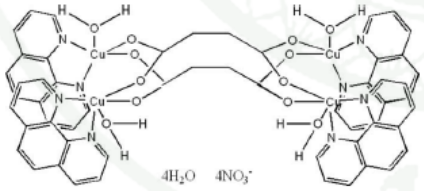

Experimental

Crystal data

$[Cu_4(C_4H_4O_4)_2(C_{12}H_8N_2)_4(H_2O)_4](NO_3)_4\cdot 4H_2O$
M_r = 1599.29
Monoclinic, $P2_1/c$
a = 8.9180 (1) Å
b = 34.1090 (2) Å
c = 10.3620 (2) Å
β = 96.031 (1)°
V = 3134.51 (7) Å^3
Z = 2
Mo $K\alpha$ radiation
μ = 1.44 mm^{-1}
T = 293 K
0.20 × 0.19 × 0.10 mm

Data collection

Bruker SMART 1K CCD diffractometer
Absorption correction: none
23089 measured reflections
8980 independent reflections
7772 reflections with $I > 2\sigma(I)$
R_{int} = 0.018

Refinement

$R[F^2 > 2\sigma(F^2)]$ = 0.064
$wR(F^2)$ = 0.191
S = 1.05
8980 reflections
463 parameters
101 restraints
H atoms treated by a mixture of independent and constrained refinement
$\Delta\rho_{max}$ = 2.88 e Å^{-3}
$\Delta\rho_{min}$ = −1.59 e Å^{-3}

Table 1
Selected bond lengths (Å).

Cu1—O2	1.948 (3)	Cu2—O1	1.946 (3)
Cu1—O5	1.966 (3)	Cu2—O6	1.952 (3)
Cu1—N2	2.011 (3)	Cu2—N4	2.007 (3)
Cu1—N1	2.015 (3)	Cu2—N3	2.025 (3)
Cu1—O4	2.240 (3)	Cu2—O3	2.160 (3)

Table 2
Hydrogen-bond geometry (Å, °).

D—H···A	D—H	H···A	D···A	D—H···A
O3—H4···O14	0.73 (7)	1.99 (7)	2.707 (7)	169 (7)
O3—H16···O13	0.70 (6)	2.07 (6)	2.772 (6)	177 (9)
O4—H23···O12	0.82 (6)	2.27 (6)	3.015 (7)	153 (5)
O4—H24···O10^{i}	0.82 (5)	2.03 (6)	2.816 (6)	161 (8)
O13—H13*C*···O5^{ii}	0.77 (7)	2.24 (7)	3.000 (5)	167 (7)
O13—H13*D*···O10^{iii}	0.71 (7)	2.23 (7)	2.899 (7)	159 (8)
O14—H14*B*···O9^{iv}	0.83 (7)	2.15 (6)	2.846 (13)	142 (6)
O14—H14*C*···O7^{v}	0.82 (9)	2.10 (9)	2.874 (14)	158 (10)

Symmetry codes: (i) $-x, -y, -z+1$; (ii) $-x+1, -y, -z$; (iii) $x+1, y, z-1$; (iv) $x+1, -y+\frac{1}{2}, z-\frac{1}{2}$; (v) $x+1, y, z$.

Data collection: *SMART* (Bruker, 2000); cell refinement: *SAINT* (Bruker, 2000); data reduction: *SAINT*; program(s) used to solve structure: *SHELXS97* (Sheldrick, 2008); program(s) used to refine structure: *SHELXL97* (Sheldrick, 2008); molecular graphics: *SHELXTL* (Sheldrick, 2008); software used to prepare material for publication: *SHELXTL*.

The authors thank the Royal Golden Jubilee PhD Program (RGJ) for financial support.

Supplementary data and figures for this paper are available from the IUCr electronic archives (Reference: HB5112).

References

Bruker (2000). *SMART* and *SAINT*. Bruker AXS Inc., Madison, Wisconsin, USA.
Ghosh, A. K., Ghoshal, D., Zangrando, E., Ribas, J. & Chaudhuri, N. R. (2007). *Inorg. Chem.* **46**, 3057–3071.
McCann, S., McCann, M., Casey, R. M. T., Jackman, M., Devereux, M., McKee, V., & (1998). *Inorg. Chim. Acta*, **279**, 24–29.
Padmanabhan, M., Kumary, S. M., Huang, X. & Li, J. (2005). *Inorg. Chim. Acta*, **358**, 3537–3544.
Sheldrick, G. M. (2008). *Acta Cryst.* A**64**, 112–122.

CIRRICULUM VITAE

NAME : Ms. Panana Kitiphaisalnont

BIRTH DATE : April 20, 1979

BIRTH PLACE : Bangkok, Thailand

EDUCATION :

YEAR	INSTITUTE	DEGREE/DIPLOMA
2000	Mahidol Univ.	B.Sc. (Chemistry)
2004	Kasetsart Univ.	M.S. (Chemistry)

SCHOLASHIP/AWARDS : Research Fund for Thesis from the Graduate School, Kasetsart University 2001–2002
: Research Assistantship from the Thailand Research Fund (TRF) 2002 –2004
: The Royal Golden Jubilee Ph.D. Scholarship from The Thailand Research Fund (TRF) 2006 –2009
: Outstanding Poster Presentation in RGJ-Ph.D. Congress VIII April 20-21, 2007

PUBLICATIONS :

1. Kitiphaisalnont , P.; Thohinung, S.; Hanmungtum, P. ; Chaichit, N.; Patrarakorn, S. and Siripaisarnpipat, S. "Effect of metal ions and length of alkylene bridge on the strength of hydrogen bond in diiminedioxime cobalt (III) and nickel (II) complexes" *Polyhedron*. **2006**, 25, 2710-2716.
2. Kitiphaisalnont, P.; Peungsamran, N. and Siripaisarnpipat, S. "Spectroscopic Investigation of Heat Treated and Unheat treated for Ratanakiri Zircon" *J.Aust. Ceram. Soc.* 42[2] **2006**, 21-25.
3. Kitiphaisalnont, P.; Siripaisarnpipat, S.; and Chaichit, N. "Di-μ_4-succinato-tetrakis[aquaphenanthrolinecopper(II)]tetranitrate tetrahydrate" *Acta Cryst. E.* 65 **2009**, 1284.